



# **BRNO UNIVERSITY OF TECHNOLOGY**

VYSOKÉ UČENÍ TECHNICKÉ V BRNĚ

## **FACULTY OF MECHANICAL ENGINEERING**

FAKULTA STROJNÍHO INŽENÝRSTVÍ

## **INSTITUTE OF AEROSPACE ENGINEERING**

LETECKÝ ÚSTAV

# **CONCEPTUAL DESIGN OF A HEAT SWITCH INSTALLATION INTO A STRUCTURE OF SATELLITE**

KONCEPČNÍ NÁVRH ZÁSTAVBY TEPELNÉHO SPÍNAČE DO KONSTRUKCE DRUŽICE

**MASTER'S THESIS**

DIPLOMOVÁ PRÁCE

**AUTHOR**

AUTOR PRÁCE

Bc. Martin Vrba

**SUPERVISOR**

VEDOUCÍ PRÁCE

Ing. Jakub Mašek

**BRNO 2020**



# Master's Thesis Assignment

Institut: Institute of Aerospace Engineering  
Student: **Bc. Martin Vrba**  
Degree program: Mechanical Engineering  
Branch: Aircraft Design  
Supervisor: **Ing. Jakub Mašek**  
Academic year: 2019/20

Pursuant to Act no. 111/1998 Coll. concerning universities as amended and pursuant to the BUT Study Rules, by the Director of the Institute, you have been assigned a Master's Thesis entitled:

## Conceptual design of a heat switch installation into a structure of satellite

### Characteristics of the project issues:

Space exploration missions require the use of heat switches to thermally decouple the payload from the cold external environment in order to save energy. A miniaturized heat switch can be used as a versatile thermal control hardware for various types of space probes and would be installed in series between the radiator and the dissipative unit. The current switch development showed a necessity to design and analyse its interfaces according to possible installation into a structure of satellite or space probe.

### The objectives to be achieved:

- Acquaint with the problematics of heat switch installation, possible construction of probe, radiator and dissipative unit based on literature review
- Requirements proposal for heat switch development - interfaces and fixation points
- Conceptual designs of the installation and their critical assessment according to requirements
- Trade-off between concepts

### Literature on the topic:

MAŠEK, Jakub. Qualification Test of Heat Switch for Martian Conditions. Brno: Vysoké učení technické v Brně, Fakulta Strojního inženýrství, 2016, 129 s. Diplomová práce. Vedoucí práce Ing. Robert Popela, Ph.D.

Deadline for submission Master's Thesis is given by the Schedule of the Academic year 2019/20

In Brno,

L. S.

---

doc. Ing. Jaroslav Juračka, Ph.D.  
Director of the Institute

---

doc. Ing. Jaroslav Katolický, Ph.D.  
FME dean

## **ABSTRACT**

This Master thesis focuses on compiling a construction and heat-paths overview of space ships and space vehicles, which are used currently. Based on specific requirements and standards, conceptual designs are developed for the inclusion of a thermal switch into the satellite structure. In these chapters, specific parts are described, which partake on the heat conduction and are important from the construction view for these designed concepts. This Master thesis describes methods of computation of thermal conductivities and distribution of the force of gravity to the points of attachment for individual concepts. At the end, an evaluation and selection of the potential optimal concept is done.

## **KEY WORDS:**

European space agency, concept, construction, cooler, equipment, heat, isolation, miniaturized head switch, phase-change material, radiation, satellite, space, space ships, space vehicles, thermal conductivity, thermal resistance, thermal way.

## **ABSTRAKT**

Tato diplomová práce je zaměřena na sestavení přehledu konstrukcí a tepelných cest kosmických lodí a kosmických vozidel, které se v současné době používají. Na základě specifických požadavků a standardů jsou vypracovány koncepční návrhy zástavby tepelného spínače do konstrukce družice. V jednotlivých kapitolách jsou popsány určité členy, které se na vedení tepla podílí a jsou důležité pro navrhované koncepty z pohledu konstrukce. Diplomová práce popisuje postupy výpočtu tepelných vodivostí a rozložení působící tíhové síly do míst uchycení pro jednotlivé koncepty. Na závěr provádí hodnocení a výběr potenciálně nejvhodnějšího návrhu.

## **KLÍČOVÁ SLOVA:**

Evropská kosmická agentura, koncept, konstrukce, chladič, zařízení, teplo, izolace, miniaturizovaný tepelný spínač, materiál měnící stav, záření, satelit, vesmír, kosmická loď, kosmické vozidlo, tepelná vodivost, tepelný odpor, tepelná cesta.

## ROZŠÍŘENÝ ABSTRAKT

Evropská kosmická agentura (ESA), podobně jako Národní úřad pro letectví a kosmonautiku (NASA) v Americe, má snahu řešit otázku, jako jednu z mnoha, týkající se regulace odvodu tepla od přístrojů ve vesmírných satelitech nebo u vesmírných vozítek. Z potřeby tuto otázku vyřešit vznikl pod záštitou Evropské kosmické agentury projekt Miniaturního tepelného spínače. Tento projekt nakonec připadnul Leteckému ústavu Vysokého učení technického v Brně. V rámci tohoto projektu vznikl požadavek na vytvoření koncepčních designů zástavby Miniaturního tepelného spínače do konstrukce družice. Tato diplomová práce se tomuto tématu koncepčních návrhů zástavby věnuje.

V první části, která má rešeršní charakter, jsou představeny a rozebrány jednotlivé a důležité součásti pro odvod tepla v rámci celé tepelné cesty. Především jsou to prvky v rámci pasivní tepelné kontroly, do které patří také Miniaturní tepelný spínač. Je to mu tak proto, jelikož ke své funkci nevyžaduje žádný externí zdroj energie. Zároveň jsou také popsány možnosti, jak by tato tepelná cesta mohla vypadat. V rámci tepelné cesty je uvažován flexibilní vodivý člen, který by měl sloužit jako spojovací prvek mezi zdrojem tepla a Miniaturním tepelným spínačem a jeho zástavbou. Následně na základě provedené rešerše a zhodnocení podoby tepelné cesty jsou sepsány požadavky, na jejichž základě jsou navrženy koncepty zástavby Miniaturního tepelného spínače. Tyto koncepty se také odvíjí od konkrétní úvahy o pozici Miniaturního tepelného spínače.

V další části diplomové práce jsou představeny a popsány jednotlivé navržené varianty konceptů. Celkem jsou navrženy čtyři koncepty A až D, kdy každý koncept je zaměřen na jiný způsob montáže. První tři koncepty sledují záměr externí konstrukce, kdy na Miniaturní tepelný spínač není přenášeno velké silové působení, jež zachytí konstrukce. Poslední čtvrtý koncept není navržen jako externí konstrukce, ale jsou u něj upraveny pouze jeho vnější komponenty tak, aby jej bylo možné přišroubovat k jiným součástem tvořící tepelnou cestu. Různé způsoby montáže jsou navrženy z toho důvodu, jelikož se nejedná o návrh a použití finální konstrukce, aby zahrnuli co nejvíce možných případů, jak by mohl být Miniaturní tepelný spínač upevněn v těle satelitu. Konkrétní podoby všech konceptů jsou vytvořeny v programu Catia V5 R21.

Hlavní funkcí Miniaturního tepelného spínače je regulace odvodu tepla. Navržené konstrukce konceptů, jako schránky pro Miniaturní tepelný spínač, mohou tuto funkci narušit, jelikož vytváří stálou cestu pro odvod tepla a mohou tuto regulaci omezit. Z tohoto důvodu je třetí část diplomové práce věnována výpočtu tepelné vodivosti celé soustavy a samostatných konstrukcí. Cílem výpočtu tepelné vodivosti jednotlivých konceptů je zjistit do jaké míry jsou tepelně vodivé případně izolující. Podle vstupujících parametrů potřebných k výpočtu tepelné vodivosti, materiálové charakteristiky a zvolené rozměry konstrukcí na základě modelů, jsou podle literatury a popsaného postupu výpočtů, vypočítány tepelné vodivosti všech čtyř konstrukcí konceptů a celách uvažovaných sestav. Výsledná hodnota tepelné vodivosti je vždy vypočtena jako převrácená hodnota odporu proti kondukcii tepla, jelikož jednotlivé části konceptů tvoří odpory, podobně, jako v elektrickém obvodu rezistory kladou odpor elektrickému proudu proudu. Následně je tento výpočet proveden stejným způsobem pro případ, že je do stykových míst Miniaturního tepelného spínače s konstrukcemi vložena 2 mm vrstva teflonu – PTFE. Zároveň jsou tyto výpočty u každého konceptu provedeny pro dva různé typy materiálu

kvůli možnosti porovnání. U posledního čtvrtého konceptu není však tento teflonový pásek přidáván, jelikož je zde nutné naopak zajistit zachování co největší tepelné vodivosti.

Poslední část diplomové práce se zabývá a jejím cílem je zjistit rozložení a velikosti sil působící na jednotlivé šrouby, jimiž jsou konstrukce připevněny k ostatním částem tepelné cesty. Tyto síly vznikají od zatěžující síly, kterou je tíhová síla jednotlivých konceptů. Na základě požadavku od Evropské kosmické agentury, kdy je nutné, aby Miniaturní tepelný spínač a tudíž i konstrukce, vydržela 20-ti násobek běžného gravitačního zrychlení Země, jsou síly do šroubů počítány pro dvě hodnoty gravitačního zrychlení.

Výsledkem a závěrem této práce je výběr potenciálně nejvhodnějšího konceptu k použití zástavby. Výběr je proveden na základě všech vypočtených hodnot a to jak hodnot tepelných vodivostí a hmotností jednotlivých konceptů, tak hodnot rozložení působících sil na šrouby. K objektivnějšímu výběru nejvhodnější konstrukce slouží především specifický parametr. Ten uvádí do poměru hodnotu tepelné vodivosti a hmotnosti. Jelikož hlavním cílem návrhu konceptů je dosažení co nejnižší celkové hmotnosti a zároveň dosažení co nejnižší tepelné vodivosti samotných konstrukcí, je tento parametr ideálním ukazatelem. Pouze u konceptu kde neexistuje externí konstrukce, je cílem dosažení naopak co největšího specifického parametru. Je to z toho důvodu, že potřeba v tomto případě zajistit naopak co největší tepelnou vodivost. V závěrečné diskusi jsou uvedeny všechny konkrétní důvody pro výběr jednoho z konceptů a zároveň pro výběr jednoho z použitých materiálů.

## **BIBLIOGRAFICKÁ CITACE**

VRBA, Martin. *Koncepční návrh zástavby tepelného spínače do konstrukce družice* [online]. Brno, 2020 [cit. 2020-06-26]. Dostupné z: <https://www.vutbr.cz/studenti/zav-prace/detail/125296>. Diplomová práce. Vysoké učení technické v Brně, Fakulta strojního inženýrství, Letecký ústav. Vedoucí práce Jakub Mašek.

## **ČESTNÉ PROHLÁŠENÍ**

Prohlašuji, že jsem diplomovou práci na téma *Koncepční návrh zástavby tepelného spínače do konstrukce družice* vypracoval samostatně s využitím uvedené odborné literatury a pramenů.

V Brně dne 26. 6. 2020

.....  
Martin Vrba



## **PODĚKOVÁNÍ**

Děkuji leteckému ústavu VUT v Brně za poskytnutí odborné literatury a především svému vedoucímu Ing. Jakubu Maškovi za odborné vedení při tvorbě diplomové práce, vstřícný přístup a věcné připomínky. Dále bych chtěl poděkovat přátelům a své rodině za podporu během studia.



## Content

Introduction.....	13
1. Technology of Miniaturized Heat Switch.....	15
1.1. Functional specification.....	15
1.2. Usage possibilities.....	17
1.3. Current design.....	19
2. Heat transfer.....	21
2.1. Radiation.....	21
2.1.1. Solar Radiation.....	23
2.1.2. Albedo radiation.....	23
2.1.3. Planetary radiation.....	24
2.2. Convection.....	24
2.3. Conduction.....	25
2.4. Combined Modes of Heat Transfer.....	26
3. Thermal control of satellites.....	27
3.1. Heating and heat dissipation.....	28
3.1.1. Active thermal control.....	29
3.1.2. Passive thermal control.....	30
3.2. Supporting structure.....	30
3.3. Arrangement of elements for heat dissipation.....	33
3.3.1. Radiator.....	34
3.3.2. Louvers.....	36
3.4. Insulations and surface coating.....	38
3.4.1. Thermal surface finishes.....	38
3.4.2. Insulations.....	40
3.5. Thermal way.....	43
3.6. Fastening.....	45
3.7. Prerequisites for construction of MHS.....	46
4. Thermal switch installation design.....	48
4.1. Requirements for conceptual designs.....	50
4.2. Definition of parameters.....	51
4.3. Concept A.....	53
4.4. Concept B.....	55
4.5. Concept C.....	57
4.6. Concept D.....	59

4.7. Summary of conceptions .....	61
5. Thermal control of concepts.....	63
5.1. Calculation procedure.....	63
5.2. Outputs.....	64
6. Force analysis of concepts .....	70
6.1. Calculation procedure of magnitude of forces.....	70
6.2. Magnitude of forces of concept A.....	72
6.3. Magnitude of forces of concept B.....	74
6.4. Magnitude of forces of concept C.....	78
6.5. Magnitude of forces of concept D.....	80
7. Discussion .....	84
8. Conclusion.....	87
9. Bibliography.....	89
List of figures .....	93
List of tables.....	95
List of short cuts and symbols.....	96
Appendix.....	98

# Introduction

Since the first spacecraft launch into space in the year 1957, hundreds of spacecraft and space vehicles have been built in support of scientific, military, and commercial missions. In order for the spacecraft and space vehicles to perform their function, systems that will ensure proper operation are needed. One of these systems in spacecraft and space vehicles, which do their mission away from Earth's atmosphere is thermal control. Spacecraft thermal control is integral to a mission success. The process of thermal control for a spacecraft involves managing the energy entering and leaving the spacecraft to ensure that the components of the spacecraft remain within an acceptable temperature range. Spacecrafts perform optimally and have longer working lives when the temperature of their components remains within these boundaries, often near the temperature at which they were fabricated. Heat removal from electronic units is a foremost spacecraft concern, and thus the problem of developing an optimal conductive interface between unit baseplate and spacecraft mounting is critical.

Such an indispensable component in the whole thermal regulation cycle can be the Miniaturised Heat Switch (MHS). In the year 2012 a project was created in Italy for the development of the before mentioned MHS. The first developer in this project under the auspices of the European Space Agency MHS was the company AeroSekur, later AresCosmo. This company left the project and since Brno University of Technology (BUT) was already involved in this project from the year 2015 it received the project to complete it. During the development of the MHS, Thermo-vacuum test chamber for testing in simulated Martian conditions is also developed. MHS is also considered for the use on space vehicles on Mars.

The project framework, in addition to the development of a new MHS, also entails the creation of a new construction design of this developed switch integrated into the satellite structure. This Master's thesis is focused on this topic. For individual concepts, the basic structural arrangement of satellites together with the description of the essential parts of thermal regulation is first described. Also basic requirements rising from ECSS standards European Space Agency (ESA) are mentioned. Then, concepts and computational models for thermal energy transmission and strength checks are introduced. Finally, these conceptual designs are compared based on the requirements.



# 1. Technology of Miniaturized Heat Switch

The numerous electrical components on a spacecraft present thermal-control challenges. High-power dissipating components must be prevented from overheating conversely, components that are only activated occasionally must be prevented from cooling to temperatures below operational level in order to save energy. The ideal for such applications is the use of phase-change materials (PCM).

The Miniaturized Heat Switch is clearly a mechanical device, which includes PCM. MHS serves as a component, that allows heat transfer from the interior equipment (hot interface) of the spacecraft and space vehicles onto the radiator (cold interface), which radiates the heat into space. The heat transfer is controlled by a variable conductivity based on temperature. In the state ON it allows the transfer of heat energy onto the radiator and in the state OFF prevents this transfer - isolates. When the temperature on the hot side drops below a predetermined limit, usually this limit is the solidification temperature of actuator (PCM), this heat transfer is canceled via the MHS. This circumstance is very important for saving the energy produced. Based on these attributes is the MHS a perfect fit for continuously operating systems, which need to keep a very thin temperature interface. It is also applicable within systems with frequent temperature fluctuations. Heat switches thus function similarly to a diode or variable-conductance heat pipes. However, they achieve temperature control by modulating and conduction paths rather than a two-phase flow process. [18][21]

## 1.1. Functional specification

For the development of MHS, basic requirements by ESA have been established. These requirements, on which the company AeroSekur developed a preliminary design, are listed in the document ESA SOW Report [18]. Subsequently in this report [34] company AeroSekur stated additional requirements for the project needs. Such stated requirements are divided into multiple sections:

- Functional & Performance Requirements
- Interface Requirements
- Environmental Requirements
- Physical & Resource Requirements
- Operational Requirements
- Product Assurance Requirements
- Design Requirements
- Verification & Testing Requirements

Also the requirements for mechanical, vibration and radiation tests are listed. And finally the end product (system) definition and breakdown.

The Heat Switch shall consist of: [18]

- a. Hot mounting interface
- b. Cold mounting interface
- c. Switching device to vary the thermal conductance between the hot and cold interfaces

The heat switch shall be a standalone item ready to be mounted between a unit and radiator.

ESA at the same time provides general recommendations in their standards as to what characteristics should the PCM have. The ideal PCM would have the following characteristics: [13]

1. Melting point within the allowed temperature range of the thermally controlled component. In general between 260 K and 315 K
2. High heat of fusion. This property defines the available energy storage and may be important either on a mass basis or on a volume basis
3. Reversible solid-to-liquid transition. The chemical composition of the solid and liquid phases should be the same
4. High thermal conductivity. This property is necessary to reduce thermal gradients. Unfortunately most PCM are very poor thermal conductors, so that fillers are used to increase the conductivity of the system
5. High specific heat and low density
6. Long term reliability and stability during repeated cycling
7. Low volume change during phase transition
8. Low vapor pressure
9. Non-toxic
10. Non-corrosive. Compatible with structural materials
11. No tendency to supercooling<sup>1</sup>
12. Availability and reasonable cost

In these standards, the best PCM specific variants and their characteristics are listed, which were processed by the company Dornier Systems. [7]

---

<sup>1</sup>Supercooling is the process of cooling a liquid below the solid-liquid equilibrium temperature without formation of the solid phase. Supercooling when only one phase is present is called one-phase supercooling. Supercooling in the presence of both solid and liquid, or two-phase supercooling, depends upon the particular material and the environment surrounding it. The best way to reduce supercooling is to ensure that the original crystalline material has not been completely molten. In such a case the seeds which are present in the melt tend to nucleate the solid phase when heat is removed. Nucleating catalysts are available for many materials. [13]



## 1.2. Usage possibilities

Heat switches could serve as the basis for an entire spacecraft thermal-control system, but such an application would require a shift in philosophy, beginning in the early stages of the design process. Examination of a typical conventional thermal design reveals why heat switches could be desirable as the basis for a spacecraft thermal-control system. The industry standard for spacecraft thermal control involves connecting internal heat-producing components to external radiator surfaces through either heat pipes or spacecraft structure. These connections from the components to the radiation plate, which generate thermal energy, must ensure a sufficiently large heat dissipation from them. This means that it must have high thermal conductivity. Radiators are then sized so that, in the worst-case hot mission environment and worst-case heat dissipation of the components, they still run cold enough to keep all components below their upper temperature limits. A more detailed description of radiators is in Chapter 3.2.1.

In general, heat switches can control spacecraft component temperatures either from a location between an insulated spacecraft structure and an external radiator or from between the components themselves and the structure of the spacecraft. These two options lead to somewhat different switch operating modes. Both these options are shown in figures 1.1 and 1.2. The first option, where the MHS is positioned between the components and the spacecraft structure, is typical for space vehicles, which fulfil their mission on Mars for example. The second option of MHS structure is typical for use in satellites and probes that travel through open space and are exposed to solar and cosmic radiation, and vacuum. However, it is not necessary to use one method of placement only for satellites or space vehicles. The placement from figure 1.1 can be used in satellites and the placement in figure 1.2 can be also used in space vehicles.

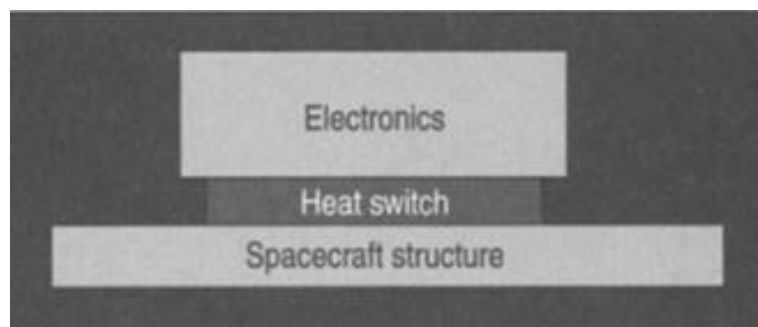


*Figure 1.1: First type of location of heat switch [21]*

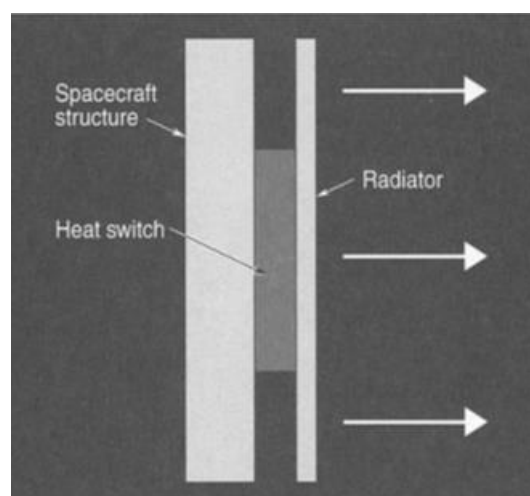


*Figure 1.2: Second type of location of heat switch [21]*

In general, MHS are devices, which allow a passive heat dissipation or isolation. The heat dissipation or isolation principle itself, in MHS, can be based on multiple systems – “switching” principles: [13][21]

- Paraffin heat switches
- Diaphragm Thin Plate Heat Switch
- Shape Memory Heat Switches
- Cryogenic Heat Switches
- Gas-Gap Heat Switches
- Differential Thermal Expansion Heat Switches

For the discovery of usage possibility of PC working materials an experimental investigation has been performed by DORNIER SYSTEM. Several PCMs have been tested under repeated heating and freezing cycles. The main purpose of these tests has been the detection of eventual supercooling phenomena. An aim of experimental testing by the company DORNIER SYSTEM was finding out the variables having any influence on the supercooling behaviour of the PCM [13][21]

- Total number of cycles
- Cooling rate
- Type of container

Testing materials: [13][21]

- Dodecane
- Tetradecane
- Hexadecane
- Acetic acid
- Disodium hydroxide heptahydrate
- Distilled water

The resulting of testing materials can be found in literature [13][21]. Summary of the main results:

- Water and paraffins did not show any tendency to supercooling
- Acetic acid showed supercooling of different orders of magnitude
- Supercooling of disodium hydroxide heptahydrate amounted to 3 - 3,5 K regardless of cooling rate and number of temperature cycles.

The heat switch, which an Italian company started to develop and then it was taken over by BUT, is a paraffin heat switch. Before the project was given to BUT for completion, the Italian company designed and made a first prototype. They also undertook basic testing of the created heat switch. Summary of this testing and the detailed description of the original MHS construction can be found in the literature [4][5]. The general construction description of this prototype is outlined on the next chapter. Due to the fact, that the original design does not meet the ESA requirements, problems are also mentioned that need to be solved.

### 1.3. Current design

The main function of MHS based on paraffin is the inner structure ability, which during the warming of paraffin to its melting point and higher, when it increases its volume, to move and press the part cold plate (R5) to the contact plate (R25, R27). During the contact of these parts heat may traverse through the whole miniaturized thermal switch – STATE ON. In the basic condition – STATE OFF, when the heat can't traverse, is the initial distance between the mentioned parts 1,7 mm within the requirements of ESA[3]. This adjustment allows the construction of the part bellow assy (R10). After cooling the paraffin, the MHS is returned to the original position by a spring mechanism.

Design MHS is adopted from the company AeroSekur. In general form is this design, see figure 1.3, based on several main parts. All the individual parts of the MHS are described in Annex A.

The main outer structure is made of hot and cold plates on both sides of the MHS and of three columns – Elastomer insulator (R20, R21, R22) between these parts. Hot plate represents a part of base plate (R1, R6, R15). Heat energy from different devices is brought onto the hot plate and from the cold plate is this energy drained away. The main function of the columns is to hold up the whole structure of MHS, where they permanently hold the distance between the hot and cold plate. At the same time, they serve as isolators, so that the diverted heat energy isn't returned to the base plate.

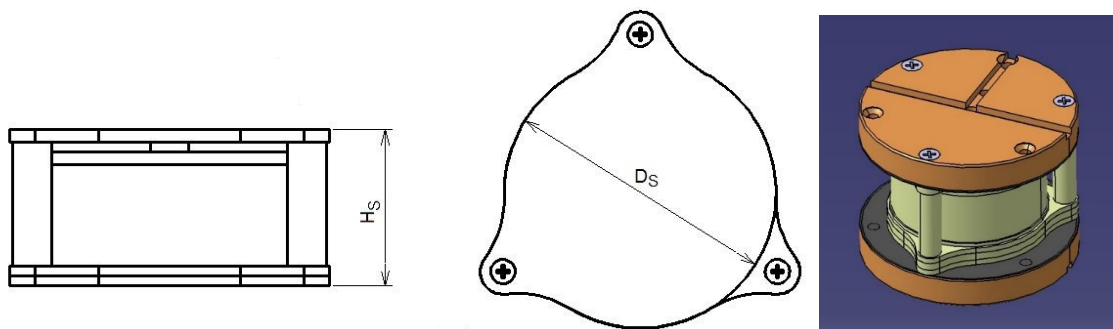


*Figure 1.3: Original concept of MHS [4]*

Basic dimensions MHS:[27] [33]

$$D_s = 42 \text{ mm}$$

$$H_s = 26,2 \text{ mm}$$

$$A_s = 1564,53 \text{ mm}^2 - \text{input surface for heat transfer}$$

- The most important part of MHS is a conductive copper braid structure. This structure must divert the heat energy from the base plate onto the cold plate when the MHS is in state ON. One of the requirements given by ESA is the conductivity of this structure, that must have the minimal value of  $1,5 \text{ W} \cdot \text{K}^{-1}$ . As the conductivity of the original structure, figure 1.4, is lower than required, better structure must be developed. This issue is addressed by Bc. Jakub Černoč in his Master's thesis Flexible structure development for efficient heat transfer. [2]

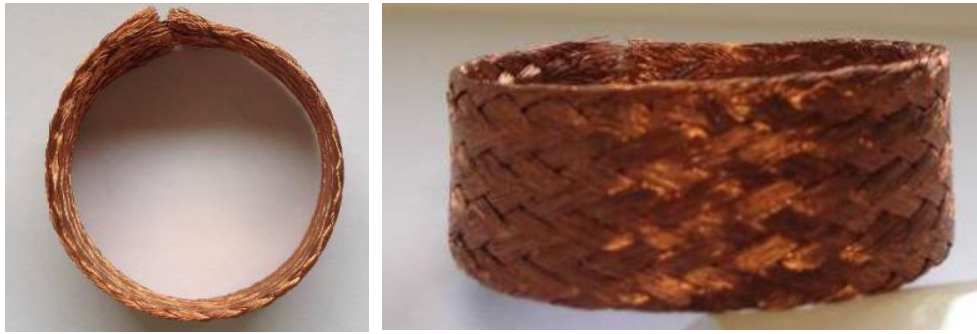


*Figure 1.4: Original conductive structure [4]*

- The inner part of the MHS is a box, that contains PCM. PCM secures the main function of the MHS – switch from state OFF into state ON, when heat transfer through MHS is allowed. The medium, that during a temperature increase is stretched enough, that it moves the whole inner structure of the MHS and switches into the state ON, is paraffin. During the original testing was as paraffin used hexadecane  $C_{16}H_{34}$ . An essential characteristic of hexadecane is its low melting point of 18 °C. Part of the inner structure is also a spring mechanism, which secures the return of PCM into the original position, when it is cooled down.

Currently, there is an effort to improve the current design in many ways. Intensive inter-institutional cooperation on this project is taking place at the Faculty of Mechanical Engineering. The most important areas for the current design improvement are:

- Improvement of the heat conductivity of the flexible structure
- Concept change of the paraffin box
- Modification of the external construction
- Finding suitable materials and optimal production possibilities

And lastly the conceptual design of a heat switch installation into a satellite structure, which is the assignment and subject of this Master thesis. These concepts and their installations are analysed in the fourth chapter.

## 2. Heat transfer

Throughout its lifespan and mission fulfilment, the satellites meet different kinds – modes of heat transfer. There are total of three modes: heat transfer by convection, conduction and radiation. The most usual methods of heat transfer are only conduction and radiation. Conduction takes place between individual devices, components and the satellite construction. Radiation then forms the largest part of heat transfer in open space. Radiation from the Sun or other cosmic bodies falls onto the satellite and at the same time within the internal thermal control, the satellite is trying to radiate the excess heat generated by the devices into space. [37] Most of the convection is encountered by space vehicles, which fulfil their mission on planets with atmosphere, for example on Mars. As such, the satellite encounters convection only during heat transfer from fluids in closed vessels. [6] In figure 2.1, all three modes of heat transfer are schematically shown.

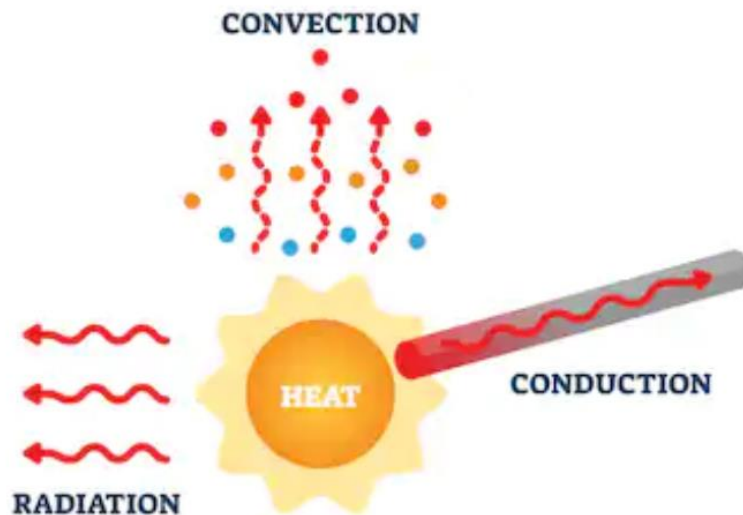


*Figure 2.1: Modes of heat transfer [39]*

### 2.1. Radiation

Radiation is a physical process, in which the substance – mass emits into the space energy in the form of electromagnetic radiation – electromagnetic waves. Radiation transfers thermal energy even in vacuum, where it is not possible to mediate conduction or convection. The energy that is radiated by radiation depends on several factors:

- Body temperature – amount of radiated energy is described by Stefan-Boltzmann law or Planck radiating law.
- Surface color – the least amount of heat is radiated by silvered shiny surfaces, the largest amount by black surfaces. At temperatures above 1000 °C however, most materials with small variations behave similarly like completely black bodies. [43]
- Area volume - the energy emitted by the radiation is directly proportional to the area volume of the radiating body

For the radiated thermal energy through radiation apply the optical laws similarly, as for all other electromagnetic waves. From a thermodynamic view, radiation is a heat transfer at any wavelength. In the narrower sense, it is mostly infrared radiation.

The total radiation intensity of an absolutely black body describes the Stefan-Boltzmann law. This law says, that intensity  $E_0$  [ $\text{W}\cdot\text{m}^{-2}$ ] increases with the fourth power of temperature  $T$  [K], equation 2.1: [21][43]

$$E_0 = \sigma \cdot T^4 \quad (2.1)$$

where  $\sigma = 5,67 \cdot 10^{-8}$  [ $\text{W}\cdot\text{m}^{-2}\cdot\text{K}^{-4}$ ] is the Stefan-Boltzmann constant. For a „grey body“ this law can be rewritten into the form: [21][43]

$$E_g = \varepsilon \cdot \sigma \cdot T^4 \quad (2.2)$$

where  $E_g$  [ $\text{W}\cdot\text{m}^{-2}$ ] is the radiation intensity of a grey body and  $\varepsilon$  [-] is the emissivity of the body surface. Emissivity is defined as the ratio of the radiation intensity of a real body to that of an absolutely black body with the same temperature. Emissivity is defined in the range  $0 \leq \varepsilon \leq 1$ . For a body with a finite surface on which an amount of energy falls or the body emits this energy through this surface, this law can then be rewritten in the form: [21][43]

$$E_s = \varepsilon \cdot A \cdot \sigma \cdot T^4 \quad (2.3)$$

where  $E_s$  [W] is the radiant performance and the  $A$  [ $\text{m}^2$ ] is body surface.

The computations of specific cases of radiation and absorption for different surfaces can be found in ECSS standards for example [9][12][21], as well as in literature [37][43]. In figure 2.2, three modes of radiation that can occur are shown: solar radiation, albedo radiation and planetary radiation.

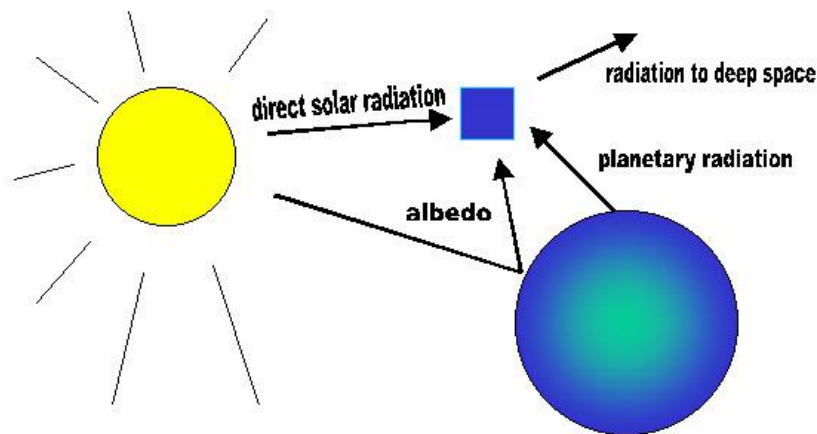


Figure 2.2: Modes of radiation [31]

### 2.1.1. Solar Radiation

The radiant energy from the Sun is the most significant heat source. The radiation is nearly constant, and is equal along all directions. Sunlight, that passes through the Earth's atmosphere and falls onto the surface is called **total solar irradiance – solar constant  $G_s$** . The solar constant is „*the rate at which solar energy is incident on a surface normal to the Sun's rays at the outer edge of the atmosphere*” in [ $\text{W} \cdot \text{m}^{-2}$ ] [43] Due to the Earth's elliptical orbit, the solar constant will vary based on the time of year. The Earth is farthest from the Sun during the northern hemisphere's summer, and the minimum value of the solar constant is about  $1322 \text{ W} \cdot \text{m}^{-2}$ . When the Earth is closest to the Sun, during the northern hemisphere's winter, the solar constant is about  $1414 \text{ W} \cdot \text{m}^{-2}$  [21]. The value of the total solar irradiance can be used to estimate the effective surface temperature of the sun from the requirement that

$$(4 \cdot \pi \cdot L^2) \cdot G_s = (4 \cdot \pi \cdot r^2) \cdot \sigma \cdot T_{sun}^4 \quad (2.4)$$

where  $L$  [m] is the distance of the Earth from the Sun and  $r$  [m] is the radius of the Sun. Similarly, it is possible to estimate the effective surface temperature of other bodies.

Body in room temperature radiates with greater wavelengths than the radiation coming from the Sun. This allows for selection of surface finishes which have a low absorptivity in the short-wavelength part of the infrared spectrum, and a high emissivity in the long-wavelength part of the spectrum [21].

### 2.1.2. Albedo radiation

Albedo is a measure of the reflectivity of a body – of its surface. This is the ratio of the reflected electromagnetic radiation to the total incident radiation and is expressed as a percentage. In table 2.1 the albedo values of the planets of our solar system are given.

$$Albedo = \frac{\text{reflected electromagnetic radiation}}{\text{incident electromagnetic radiation}} [\%]$$

**Table 2.1:** Albedo of planets [3]

<b>Planet</b>	<b>Albedo</b>
Mercury	6 %
Venus	75 %
Earth	30 %
Mars	16 %
Jupiter	43 %
Saturn	61 %
Uranus	35 %
Neptune	51 %

### 2.1.3. Planetary radiation

Sunlight, that falls down on Earth or any other planet and at the same time isn't reflected, is absorbed and then radiated from the planet as IR energy. It is therefore the energy that anybody has received and then radiates part of it back into space. The intensity of energy emitted from the planets is given: [21]

- The local temperature of a given point on the planet
- The amount of cloud cover or atmospheric density

In general, however, the IR energy from planets is very small compared to, for example, albedo radiation. [21]

## 2.2. Convection

Heat transfer by convection takes place as the fluid moves and heat is exchanged. The flowing fluid transfers or removes heat from the surface of the surrounding bodies. Convection can occur not only between a liquid and a solid, but also between two gaseous or two liquid substances, or between a liquid and a gaseous substance. [43] From Newton's law of cooling, which says the temperature difference between the temperature of an object  $T$  [K] and the temperature of its surroundings  $T_\infty$  [K] decreases exponentially with time, an equation can be derived for the rate of convection heat transfer [43]

$$Q_v = h \cdot A \cdot (T - T_\infty) \quad (2.5)$$

where the rate of convection heat transfer is  $Q_v$  [W] and  $h$  [ $W \cdot m^{-2}$ ] is the convection heat transfer coefficient. Table 2.2 gives some examples of values of heat transfer coefficient. In satellite thermal analysis, convection will take place during ground operations, ascent, and through the use of thermal control measures such as heat pipes and pumped fluid loops [b].

*Table 2.2: Examples of heat transfer coefficient [43]*

Type of convection	<b>h</b>
	[ $W \cdot m^{-2}$ ]
Free convection of gases	2 – 25
Free convection of liquids	10 – 1000
Forced convection of gases	25 – 250
Forced convection of liquids	50 – 20 000
Boiling and condensation	2 500 – 100 000



## 2.3. Conduction

Heat conduction is a way of spreading heat in solid bodies whose different parts have different temperatures. Heat is also propagated by conduction in liquids and gases, where it also applies heat transfer by convection. Conduction is one of heat transfer, during which particles of the material with higher middle kinetic energy transfer part of their energy, through mutual collisions, to particles with lower middle kinetic energy [43]. Particles don't change their location though, but rather they oscillate around their equilibrium position.

If the heat flux is homogeneous and stable, the amount of heat that passes through the surface area in time  $t$  [s] to the depth  $d$  [m] can be written as

$$Q = \lambda \cdot A \cdot t \cdot \frac{\Delta T}{d} \text{ [J]} \quad (2.6)$$

where  $\lambda$  [ $\text{W} \cdot \text{m}^{-1} \cdot \text{K}^{-1}$ ] is the coefficient of thermal conductivity and  $\Delta T$  [K] is the temperature difference. In figure 2.3 are given examples of range of thermal conductivity of various materials at room temperature and in the table 2.3 are given examples of thermal conductivity of some materials.

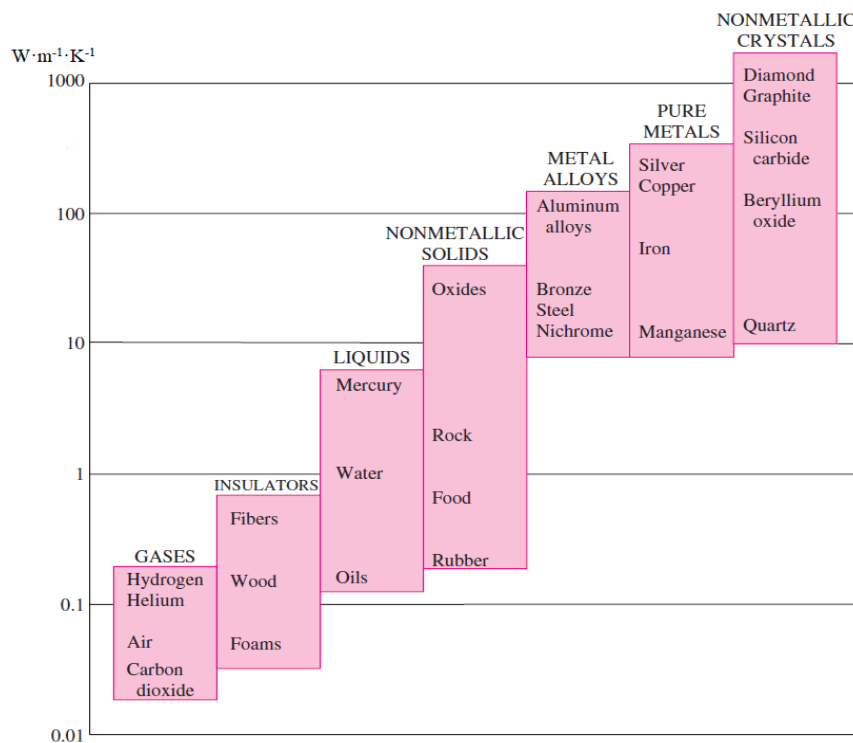


Figure 2.3: The range of thermal conductivity of various materials at room temperature [43]

Table 2.3: The thermal conductivities of some materials in 25 °C [43]

Material	$\lambda$
	[ $\text{W} \cdot \text{m}^{-1} \cdot \text{K}^{-1}$ ]
Diamond	2300
Silver	429
Copper	386
Gold	317
Aluminium	237
Iron	80
Human skin	0,37

The heat conduction rate determines the thermal conductivity. The thermal conductivity coefficient allows to compare substances according to their thermal conductivity. According to this coefficient, substances are divided into [21]

- thermal conductors - substances with a high rate of heat conduction and a large coefficient of thermal conductivity
- thermal insulators - substances with low heat transfer rate and low thermal conductivity coefficient

## **2.4. Combined Modes of Heat Transfer**

It is not possible, that in any body (solid matter) the three variants of heat transfer (radiation, convection and conduction) would exist at the same time. For semi-transparent solids, radiation and conduction heat transfer can occur, but radiation cannot occur with opaque solids. At the same time, in general, convection cannot occur in solids. [6]

### 3. Thermal control of satellites

In general, satellites and space vehicles are designed so that a compromise between stability, robustness and weight of the construction is maintained. This compromise must be maintained due to the parts of the flying phase that are most at risk. These parts are the start and the release into orbit and after that, for the space vehicles, the entry into the atmosphere of another planet and the landing. For these space devices, the weight question is asked to a greater extent, than it is in aviation. This is primarily due to economic reasons, where greater weight released into orbit is more expensive. Other reasons that must be taken into account for maintaining the compromise are individual influences that affect the satellites and space vehicles not only during the critical phases, but also during the fulfilment of predetermined missions.

The most important factors that affect the construction of these space devices during critical flight phases are overloading and vibrations. [21][36] These two factors place the greatest emphasis on the space vehicles construction itself, both in the terms of strength, but also in terms of a stable grip of all carried devices and all support systems that ensure the fulfilment of the planned mission. During the start and the release into orbit, but primarily during the entry into the atmosphere from orbit and landing even mechanical shocks are important. [21]

Beyond these critical phases, which place the greatest emphasis on the construction of the space vehicles, an essential phase of such space vehicle is the life phase, when it is fulfilling the predetermined mission. This is the longest part of its life. The main decisive factor in this phase are the thermal conditions and the total heat regulation. Satellites fulfilling missions around planets, not only around our Earth, and also satellites wandering through empty space must deal with effects, for example: [21][36][43]

- Effect of sunlight and solar winds
- Changes – temperature fluctuations (thermal cycles) due to the times when they are exposed to sunlight and when, on the contrary, they are not
- Orbital environment: atmosphere or space debris
- Aerodynamic heating

The system responsible with dealing with these effects is the thermal regulations system. This diploma thesis deals with this system. Other systems contained in satellites or in space vehicles also contribute to the need for thermal regulation, due to the fact that they need a small temperature range for proper function or that through their activity they affect other systems. For example: [24][37]

- Propulsion system
- Orientation and stabilization system
- Navigational system
- Thermal protection (partly falls under the thermal regulation system)
- Life support system – only in the case of space stations
- Batteries
- Other electrical equipment or working tools

The following chapters describe the method of thermal regulation of satellites and space vehicles, as well as inner structure of these space devices, which are needed for the design of MHS installation into the structure.

### 3.1. Heating and heat dissipation

Satellites and space vehicles must use specific techniques for thermal regulation and specific hardware devices to achieve correct functionality of all appliances and systems carried onboard. During the design of these devices is it necessary to adhere to the volumetric efficiency<sup>1</sup> and low weight.

For thermal regulation and the temperature management two basic approaches are used: passive and active temperature management. For most satellites, a combination of passive and active temperature management is used, even though the passive method predominates. These passive elements are then supplemented with active elements, so that the most effective and required reaction speed is reached.

The thermal requirements of devices and appliances onboard are main factors during the construction of the thermal regulation system. The goal of the thermal control system (TCS) is to keep all devices running in the permissible temperature range. All electronic devices onboard the space ship, such as cameras, data acquisition devices, batteries and others, have a fixed operating temperature range. Keeping these devices in their optimal operating temperature range is essential for every mission. Examples of temperature ranges include:

*Table 3.1: Examples of temperature ranges [24]*

Components	Temperature from	Temperature to
	°C	°C
Batteries	-5	20
Propulsion components	5	40
Cameras	-30	40
Infrared spectrometers	-40	60
Inactive structure	-100	100

Within TCS there are two types of thermal control methods. The first method is the active thermal control (ATC) and the second is passive thermal control (PTC). The main difference between these methods of thermal control is their function. The parts of ATC during the thermal control perform a specific mechanical movement and need to consume the supplied energy. Whereas PTC perform their function without mechanical movement and supplied energy consumption.

---

<sup>1</sup>Volumetric efficiency in relation to space equipment means efficient use of space based on required function of given device. [21]

### 3.1.1. Active thermal control

Especially with satellites, that perform their missions in outer space or with satellites, that orbit different planets, occur higher temperature fluctuations than they are able to resist. Even with their construction, heat shields, insulation or different surface finishes. Therefore some active parts for thermal control are sometimes required to protect components during cold conditions or to replace the heat that is lost when the electrical equipment is turned off. During ideal conditions the thermal regulation of satellites would be achieved through passive methods. However, since there exist specific devices that are sensitive to temperature, such as infrared sensors, these passive methods are not enough.

Active temperature regulation system uses mechanical or thermoelectric devices. These devices can use even movable parts and thus become less reliable. Active systems should then be used only when it is not possible to use only the passive systems. [22]

The most common part in spacecrafts in the active temperature regulation system is a so called Heater, figure 3.1. It consists of an electrical resistive part placed between two layers of flexible insulating material, such as Kapton or FEP Teflon qualified (NASA S-311-79) [14]. Heater can contain one or more circuits, depending whether redundancy is required.

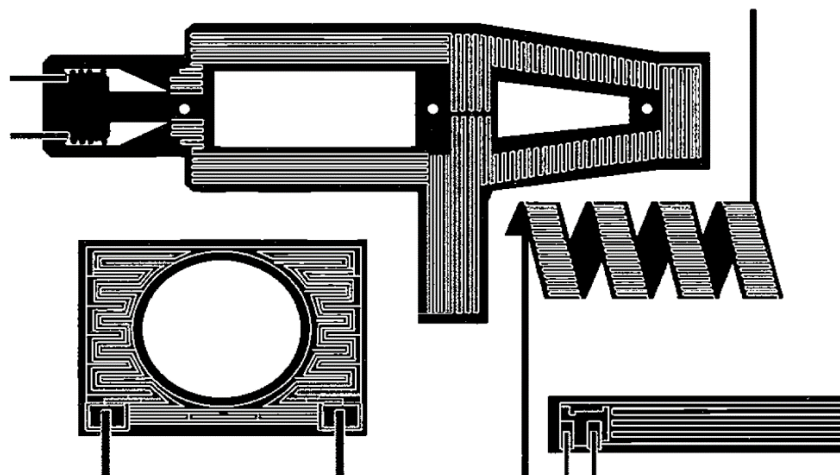


Figure 3.1: Heater [21]

Other parts of ATCS can be heat pipes or louvers – chapter 3.3.2.

Heat pipes can fall into both types of thermal control. Heat pipes use a closed two-phase flow fluid cycle with an evaporator and a condenser for the transportation of relatively large amount of heat from one place to another. They work on the principle of heated liquid evaporation at the place of the heat source and subsequent liquid condensation in condenser. [21] This cycle of evaporation and condensation is shown schematically in figure 3.2.

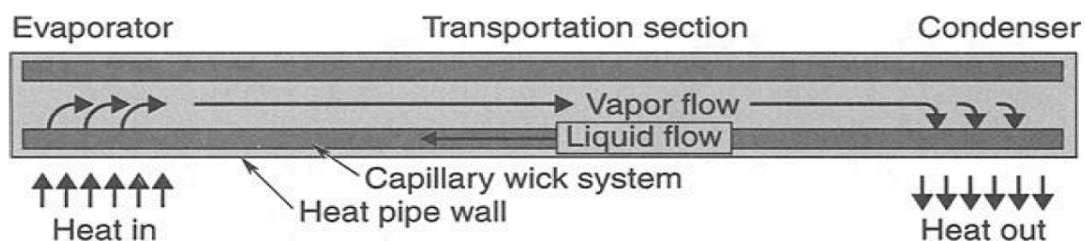


Figure 3.2: Heat-pipe schematic [21]

### 3.1.2. Passive thermal control

Unlike the active parts for thermal control in satellites, which are protected by different devices against very low temperatures, the passive parts for thermal control work differently. Their main goal is to protect devices from overheating, either through heat insulation from outer heat flow (such as the Sun or albedo radiation), or through correct heat dissipation from inner sources (such as heat emitted from an internal electrical device). Heat is dissipated from the inside of the satellite onto specific panels - Radiators, which are constructed so that the supplied heat was emitted to the greatest extent into outer space.

Passive thermal control system includes other parts, such as: [21][36]

- Multilayer insulation (MLI), which protects the cosmic ship from excessive solar or planetary heating as well as from excessive cooling from exposing to deep space
- Coatings, that change thermos-optic attributes of outer surfaces
- Thermal fillers for improving thermal bonds on selected interfaces (for example, thermal way between an electric device and its radiator)
- Thermal pads to decrease thermal bonds on selected interfaces
- Thermal doublers that spread on the radiator surfaces heat scattered by radiation
- PCM actuators, which are contained, for example in MHS

In the following chapters, the essential components involved in thermal regulation are described. The typical satellite construction is described as well as individual parts of TCS that are adapted to this construction. MHS technology is a part of the passive thermal control system (PTCS) and for this reason only parts of this system are described. However, one part from the active thermal control system (ATCS) is mentioned and that part is Louvers, because this part is most often used in combination with PTCS.

## 3.2. Supporting structure

The supporting structure is the most important part of each spacecraft. The structure provides a strong supporting framework to house payloads, instruments and satellite subsystems, especially through the stresses of launch. From shape to strength requirements of the supporting structure all other requirements are derived, for example: [6][21]

- Shape and likeness of the spacecrafts
- Carrying capacity – amount and weight of the carried payload
- Propulsion system – types and placement
- Mounting options and fixation options of all inner equipment as well as outdoor equipment that protect the spacecraft from various external influences

On a general scale the structure has to be light enough to be launched while also being strong and stiff enough to support the payload and endure launch loads without bending or breaking.

Any structural distortion could impact the operations of telescopes, imagers or antennas precisely mounted on the satellite.

The typical supporting structure that is used on the satellites in orbit of Earth or other planets and in landers that land on Mars for example has the same foundation for every spacecraft. Such a foundation is based on one or many smaller inner beams, where individual boards are mounted - baseplates, which can carry devices or separate individual parts of the spacecraft. An example can be the inner structure on the figure 3.3 from the International Ultraviolet Explorer (IUE).

Landers, which can land on Mars for example, are handled in a remarkably similar way. As an example, in figure 3.4, the structure of the InSight lander that landed on Mars is shown. In this case however, the central beam is missing. The desk, on which all the devices are mounted (Component deck), is a part of the supporting structure that provides support on the surface of Mars. The load-bearing structure consists of a beam structure, which includes the support legs of the lander. [23]

When considering the use of materials for such supporting structures, it is possible to proceed from the basic and typical requirements:

- Sufficient strength
- Low weight
- Required thermal conductivity

In some cases, there is a requirement for the supporting structure to partially participate on heat dissipation from equipment. However, this is not a rule. [21] [37]

Based on these requirements, such materials are chosen for the supporting structure, the most typical representatives of which can be found in the literature [8]. They are largely metallic materials, but in special cases and based on specific requirements composite materials can also appear. Most often aluminium-titanium alloys are used, such as:

- Al – Cu
- Al – Mg – Si
- Ti – Al – Sn
- Ti – Al – V

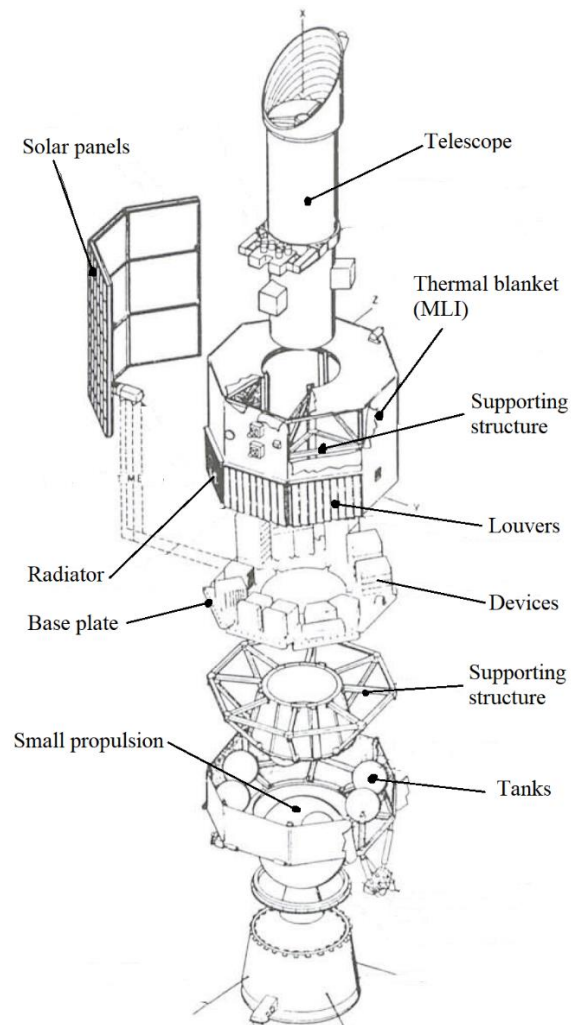


Figure 3.3: Structure of IUE [16]

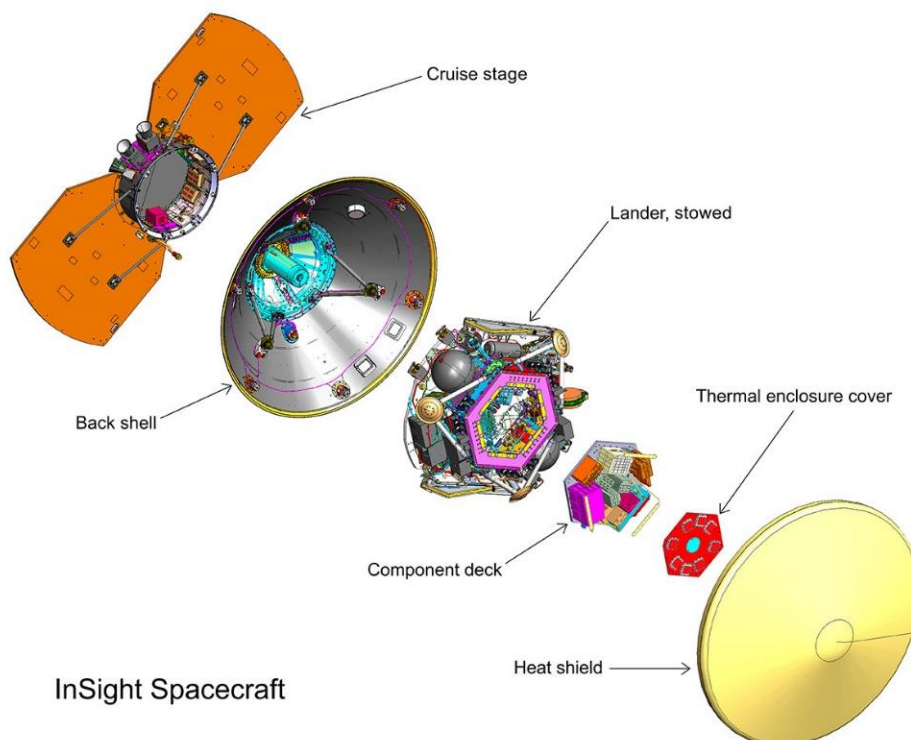


Figure 3.4: Structure of InSight [23]



### **3.3. Arrangement of elements for heat dissipation**

All spacecrafts carrying out their missions in Earth's orbit or other planets optionally moons or fulfil their mission somewhere else in our Solar system carry on board different measurement and detection devices. All this equipment requires, for their functionality, a source of electricity, electrical wiring and other components that generate heat through their service, which is required to be taken away to ensure safe, reliable and effective operation. Due to the possibilities of fast heat dissipation and at the same time of the shortest path, that the heat must travel are these devices, that generate heat, placed at the edge of spacecraft as much as possible. Respectively they are placed closer to parts, such as a radiator, which performs the dissipation of excessive heat into outer space through radiation. This radiator is closely described in the next chapter. This position is important to avoid these mentioned requirements:

- Fast heat dissipation
- Short thermal way

If these problems would not be avoided, radiation or heat conduction to other devices could happen. In satellites with a cylindrical, octagonal or other body it is easy to distribute these devices around the satellite perimeter so that they would be located as close as possible to the radiators. In satellites or space vehicles with an irregular body and baseplate this distribution is more difficult.

Within PTCS, all necessary parts that participate in the heat regulation of devices, can be: [6]

- Insulations
- Tapes
- Sunshields
- Radiators
- Heat-pipes
- Heat switches including PCM materials
- Multilayer Insulation
- Surface finishes

As an addition to PTCS, one part from ATCS is used very regularly - Louvers. However, it is not necessary to use all parts at once. Usually, only a specific combination of these parts is used. In the following chapters, the most important parts are described, which are a part of the assumed thermal way for this Master thesis, which is described in chapter 3.5.

### 3.3.1. Radiator

The radiator is a component located on the end of the thermal way, where the heat is taken away from the devices onto the radiator surface and after that the heat is emitted to the greatest extent into space outside of the spacecraft. Regardless of the radiator configuration, whether it is a simple and basic flat board panel on the external side of the satellite, or it is a panel, that is not a part of the construction (Deployable Radiators), radiators dissipate heat from their surface through IR (infrared) radiation. The radiating power of radiators depends on the surface emissivity and temperature of the radiators. The radiator must dissipate waste heat from the cosmic ship as well as all the heat and radiation, that falls on it from the vicinity or other surfaces of the spacecraft. Most of the spacecraft's radiators rejects between 100 and 350 W internally generated waste heat from Electronics per square meter. The upper end of this range is typical for a radiator that runs at a relatively high temperature (around 40 ° C) and receives a small amount of heat from the vicinity or other surfaces of the spacecrafts. The lower end of this range can represent a radiator running below room temperature on the lower Earth's orbit. Higher emissivity and low radiation absorption is achieved through a special surface modification. Among typical surface modifications, that are described in chapter 3.4, include quartz mirrors, silver-plated or aluminized teflons and white color. [12][21]

Depending on how the heat is transferred from the source to the radiating surfaces, radiators can be classified as follows:

**Table 3.1:** Types of radiators [12]

TYPE	CONNECTION TO THE HEAT SOURCE
Passive Radiators	Direct
	By means of Heat Pipes
	By means of Phase-Change Materials (PCM)
Active Radiators	By means of Fluid Loops
	By means of Fluid Loops plus Heat Pipes

For the purpose of this Master thesis, passive radiators with phase change materials are substantial. In these systems is the heat transfer to the radiator controlled through PCM, which melts during periods of high heat dissipation and solidifies again as the temperature drops.

The radiator itself is in its simplest form a flat, usually aluminium, board with the structure similar to the composition of composite materials. In this case, honeycomb core and thin boards that surround the core are made from aluminium. These faceplates don't have to be made exclusively from aluminium, but other metals with good thermal conductivity can be used. The purpose of a metal core and faceplates is that the radiator can also partially function as a construction panel. In such a case, its weight is a part of the supporting structure of the spacecraft. Disadvantage of such an adaptation can be that a small portion of heat transferred from the spacecraft interior to the radiator can be returned back through the faceplates. In figure 3.5 a Body-Mounted radiator can be seen that is connected through screws to the construction (isn't part of the spacecraft construction). Batteries are assigned to the radiator as an example of a possible arrangement. To prevent the mentioned backward heat transfer from the radiator to the construction itself, different surface adjustments are applied and very thin foil is used (in

millimetres) from teflon for example. [21] Such methods are used in all possible forms of a radiator.

The position of the radiator on the satellite or space vehicle is already obvious from its function. For satellites orbiting, the most suitable placement is the side facing the planet, since in such a case a minimum of radiation falls on the radiator. The other option is the case, in which Louvers are used in front of the radiators. Louvers are described in the next chapter. Thanks to their function, the radiator can be placed anywhere on the spacecraft, where it does not influence other parts of the spacecraft with the radiated heat and thus resisting the radiation from the Sun.

Generally, radiators have some pros and cons: [12]

Pros:

- They are simple and light
- Practically indefinite service life
- Operation of devices not restricted
- Power supply is not required

Cons:

- Limited heat capacity
- Require correct placement on the spacecraft
- Prone to contamination by out gassing

For the design of the radiators and the possibility of connecting a thermal way to it, there are some construction rules, which specify certain parameters: [12] [21]

- o Maximum permissible power of the cabinet with electronics per square centimetre
- o Maximum overall performance
- o Thermal conductivity of the radiator
- o Sense of incorporation of radiators into the spacecraft

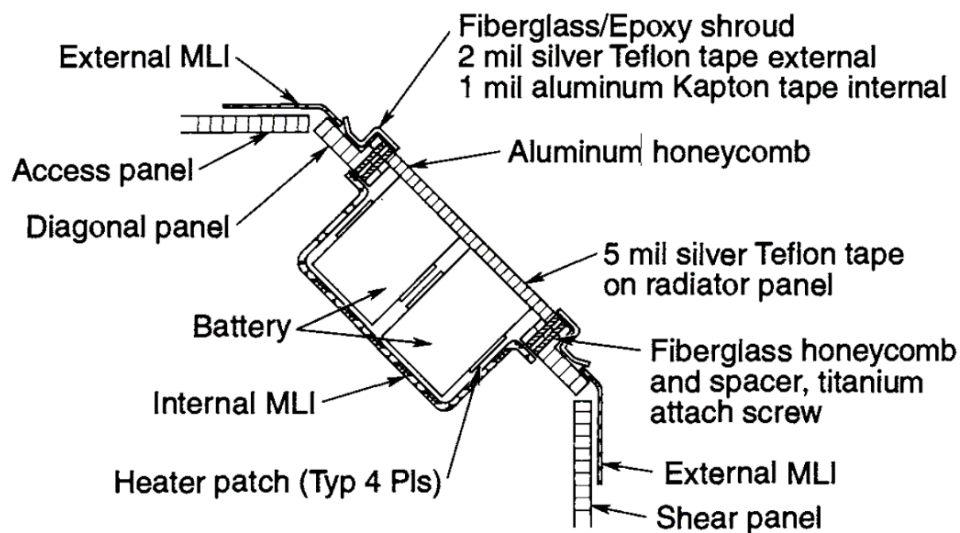


Figure 3.5: Radiator [21]

### 3.3.2. Louvers

Louvers are active thermoregulation parts, which are used in different forms on many spacecrafts. It is a controlled movable element, which is able during its activation almost completely impede incoming radiation from the vicinity. Their functionality is completely identical as with ordinary louvers on every window in apartments. In general, a louver in its fully open state<sup>1</sup> can reject six times as much heat as it does in its fully closed state<sup>1</sup> [15] Louvers find application nearly everywhere, where a cyclic change of incoming radiation occurs. While most commonly placed over external radiators, louvers may also be used to modulate heat transfer between internal spacecraft surfaces, or from internal surfaces directly to space through openings in the spacecraft wall. [21]

Louvers consist of five main components: [15]

- Base frame
- blades
- Action elements
- Radiation sensors
- Construction elements

In figure 3.6 a typical louver is showcased mounted via a radiator. Louvers can be controlled through different controlling units – Action elements. These controlling units move the blades based on the perceived radiation from the sensors and also based on the incoming heat from the radiators. The most commonly used louver assembly is the bimetallic, spring-actuated, rectangular-blade (venetian-blind) type. Other used types of controlling units are Bourdon spirals<sup>2</sup> and electrical devices. In figure 3.7 is this mechanism illustrated. The whole system of opening and closing can be theoretically prone to loss of reliability. This can be eliminated through the implementation of Action elements for every blade individually, not one or two Action elements for all blades. In the case of one controlling unit failing, all blades will not be lost.

The material, from which louvers are made in most cases, is aluminium. It is used to make the frame as well as the blades. However, a higher polishing rate is required to achieve low emissivity and anodized on the interior side [37]. Louvers are connected to the spacecraft construction through screws in the frame.

Thanks to the full automation of the whole system, louvers are able to maintain very small temperature range and balance all changes of incoming and outgoing radiation.

---

<sup>1</sup>The main reason for using louvers is the prevention of receiving radiation from the vicinity. For this reason, the state is open when all louvers are retracted and refuse incoming radiation, and the state is closed, when the louvers are pulled out.

<sup>2</sup>Bourdon spiral is a deformation element that can be curled into an oval profile, spiral or a helix. Typical use is in tubular pressure gauges.

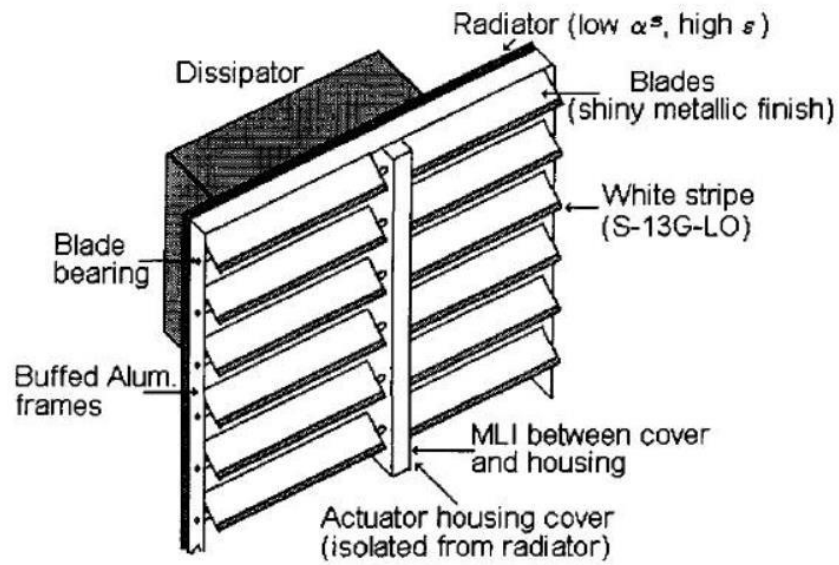


Figure 3.6: Louvers [37]

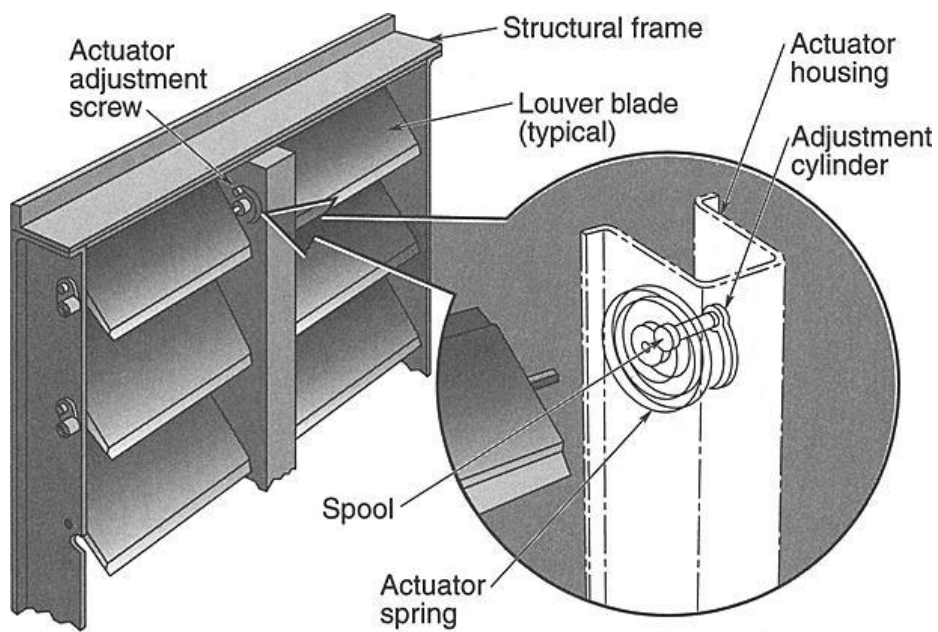


Figure 3.7: Detail of control element [21]

### 3.4. Insulations and surface coating

#### 3.4.1. Thermal surface finishes

For materials that are used for the creation of satellite parts, there is an effort to influence their heat absorption. For the outer side of the satellite, the effort is in limiting the absorption and for the inner side in improving the heat transfer from sources to the satellite walls, where this heat can dissipate. [21] For this reason, since the launch of the first satellite into orbit, there is an effort to develop such a surface finish (optionally an insulating material) that will have the required attributes for the purpose of thermal regulation. These coating materials have evolved to the point, where reasonably stable coatings are available, that give any desired value of the hemispherical total emittance  $\epsilon$  between 0,1 and 0,9 for any desired value of the solar absorbtance. [9] For these coatings to be capable of this, there is a number of different types of coating that are wavelength-dependent. In figure 3.8 used materials and insulation systems are shown. At the same time, figure 3.8 showcases the comparison of coefficient  $k_{eff}$  of thermal conductivity with other used materials.

Thermal control coatings are typically classified as: [6]

1. Solar reflectors
2. Flat coatings
3. Solar absorbers

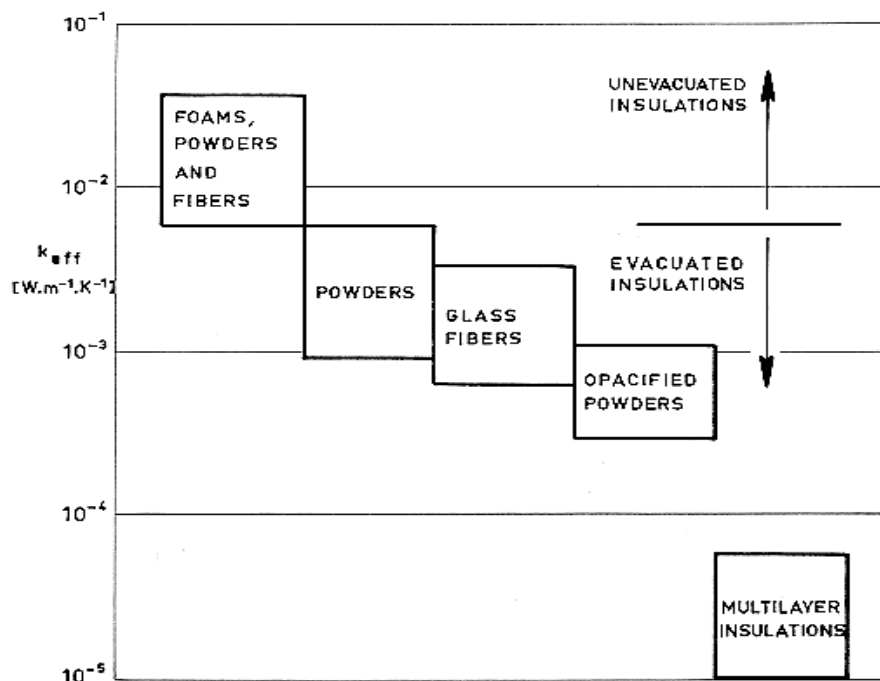


Figure 3.8: Effective thermal conductivity of MLI as compared with other insulation materials

Solar reflectors have a low solar absorptivity and a high emissivity, which makes them useful in solar and albedo environments. Flat coatings reflect and absorb almost equally, and are frequently used inside of satellite enclosures to enhance radiant heat sharing. Solar absorbers have a high solar absorptivity and a low emissivity, making them nonideal for satellite surfaces.

Solar absorbers are also sometimes used with other coatings in combination patterns to tailor surface properties. [6] [37]

The main exterior surface finishes that commonly appear on many spacecrafts are outer layer of isolating blankets, cooler coatings and color (especially white or silvered). On the other hand, the interior of the spacecraft has a tendency that every electronic box and other components together with construction panels are usually painted and treated to achieve the highest possible emissivity. Naturally, components that are sensitive to heat, that do not disperse a great amount of heat, such as fuel lines or tanks, are treated with an appropriate surface treatment based on aluminium or gold. [21]

The outer-cover layer of insulation blankets is usually made of aluminized Kapton, black Kapton, or Beta cloth. Aluminized Kapton is a gold-coloured material that has a moderate solar absorptance, a high IR emittance, and a typical thickness of 0,025 to 0,076 mm. Black Kapton has a high solar absorptance because it is loaded with carbon to improve electrical conductivity for blanket-grounding purposes. Beta cloth is a very tough Teflon-coated glass fabric that has a low solar absorptance and high emittance.

Much of the different types of surface finishes and their optical attributes are listed in literature [9] [21]. Here, through figure 3.9, only the attribute range that is available for different types of materials is listed.

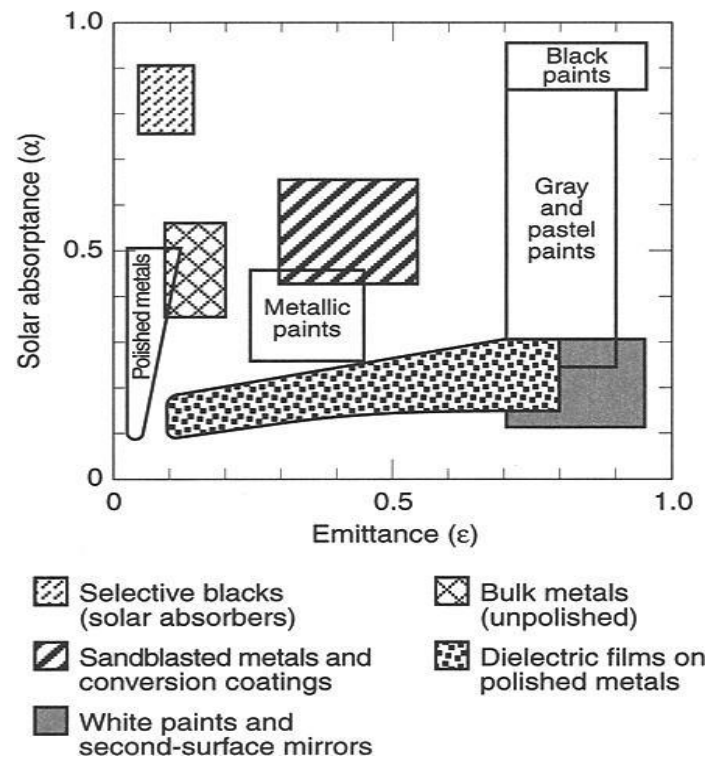


Figure 3.9: Surface properties by type of finish [21]

The basic requirement for a coating to be used in spacecraft is long-term space stability for periods of months and even of years. This objective, however, has not yet been achieved in many instances. The problem of selecting the specific coating is somewhat circumvented by the use of mosaics or coating patterns, normally combining white and black paints. [9]

### 3.4.2. Insulations

The main reason for using insulation systems is the minimalization of heat exchange, either from the point of view of conduction, so from radiation. Thermal insulation acts as a barrier against radiation and prevents dissipation of excess heat. For these insulation systems for usage in space, these materials are used primarily:

- Foams
- Fibrous insulations
- Single-layer radiation barriers
- Multilayer insulation (MLI)

Foams are primarily used for encasement of different components or in combination with other insulations. Their advantage is also a small disadvantage. They are largely formed by air. The disadvantage is that in the moment of entering a vacuum space, it changes its volume. The advantage however, is that by removing air they have a lower thermal conductivity and thus better insulate. [10]

The usage of fibrous insulations is preferred primarily, where a high temperature increase can occur, or there is a risk of fire. Also, they are often used as spacers for multilayered insulation. Their application is largely reserved for external use. [10] To give an idea of thermal conductivity of different materials of fibrous insulations a graph is given here in figure 3.10. This is a dependency of thermal conductivity on temperature.

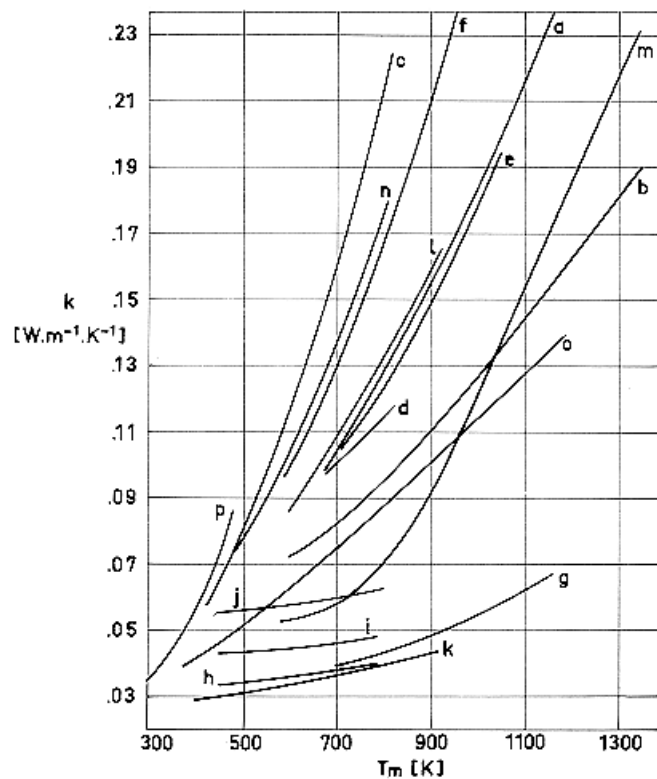


**Figure 3.10:** Thermal conductivity vs. mean temperature for several fibrous insulations [10]



**Table 3.2:** Explanations for the graph [10]

Key	Insulation	$\rho$ [kg.m <sup>-3</sup> ]	Key	Insulation	$\rho$ [kg.m <sup>-3</sup> ]	Key	Insulation	$\rho$ [kg.m <sup>-3</sup> ]
a	Fiberfrax Lo-Con	96	g	Min-K 2000	320	l	Micro-Quartz	48
b	Fiberfrax Paper	192	h	Min-K 2000	400	m	Dyna-Quartz	155
c	Kaowool bulk	48	i	Min-K 2000	480	n	Thermoflex	48
d	Kaowool bulk	160	j	Min-K 2000	561	O	Thermoflex	384
e	Refrasil Batt A-100	56	k	Min-K 1301	320	P	Micro-lite AA	24
f	Refrasil Batt B-100	48						

MLI blankets are the most common insulation. Most today spacecrafts are covered with MLI, with cut-outs provided for areas where radiators reject internally generated waste heat. MLI blankets are also typically used to protect internal propellant tanks, propellant lines, and solid rocket motors. Instead of MLI, single-layer radiation barriers are used in some cases. The case being, when lower level of insulation is required, as the single-layer radiation barriers are lighter and cheaper. [21] The outer cover can be made from Teflon, aluminized Kapton, black Kapton, or Beta cloth, which is a Teflon coated glass fabric.

MLI is composed of multiple layers of low-emittance films. The simplest composition of MLI is a layered blanket assembled from thin, 0,25 mm thick, embossed Mylar sheets, each with a vacuum-deposited aluminium finish on one side. Figure 3.11 showcases the composition of MLI. As a result of the embossing, the sheets touch at only a few points, and conductive thermal ways between layers are thus minimized. A more complex and higher performance construction is composed of Mylar film metalized (with aluminium or gold) on both surfaces with silk or Dacron net as the low-conductance spacers.

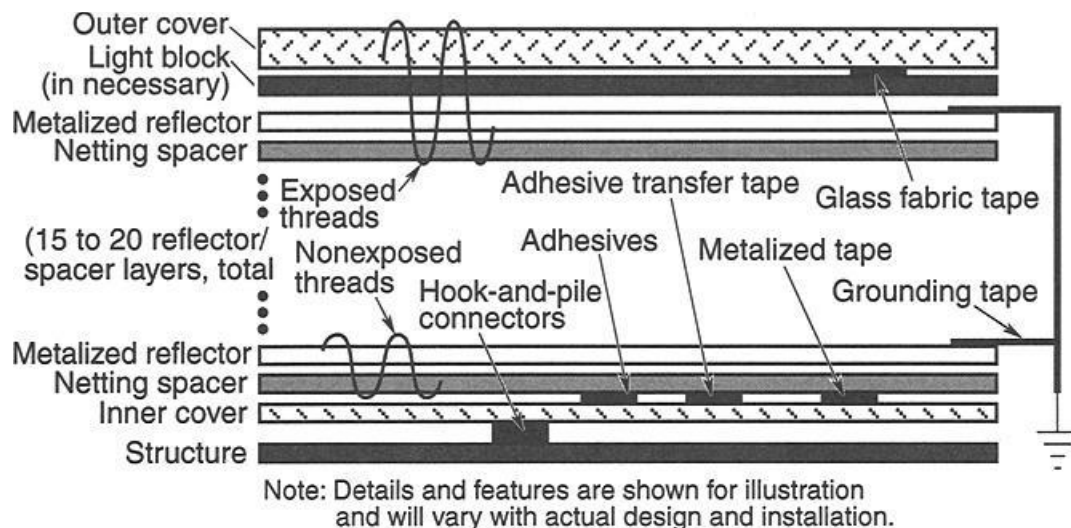


**Figure 3.11:** Composition of a typical MLI blanket [21]

Heat transfer through MLI is a combination of radiation and solid conduction. These forms of heat transfer are minimized in different ways. Radiative heat transfer is minimized by interposing as many enclosing reflective surfaces (metalized sheets) as is practical between the object being insulated and its surroundings. Solid-conduction heat transfer is minimized by

keeping the density of the low-conductance spacers between the reflective surfaces as low as possible and making the blanket "fluffy" to minimize contact between layers. [21] [37]

MLI insulation and their configurations are usually attached to spacecrafts by bonding or with velcro strips. As it can be seen in figure 3.11 grounding strips are incorporated into MLI insulation due to the discharge of electric charge. The space between layers is evacuated to decrease gas conduction. For space applications, proper venting of the insulation inner space should be provided to avoid undue pressure loads on the shields during ascent flight, to achieve an effective depressurization during re-entry. [10] Coefficient  $k_{eff}$ , which is listed in figure 3.8, is used to describe the transfer of heat through MLI, because they are composed of multiple layers with different thermal conductivity. [21] [10] At the same time, it is necessary to add that thermal conductivity of MLI insulation is dependent on the pressure of the surrounding atmosphere. This needs to be taken into consideration for missions that include landing and movement on the planets, such as Mars, or for atmospheric probes. As an example a graph is given, figure 3.12, that showcases the dependence of thermal conductivity of some MLI on pressure.

Other examples and especially different parameters of MLI insulations can be found in before mentioned literature [10] [21] [37].

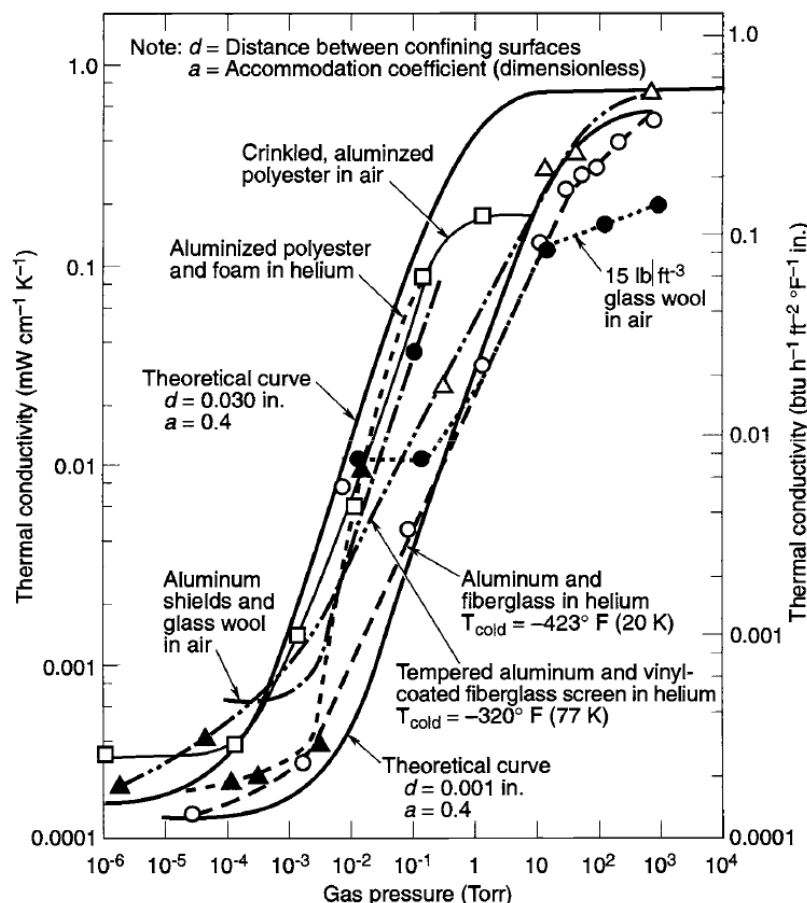


Figure 3.12: Effect of gas pressure on thermal conductivity [21]

As it was mentioned at the beginning of this chapter, MLI insulation represents with its attributes a very good option of usage as an isolation of conduction. For this reason, it is possible to consider their application and use for concepts of MHS installation in satellite construction.

### 3.5. Thermal way

In most cases, electrical and other units are designed so that thermal energy is transferred to the base plate. This heat is then transferred through conduction into the supporting part of the cosmic ship structure and from there, through different methods and paths, into the surrounding area of the spacecraft. Lower number of units is partially (sometimes for the most part) cooled by radiation. Such units are designed so that heat could be radiated from specific surface areas, except the mounting surface, into the surrounding space of the spacecraft or directly into space. This way isn't used so much and the effort is to insulate electronic components and heat conductors as much as possible in such a way, where heat transfer will be achieved only through conduction. This is achieved by low emissivity finishes and cable wraps.

If the heat dissipation from the devices is routed through the structure, the temperature rise should be small. This requirement is important, because every device inside the spacecraft is exposed to this temperature rise. Most of the cabinets for electronics, figure 3.13, of spacecrafts has a base of size from 100 x 150 mm to 450 x 600 mm, with performance levels sometimes exceeding 1 000 W. Not every electronic device is closed into a box. There are many components and devices that are directly connected to the baseplate. [21]

In the case, that electronic or other components, that generate heat, are closed in cabinets or boxes, then these boxes are attached on the baseplate through screws. If the electronic cabinets are made of „plates“ or modules, figure 3.14, then the screws are arranged along 2 opposite sides of the base plate.

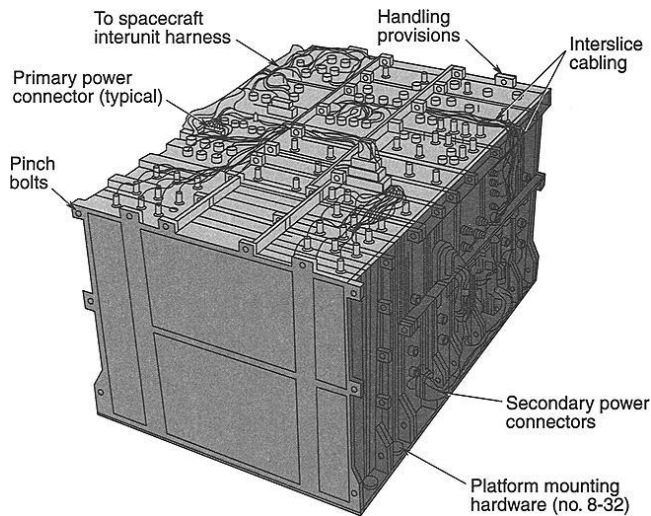


Figure 3.13: Electronic box [21]

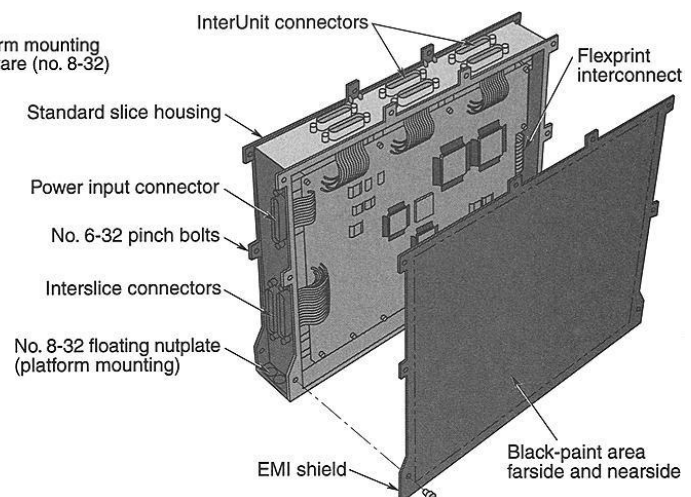


Figure 3.14: Electronic box built up from modules [21]

Flange mounting is advantageous, because it allows the bolts to be accessible and thus allows torque to be applied from above.

According to different tendencies from NASA or from ESA, there is an attempt to limit the transfer and conduction of heat through the supporting structure. It is due to already mentioned reasons, as on the baseplate and supporting structure are also different devices attached, where heat is transferred from one device to another through conduction. This way, the heat dissipation from all devices is less effective. Such a problem can be completely eliminated by using the project MHS from ESA for example. MHS can be used for thermal ways with wires of solid conductivity. Another option is a thermal way with wires of variable conductivity such as Heat-pipes (more detailed description can be found in literature [11][21][37]). As it was mentioned before in previous chapters, this MHS should serve as a switching component in a created thermal way that goes off the baseplate and supporting structure. This heat path is led directly from the heat source through MHS to the radiation plate and this can be realized in two ways.

The first, the easiest option, is to lead the thermal way through the MHS. This means that the heat source (device, component or electronic box) is so close to the radiator, that it is possible to put only the MHS between the heat source and the radiator. The heat is thus directly led from the source through the MHS to the radiation plate.

The second option is in the case of the heat source not being in such proximity and it is required to transfer heat at a greater distance. In order to realize such a path, a special conductive component with solid conductivity is required, which will ensure the heat transfer from the source to the radiation plate. This special component could be a thermally conductive component that has two ends for gripping and between these ends is located a flexible conductive structure. In figure 3.15 a copper component is shown, from the catalog of the company TAI [1], which is able to ensure heat transfer in this required way. The material, from which the flexible structure is made, doesn't have to be only copper, or copper fibres. Other alternatives are graphite fibres or graphene foil.

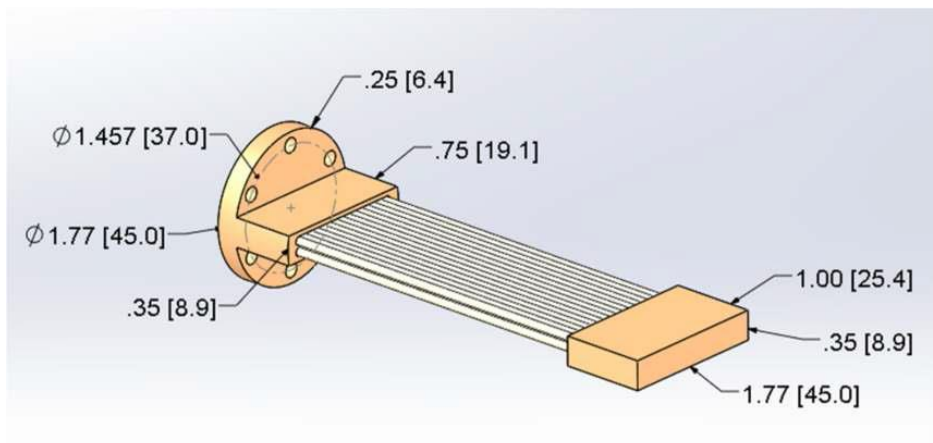


**Figure 3.15:** Thermally conductive component from the company TAI [1]

### 3.6. Fastening

Both types of anticipated thermal ways from the previous chapter always end on the radiation plate. That means, that the construction for MHS or the very MHS needs to be firmly connected to the radiation plate. It is impossible to drill a classic thread for a screw into the radiation plate, as it is created from honeycomb-sandwich structures and another solution is therefore needed. The main reason is the structure of honeycomb core itself as well as the load transfer. The load must be established into both surface panels and the honeycomb cannot resist the local pressure. [35] The best option today are inserts, thanks to which it is possible to establish a screw connection into the honeycomb sandwich structure. Their applications are given by prescribed standards. ESA released, as a guide for their use, the document *Insert design handbook*. [17]

An insert is part of a detachable fixation device, which enables the interconnection of honeycomb-sandwich structures or enables fixed connection between such structures and other structural parts, e.g. frames, profiles, brackets or mounting of equipment, e.g. boxes, feed lines, cable ducts. The material used for the created inserts can be aluminium, titanium or steel. The most used type are inserts potted by means of curing epoxy resin. A basic shape of a normal potted insert, incorporated in honeycomb-sandwich structures by potting is shown in figure 3.16 and in the figure 3.17 a cut through a classic insert from the *Wilhelm Böllhoff GmbH & Co. KG* is shown.

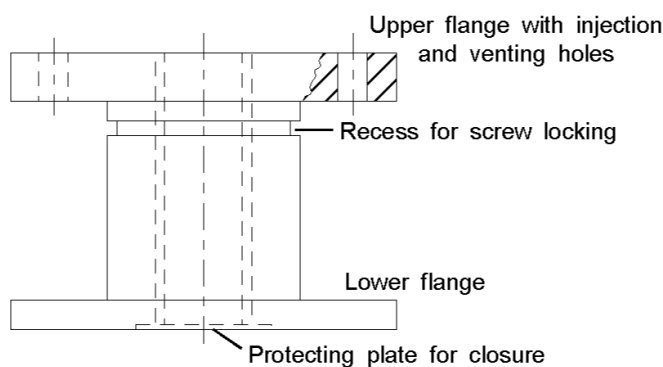


**Figure 3.16:** Typical Insert [17]



**Figure 3.17:** Typical basic Insert [42]

There are three basic options of insert usage: partially potted, fully potted, and through the thickness, figure 3.18. In figure 3.19 a real insert in the honeycomb sandwich structure panel is shown.

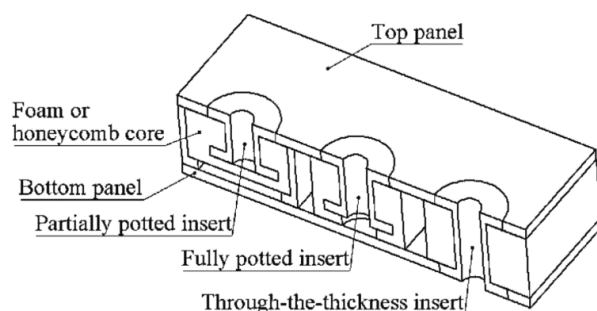


**Figure 3.18:** Three types of insert assembly [35]

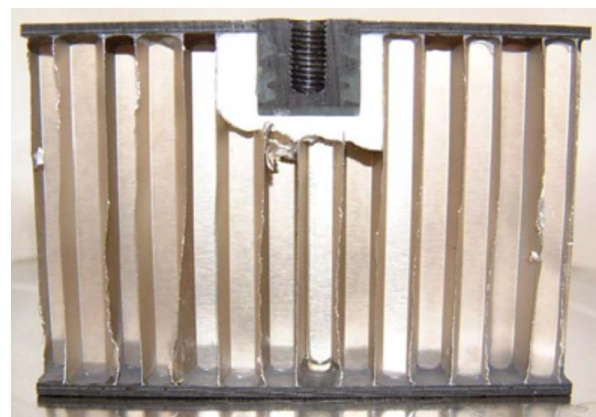


**Figure 3.19:** Partially potted insert [19]

In case the MHS could not be attached through screws and inserts into the radiation plate, there is another option. This option is by using a so called flange, figure 3.20. This flange would be set into the satellite wall, for example from a carbon composite and bolted to it. After that, the MHS would be bolted to the flange. In this case, the radiation plate would be suspended in front of this wall.

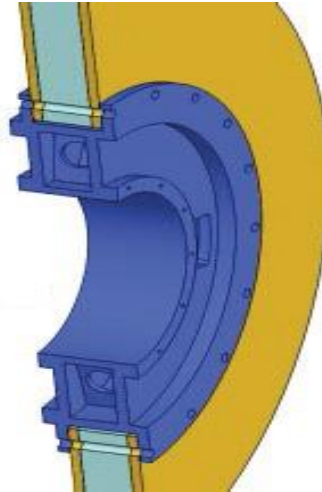


*Figure 3.20: Cut of insert [35]*

### 3.7. Prerequisites for construction of MHS

Based on the MHS function, when it is capable thanks to PCM materials, purely automatically only based on the current temperature, to regulate the heat transfer through conduction from different devices, it is possible to create basic assumptions for the concept design of the MHS development. Previous chapters show that the MHS as a switching component falling into the category of passive heat regulation, must be included into the thermal way, which requires at the moment of need a fast transfer of heat and at the same time energy savings at lower power.

One of the prerequisites for the specific construction is the fact that it has to allow the MHS to fulfil its function and not to limit it in any way and not to reduce its effectiveness. If heat is transferred to the MHS through conduction, for example by using a conductive component from figure 3.14, the construction must secure that the heat will be forwarded to the MHS to the maximum extent. This may result in another prerequisite for the construction. Due to the functionality testing of MHS in the Institute of aerospace engineering laboratories it was discovered, that during the state ON there is a slight deflection of its part (Baseplate and Contactplate), by using such a conductive component that has to transfer and forward the heat to MHS, then the contact area between these components will be reduced and deformed. The construction can theoretically help eliminate this problem. Another important prerequisite is to limit the return – back circulation – of heat back through the thermal way or in any other way. The flowing heat in state ON traveling through MHS to the radiator can never under any circumstances return back, otherwise the whole heat dissipation would be meaningless. Similarly, this applies also in the state OFF. Here, on the contrary, it is important that the construction, when the thermal way is closed off, will not transfer heat as if it would form a conductive component. For this reason, MLI insulations, mentioned in the chapter 3.4.2, are very useful and other solid insulations, such as Teflon.

For the MHS to be a part of the thermal way, it must be through its construction firmly and reliably connected to the construction of the spacecraft. The specific method of construction will be based on the requirements of MHS location on the spacecraft in general, as well as from the requirements of location within the thermal way. From the chapters 3.2 and 3.3 and subsequently from a possible request it may result that the MHS must be placed in a variety of positions within the interior of the spacecraft. Another prerequisite of the MHS construction is its versatility. Finally, a prerequisite for such a construction is the general rule that applies in aviation and cosmonautics, where it applies even more strictly. This rule is to achieve the lowest possible ratio of fulfilment of the required function of any component depending on its weight. From a design point of view, this rule is most applicable to the strength-to-weight ratio of a given component. This is mainly for economic reasons. In aviation and aerospace, every gram of construction affects fuel consumption. Whether it is long and multiple flights of aircraft, or launching into orbit and other manipulations in space. According to NASA [44] and ULA [40], the approximate prices per 1 kg per LEO in 2017 were given, as shown in Table 3.4, on the examples of rockets:

*Table 3.4: Price for 1 kg launched into LEO*

<b>Space rocket</b>	<b>Price in \$ for 1 kg</b>
Atlas V	12 000 – 21 000
Delta IV Heavy	13 000 – 17 000
Falcon 9	3 000 – 5 000
Falcon Heavy	~ 1 500

## 4. Thermal switch installation design

Miniaturized heat switch is a component, as it was mentioned in previous chapters that allows the regulation of excessive heat dissipation through conduction and with this regulation save energy. In order for the MHS to function, it is necessary that it is a part of a complex thermal way. For the correct functionality of the thermal way and specifically of the MHS, its fixed position must be secured in the satellite. The MHS structure serves this purpose.

Because, within the thermal way itself, there exist many options of the MHS position, it is necessary, for the creation of one or more concepts, to define its specific position. From a survey of literature dealing with the problem of solving thermal regulation of satellites or space vehicles and from the construction and form of the MHS it follows, that the most appropriate and efficient location of the MHS is at the very end of the thermal way. And in such a way, that its top side, the coldplate is in direct contact with the radiation plate. Thus, more efficient heat dissipation with lower losses is achieved. Based on the existence of multiple thermal ways and multiple options of mounting the MHS structure, it is possible to construct multiple variants – configurations of the entire heating system. These variants are shown in the simple diagrams below.

Diagram legends:

1. Heat source
2. Flexible conductive component
3. MHS
4. MHS structure
5. Radiation plate
6. Board – satellite wall
7. Insert
8. Flange

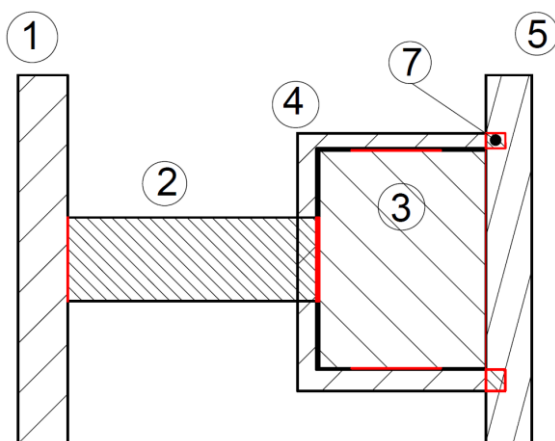


Figure 4.1: The first system diagram (platform 1)

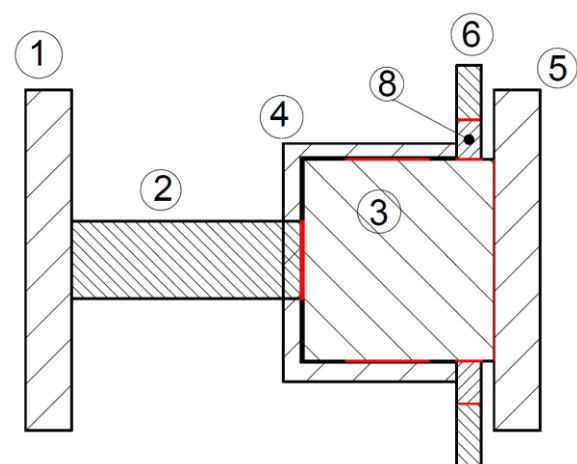
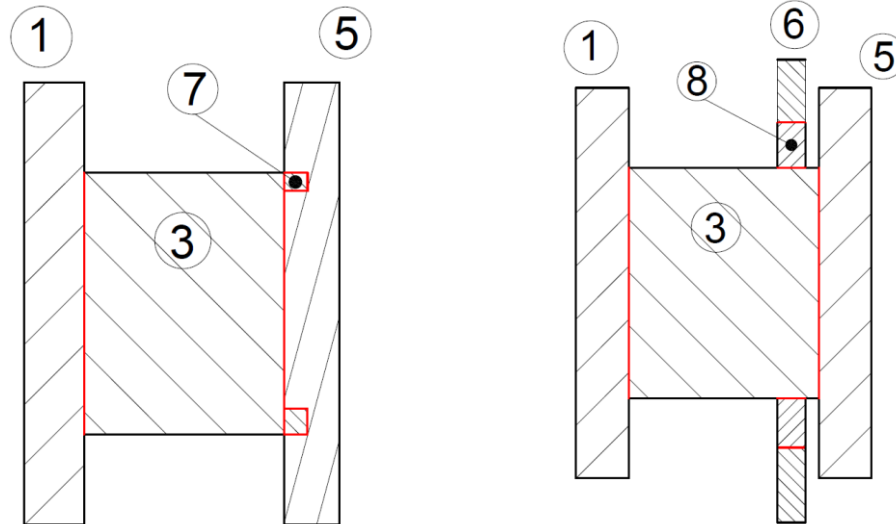


Figure 4.2: The second system diagram (platform 1)





**Figure 4.3:** The third system diagram (platform 2)    **Figure 4.4:** The fourth system diagram (platform 2)

The red color in diagrams showcases the contact surfaces of the individual components in a simplified manner.

When considering the time consumption of processing all possible usage variants of individual components, only a few are processed in this Master thesis. Specifically, only those variants with used inserts as a method of attachment. Both types of thermal ways are represented at least by one concept – two base platforms. From which of the first type of the thermal way, where the heat transfer occurs from the heat source through a conductive component and the MHS into the radiation plate, two modifications are also created in this thesis.

**Table 4.1:** List of concepts

	<b>Platform 1</b> (figure 4.1 and 4.2)	<b>Platform 2</b> (figure 4.3 and 4.4)
<b>Model</b>	Concept A	Concept D
<b>Modification 1</b>	Concept B	
<b>Modification 2</b>	Concept C	

## 4.1. Requirements for conceptual designs

Within the design requirements, similar assumptions apply to both types of MHS installations:

- Securing the position (mutual arrangement) of individual components – primarily a requirement for structures with a flexible conductive component. It is necessary, that the individual components follow each other correctly.
- Securing static fixation of all components inside the spacecraft – the structure must ensure, that during various manoeuvres of the spacecraft the thermal way will stay functional
- No spontaneous or easy loss of fixation
- Sufficient strength, firmness and stability of the structure must be secured – the structure must be able to manage required force and moment stresses so that the heat dissipation function is always ensured. This can be achieved through optimization during development.
- Minimal weight – generally important requirement in aerospace and aviation
- Easy installation – both the individual components into the structure and the structure itself into the spacecraft interior. In case of placing the structure into the spacecraft and in that regard that it is not assumed technical interventions during the mission fulfilment of the spacecraft, it is possible to consider an undetectable construction and its fixation.
- MHS construction should be least thermally conductive, so that back circulation of dissipated heat would not occur. If the dissipated heat would return through the structure, the primary function of MHS would be lost. One of the auxiliary solutions to this problem is suitable insulation.
- It is necessary that the structure will be ergonomically formed and dimensionally suitable to some extent. It should not interfere or influence the interior of the spacecraft. Within this requirement, a certain degree of versatility of the structure must be taken into account. If possible, the structure should be dimensionally adapted if necessary.
- The structure material should meet the requirements for strength, low weight and also the manufacturability requirements – from the survey of literature, ESA standards and processed materials within the MHS project from the institute of aerospace engineering follows, that the most suitable materials for the MHS construction are aluminium alloys or optionally titanium alloys.

All of these requirements serve the purpose of creating a conceptual design of a Heat switch installation into a satellite structure as well as optimizing these concepts or creating completely new concepts.

## 4.2. Definition of parameters

The creation of conceptual designs always depends on specific parameters and requirements given, that must be met with these designs. In order to be able to create conceptual designs, it is necessary to specify some parameters or components, which define the given process of designing and which are envisaged in the design.

1. The first specification is the location. For the conceptual designs for MHS structure, direct connection and the contact of contact plate (MHS) with the radiation plate, which is part of the satellite structure, is considered. For the concepts themselves, therefore, a fixed connection with the radiation plate is considered. More detailed specifications are described for each concept.
2. The mounting of conceptual designs is considered by using screws in inserts embedded into the radiation plate. In case of a thermal way without a flexible conductive component, the connection of the conceptual design with an electronics box or other auxiliary heat source structure (electronic component) by means of a screw connection is considered. Due to the fact, that the aim of this Master thesis isn't a design of a specific construction of the MHS structure, and there are no exact requirements available, no weld connection is considered.
3. For the thermal way without the flexible conductive component and only with the MHS, an electronics box wall or part of the supporting structure of any other heat source, such as a board with ideal properties for mounting the structure with screws and with any dimensions is considered. These dimensions should meet the needs of the MHS – more detailed specification is described in the relevant concept.
4. For the purpose of designing the structure concepts a simplified model of the MHS is considered, only with its external components. Since there are no (at the time of the creation of this work) requirements for the shape and dimensions of the MHS, it is possible to slightly modify them. However, the aim is to preserve the original shapes and dimensions of the MHS as much as possible.
5. Within the thermal way with a flexible conductive component a composition of these elements is considered: part of the flexible conductive component, MHS, MHS structure concept and the radiation plate. For the flexible conductive component, only the part touching, and thus transferring heat, the MHS is considered. Other elements are not that important and necessary for the design of MHS structure concepts. As it was mentioned in the chapter 3.5, the considered flexible conductive component is a selected demonstrative example from the TAI company catalog, figure 3.14. This is because the base of one terminal, which is circular, is best suited for the shape of the MHS. For the proposed concepts, in figures 4.1, 4.2 a 4.3, 4.4, two possible variants of this one terminal of the flexible component are considered. These two variants can be chosen, as TAI offers considerable variability in these products.

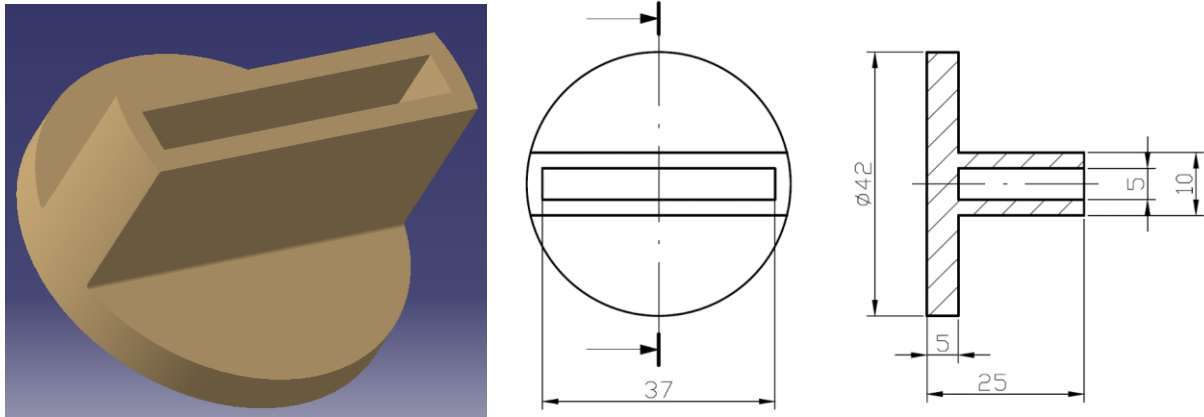


**Figure 4.5:** Basic dimensions of first type termination

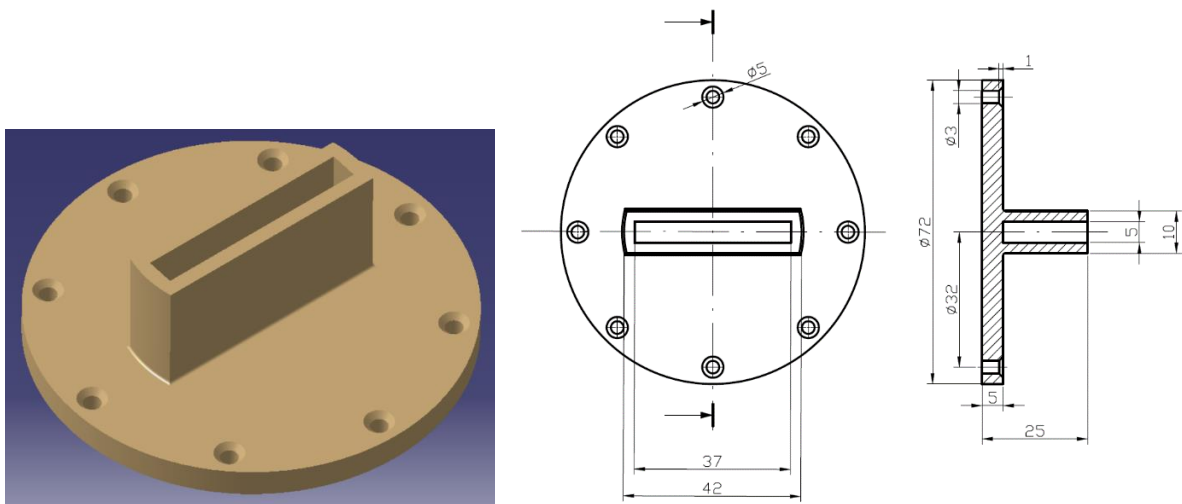


**Figure 4.6:** Basic dimensions of second type termination

6. For the purpose of this Master thesis, the radiation plate is taken as a board with the thickness of 5 mm. The determination of the remaining two dimensions, width and height of the radiator (determination of its area) is tied to its radiating power into the surrounding area. In the objectives of the project dealing with MHS, that can be found in the literature [18], a requirement of 10 W is given for the thermal output passing through the MHS and being transferred to the radiation plate. From the literature [12][21] it can be determined, by the standard and usual values of other radiators, the average area of the radiator, thanks to which the radiation plate is able to radiate power of 10 W. Also, based on the mentioned literature, it is possible to calculate the area under the conditions: [12][21]

- $\varepsilon = 0,75$  – average emissivity value
- $T = 283,15$  K – usual temperature value of radiators
- $10$  W = 10 J radiated per second

From Equation 2.2, the required size of the radiation plate is then calculated:

$$A_r = 0,03659 \text{ m}^2$$

The considered radiation plate can then be, for example, a square with an edge of 191 mm and a selected thickness of 5 mm. From this thickness, 2 mm are used for aluminum plates on both sides (1 mm each plate) and 3 mm for the height of the honeycomb core. The honeycomb core is then formed by hexagons with a width of one cell of 5 mm. The required value for the calculation of heat transfer is also the area of the entire honeycomb core. In general, the value of this area is in the range of 15 - 20% of the normal full area. When considering a core wall thickness of 1 mm, this area will be

$$A_j = 0,0063842 \text{ m}^2$$

### 4.3. Concept A

Concept A is designed within the first platform, which involves the connection of the flexible conductive component, MHS and the radiation plate. It is an external construction, figure 4.5, which secures this connection. For the concept A, the first type terminal of the conductive component is used. The construction and shape are designed in such a way, so that they create a fixed box for the MHS and the terminal of the conductive component and at the same time all force and moment actions are transmitted through it. Any forces and moments will be transmitted to the MHS only to a very limited extent.

The fixation of the MHS and the terminal of the conductive component in correct position is secured by a top and bottom tape, small beams at the top and the whole construction is firmly bolted in four beams to the radiation plate. The screws pass through the radiation plate and the whole length of the beams and it can be tightened with nuts. Expected size of the screws is M5x0,5. The whole complete set of the terminal of the flexible component, MHS, concept A, structure and the radiation plate is shown in figure 4.7.

For the needs of this concept, there is considered a small change of external parts of the MHS. For the reasons of shape and geometric simplicity are the components Coldplate and Baseplate modified into a circular floor plan. The number of beams for the structure doesn't play a role, but in the set examples the external shell of the MHS is shown with four columns.

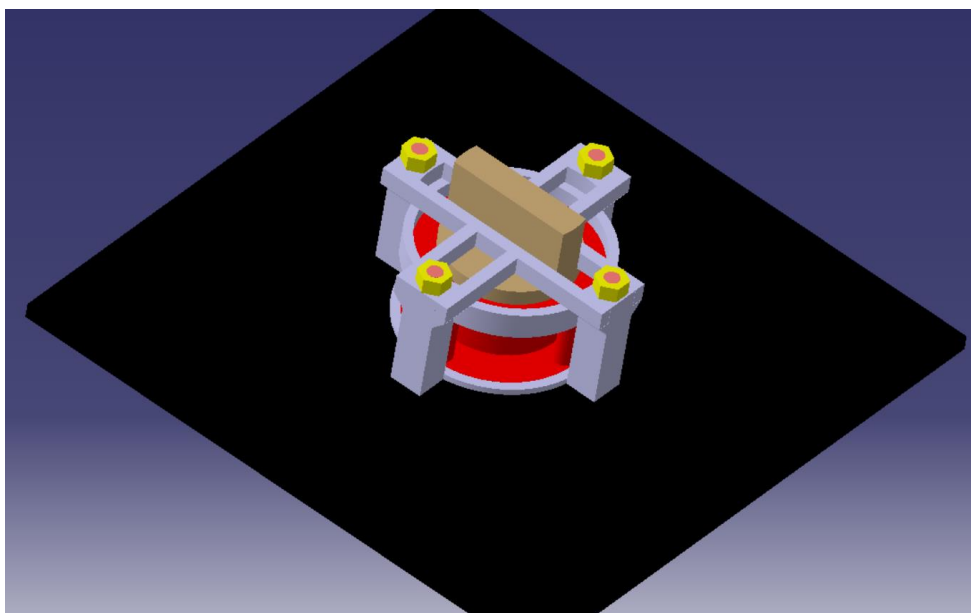


*Figure 4.7: Composition of concept A*

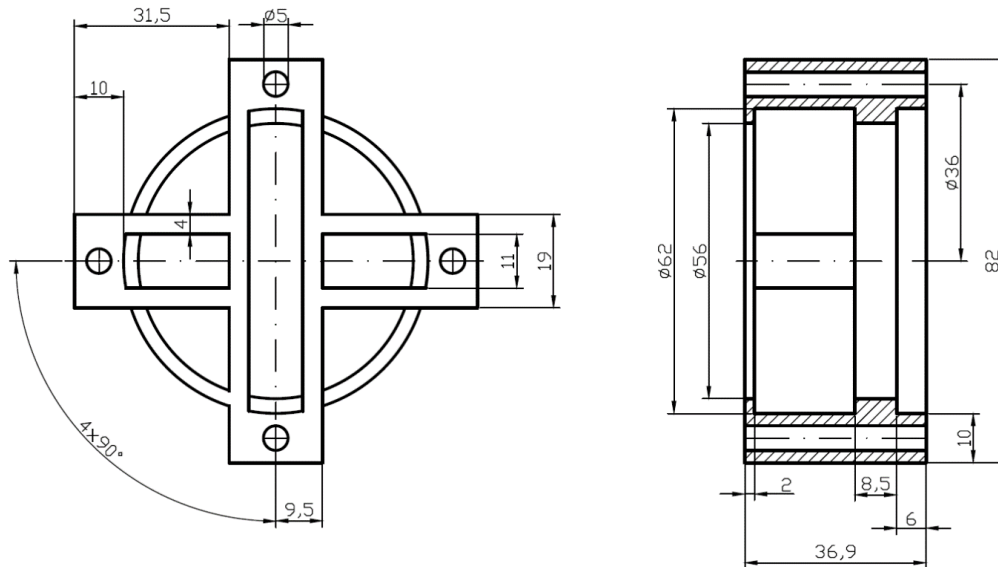


**Figure 4.8:** Basic dimensions of concept A

In figure 4.7 of the whole set, grey color represents the structure, red color is the simplified MHS model, brown represents the first type of terminal of the conductive component, pink color are the screws, yellow color are the nets and the black color is the radiation plate.

Assembly procedure:

1. Through the MHS structure (concept A) the flexible conductive component is passed from the bottom where there are no beams. It is considered, that the second terminal of the flexible conductive component has such dimensions, that it is able to pass through the opening between the beams in the top part of the structure.
2. Into the structure, also through the space without the beams, is the MHS inserted so that the area of its touches the area of the terminal of the conductive component. The dimensions of the structure are designed in such a way that the bottom areas of the beams and the bottom area of the coldplate MHS are in the same plane and touch at the same time the radiation plate.
3. This assembly is then bolted to the radiation plate with long screws and tightened with nuts.

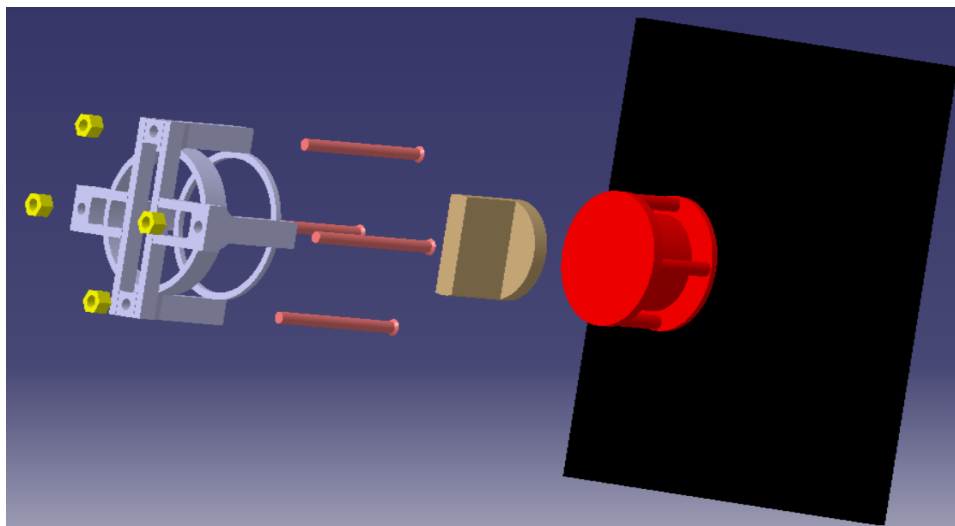


**Figure 4.9:** Disassembled assembly of concept A

## 4.4. Concept B

Concept B, similarly to concept A, is designed within the first platform. However, this is the first modification of concept A. Similarly to concept A is this concept B designed as an external structure, figure 4.8. At the same time, the first type of terminal of the flexible conductive component is also used. The structure and its shape is designed similarly to concept A so that they create a fixed box for the MHS and the terminal of the conductive component and at the same time all force and moment actions are transmitted through it. Any forces and moments will be transmitted to the MHS only to a very limited extent.

The change in concept B versus the concept A is the modification of the structure for an easier assembly of the whole set. Due to the different arrangement of the fixing beams, it is necessary to add auxiliary ribs.

The fixation of the MHS and the terminal of the conductive component in correct position is also secured by a top and bottom tape, small beams at the top and the whole construction is firmly bolted in four beams to the radiation plate. These screws, similarly to concept A, pass through the radiation plate and the whole length of the beams and it is possible to tighten it with nuts. Expected size of the screws is M5x0,5. The whole complete set of the terminal of the flexible component, MHS, concept B structure and the radiation plate is shown in figure 4.10. For a simplified view and the assembly needs is the radiation plate similar to the plate in concept A.

For this second concept B, the same changes are considered on the external members of the MHS as for concept A.

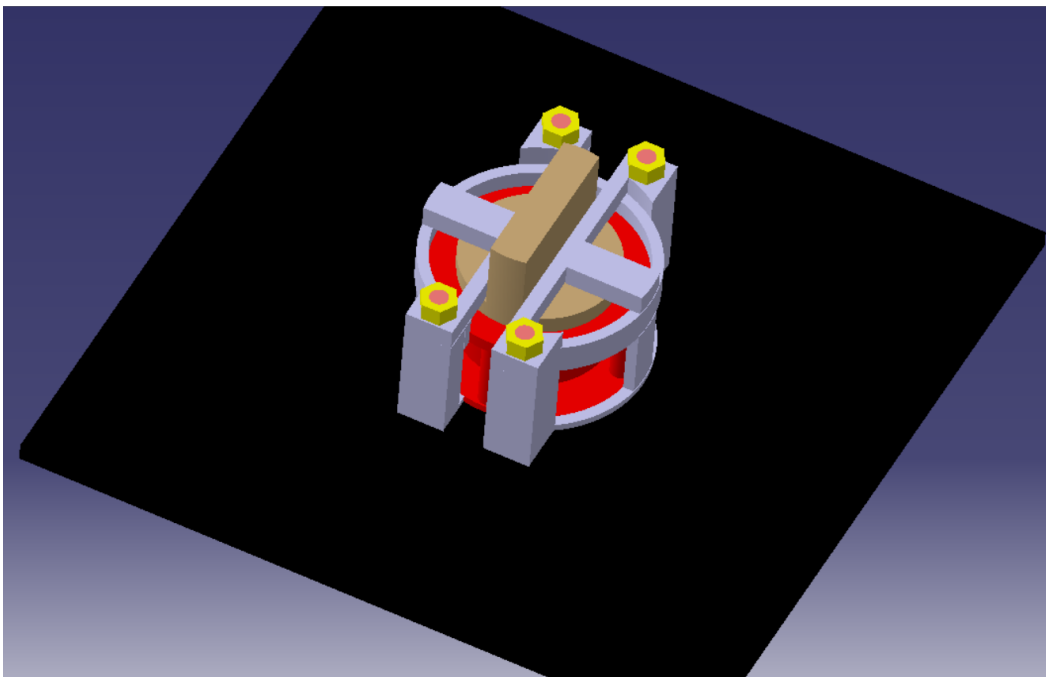


*Figure 4.10: Composition of concept B*

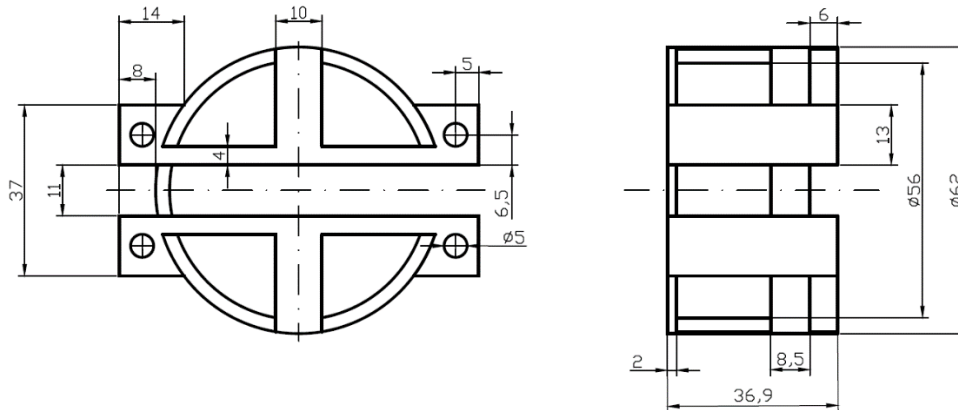


*Figure 4.11: Basic dimensions of concept B*

To showcase the whole set in figure 4.10, the same color combinations are used as in concept A. The grey color represents the structure, red color represents the simplified model of the MHS, brown color is used for the first type of terminal of the conductive component, the pink color represents the screws, the yellow color represents the nuts and the block color is the radiation plate.

Assembly procedure:

1. Due to the aimed modification – changes to the structure of concept B, it is now possible to mount the flexible conductive component from the side of the structure. This will allow for easier assembly as well as variability in dimensions and shapes of the second terminal of the flexible conductive component.
2. Subsequently, the MHS is inserted into the structure so that the area of the component baseplate touches the terminal area of the conductive component. Dimensions of the concept B structure are similarly to concept A chosen in such a way, that the bottom areas of the beams and the bottom area of the coldplate MHS are in the same plane and touch at the same time the radiation plate.
3. This assembly is then bolted to the radiation plate with long screws and tightened with nuts.

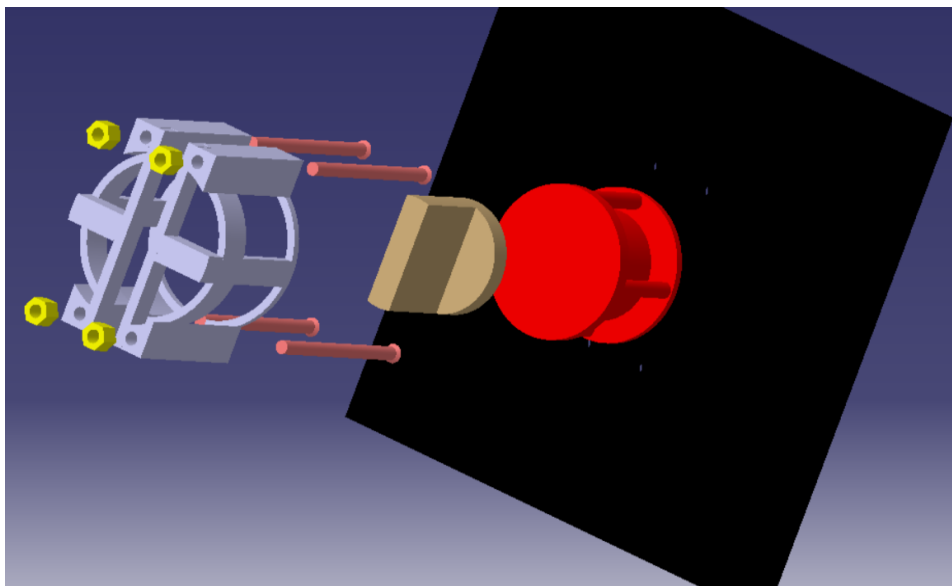


*Figure 4.12: Disassembled assembly of concept B*



## 4.5. Concept C

Concept C is the second modification of concept A. Similarly to the previous two concepts, it is a construction that creates a so called box – a fixed repository for the MHS. The modification of this concept, figure 4.11, targets this time the case when a requirement appears, which would make it impossible to mount the structure directly to the radiation plate. The structure must secure the contact of the MHS with the radiation plate as well as being attached to the frame around the radiation plate. Moreover, this concept shows the possibility, where the terminal of the conductive component isn't located inside the structure, but is externally attached to the structure by a set of screws, as it can be seen in figure 4.13. For this reason the second type terminal of the conductive component is used.

The basis of the MHS fixation is similar to the previous two concepts by using a top and bottom tape. Also for this concept, similar changes on the MHS are considered just like in the previous two concepts. At the top tape and in the beams 8 holes for screws of the estimated size M3 are prepared, by which the terminal of the flexible conductive component is bolted to the structure. The whole structure is then fixed to the frame with 4 screws of the expected size M5 at the ends of the four ribs.

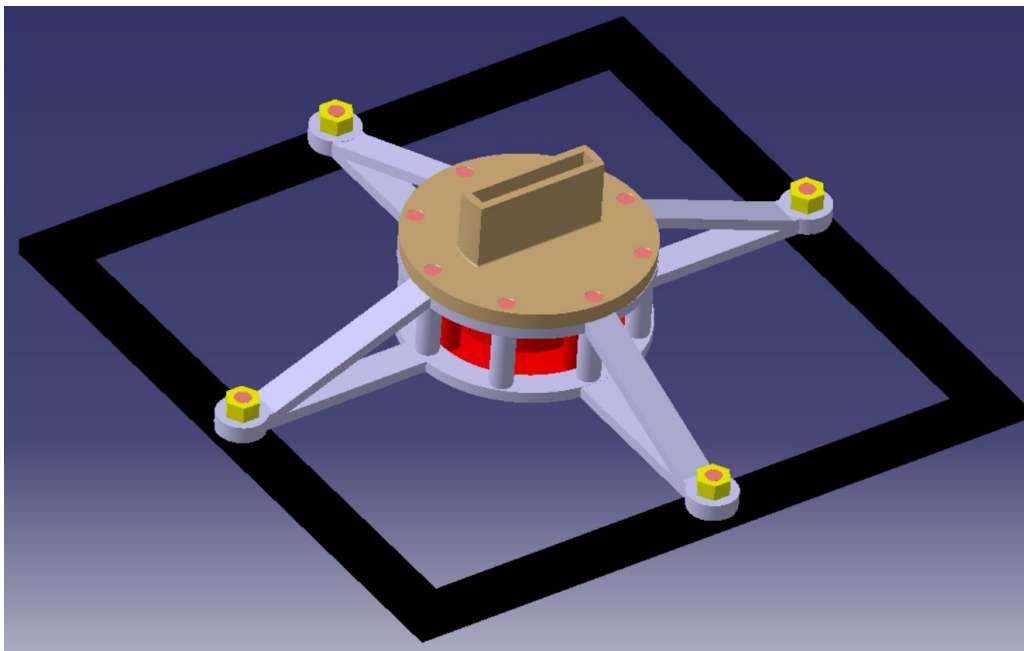


*Figure 4.13: Composition of concept C*

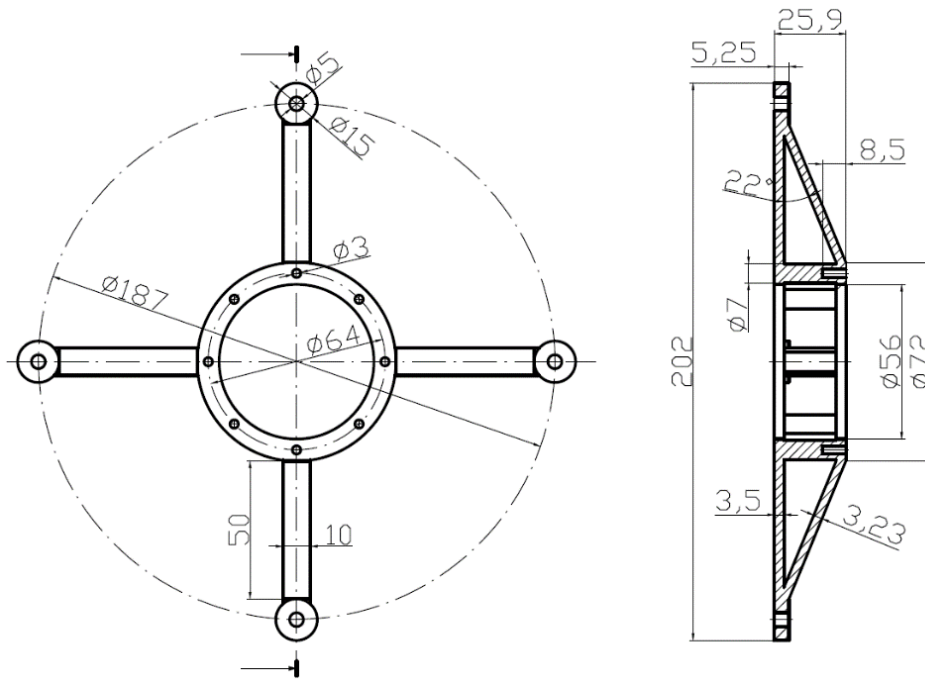


*Figure 4.14: Basic dimensions of concept C*

In the set of all components, the grey color represents the structure, the brown color represents the terminal of the flexible conductive component, the red color represents the MHS, the pink color represent all the screws, yellow color represents the nuts and the black color, in this case, represents the frame around the possible radiation plate.

Assembly procedure:

The concept C offers greater variability and thus simpler assembly of the whole set. It is possible to take the steps in a different order.

1. Screw the installation structure to the radiation plate frame using screws and nuts.
2. MHS is inserted into the structure.
3. The flexible conductive component is bolted with screws to the structure and in this way the MHS is closed in the structure and the thermal way is created.

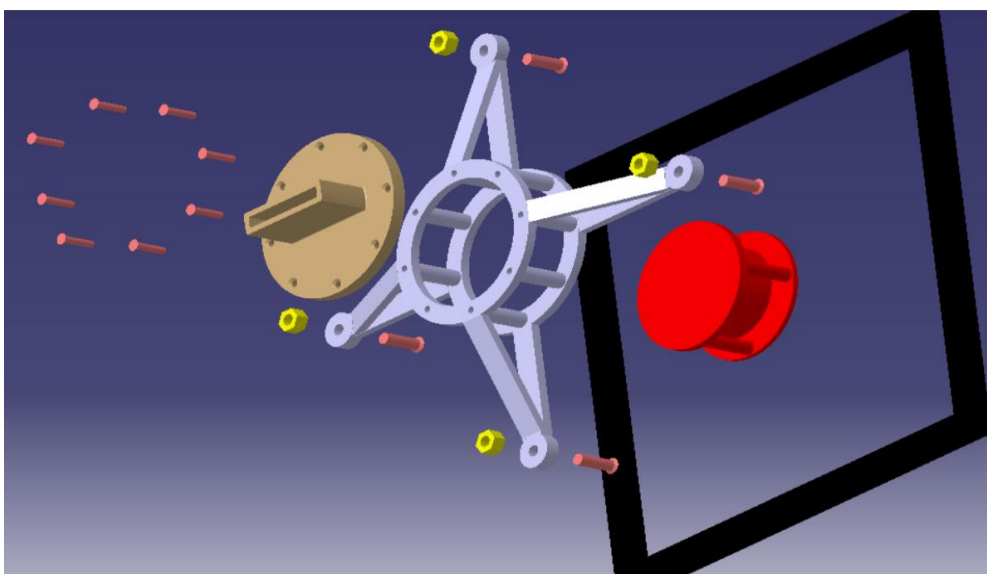


*Figure 4.15: Disassembled assembly of concept C*

## 4.6. Concept D

The concept D is not based on an external structure, as it was with the previous concepts. This is a modification of the shape and dimensions of two terminal components, baseplate and coldplate, directly on the MHS. These components are modified in such a way, that they allow fixation of the MHS to the radiation plate. At the same time, this concept is focused on the case where the thermal way is formed only with the MHS, so without the flexible conductive component. MHS is directly attached to the heat source as well as the radiation plate. Because there is no external structure here that would transfer possible force actions, these forces are transmitted through the MHS structure, primarily through its external components – baseplate, coldplate and the columns. For this reason, only these important mentioned components are considered for this concept and for an additional idea also the position and shape of the conductive structure and contactplate in MHS. In figure 4.14 the concept D is shown – modified external components of the MHS.<sup>1</sup>

In this case, a board is considered a heat source. It is a simple replacement of the heat source wall, for example of the box in figure 3.12 or 3.13, where the MHS is attached. The considered dimensions of this board are 100 x 67 mm with holes for M5 screws to mount the MHS.

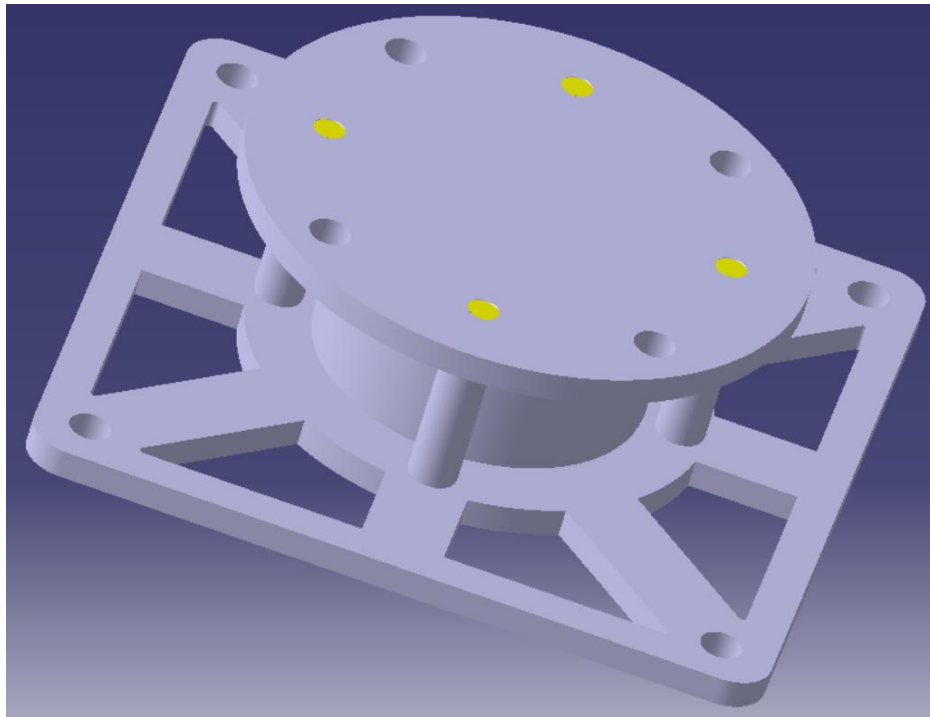


*Figure 4.16: Concept D*

---

<sup>1</sup>The yellow color represents the nuts, that hold the beams, baseplate and the coldplate.

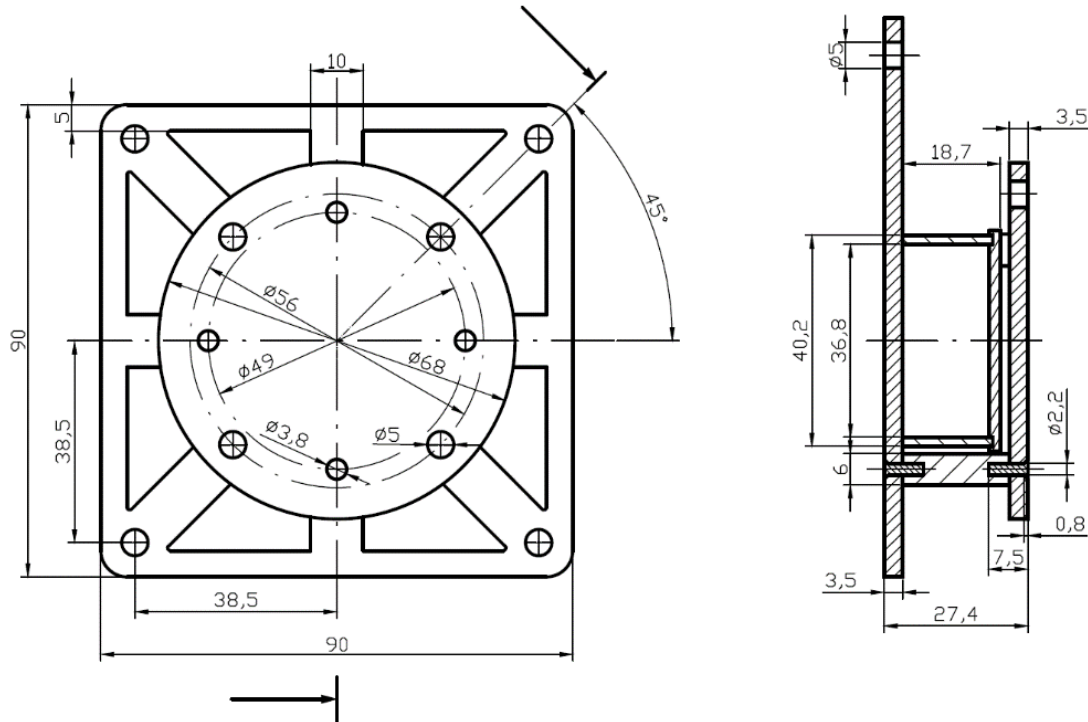


*Figure 4.17: Basic dimensions of concept D*

In the set of all components, figure 4.16, the red color represents the heat source wall, the grey color is the modified external structure of the MHS, the pink color represents the screws and the yellow color are the nuts. The black color is the radiation plate, which is reduced due to the large size. In figure 4.20, the disassembled assembly of concept D is shown in full size.

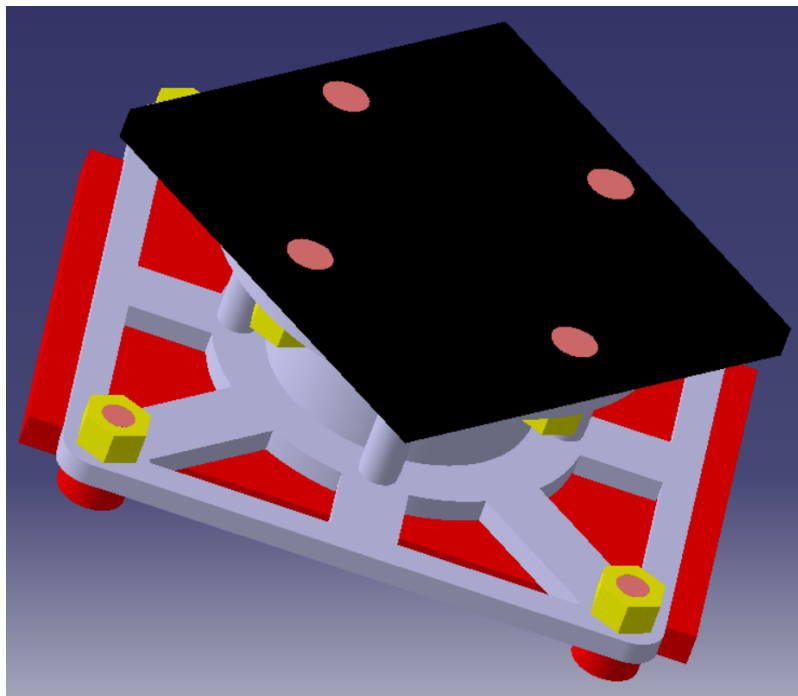


*Figure 4.18: Composition of concept D*

Assembly procedure:

As this is only a modification of the shape and dimensions of the external members of the MHS, the assembly is very simple.

1. MHS is screwed to the wall of the heat source using M5 screws.
2. And again, by using the M5 screws, the MHS is bolted to the radiation plate.

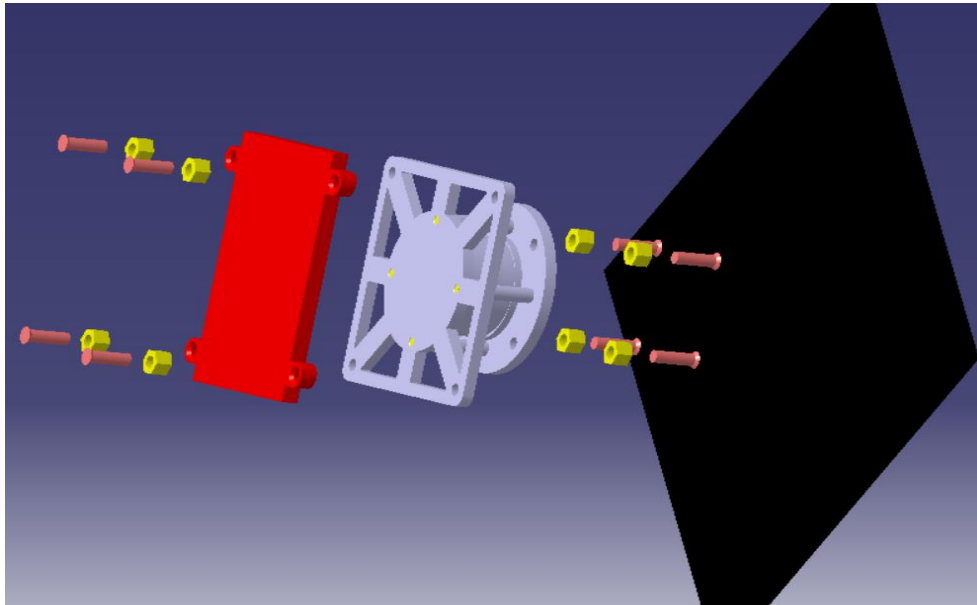


*Figure 4.19: Disassembled assembly of concept D*

## 4.7. Summary of conceptions

The proposed concepts A – D represent one type of options for firm attachment of the MHS by using Inserts. At the same time they represent two different thermal ways. Each of the first three concepts, within one of the thermal ways, focuses on a different possible problem and situation, which can be required for the final construction. Within one thermal way, 2 different types of terminals of the flexible conductive component are applied, through which the heat is transferred to the MHS from the heat source. For the second thermal way, a wall of an electronic box is used as a replacement for the heat source. In annex A a breakdown of all concepts into smaller parts is given as well as their common marking with the marking of the contact surfaces.

For the proposed concepts of MHS structure, based on literature research, materials based on aluminum alloys or titanium alloys or steel are possible. Materials that can be used as construction materials for the concepts are listed in table 4.2. Aluminum alloy 2024 T8 selected as a material for construction falls into the category "*Alloys with moderate resistance to stress-corrosion cracking*" according to the standard issued by ESA [45]. If necessary, if it is found to be unsatisfactory during control testing, this aluminum alloy would be replaced by another equivalent alloy. The mentioned steel is used in all concepts only for screws. From the mentioned copper the parts of MHS are made, which enter the calculation, and the aluminum alloy 7075 is considered a material for the radiation plate. Teflon, or PTFE, is a material that serves as an insulator due to its low conductivity. It can be used only in the first platform of concepts for limiting heat transfer to the concept structure.

**Table 4.2:** List of materials for concepts [4] [8]

	<b>Mass density</b>	<b>Yield Strength</b>	<b>Young's Modulus</b>	<b>Thermal Conductivity</b>
	$\rho$ [ $\text{kg}\cdot\text{m}^{-3}$ ]	Re [MPa]	E [GPa]	$\lambda$ [ $\text{W}\cdot\text{m}^{-1}\cdot\text{K}^{-1}$ ]
<b>Aluminium 2024 T8 (Al-Cu4Mg1)</b>	2780	400	71	120
<b>Titanium (Grade 5) Ti - 6Al - 4 V</b>	4430	965	114	6,7
<b>Cuprum – Cu OFHC (CDA110)</b>	8,9	45 - 320	130	391
<b>Aluminium - Alu 7075 T73</b>	2,81	435	72	155
<b>Steel - AISI 316L</b>	7800	290	210	16
<b>PTFE</b>	2150	35	-	0,23

Another important material property is the thermal Interface/contact conductivity. It is a property, that in units [ $\text{W}\cdot\text{m}^{-2}\cdot\text{K}^{-1}$ ] indicates the thermal conductivity of transitions of two different materials. The following table 4.3 shows the calculated numerical values of the transitions between the materials used.

**Table 4.3:** Thermal Interface/contact Conductivity

<b>Materials in contact</b>	<b>Thermal contact Conductivity</b>
	[ $\text{W}\cdot\text{m}^{-2}\cdot\text{K}^{-1}$ ]
CDA / CDA	6785,9
CDA / ALU 2024	3864,8
CDA / ALU 7075	4766,4
CDA / TI	228,6
CDA / PTFE	19,2
ALU 2024 / ALU 7075	2904,4
ALU 2024 / AISI 316L	5693078
TI / ALU 7075	275,8
TI / AISI 316L	1330729,5
AISI / ALU 7075	5966595,4
PTFE / ALU 2024	19,17
PTFE / TI	18,6

## 5. Thermal control of concepts

The primary task of the MHS structure is to ensure a firm attachment to a place, where the MHS can perform its function. That function is the regulation of the heat dissipation from devices onto the radiation plate. To ensure that this structure correctly functions, it must be firmly attached to the MHS. Due to this connection however, the heat that travels through the MHS can be partially transferred into the structure through conduction. This is undesirable, because this would mean one of the primary functions of the MHS would be lost. This function is the regulation of the heat dissipation. This could lead to constant and continuous heat dissipation through the structure. The thermal control of concepts should thus be used to determine how much heat passes through the individual structures and to evaluate the best variant on the basis of this factor.

### 5.1. Calculation procedure

In order to evaluate the individual concepts in their functionality and their ability to dissipate heat (thermal conductivity size) through the whole construction, the same calculation model for thermal conductivity was established for all concepts. All of the concepts need to be compared not only in the size of their thermal conductivity, but also primarily in a specific number. This specific parameter  $S_p$  puts into proportion thermal conductivity  $C$  [ $\text{W} \cdot \text{K}^{-1}$ ] and weight  $m$  [kg] of the miniaturized thermal switch.

$$S_p = \frac{c}{m} \quad (5.1)$$

The computational model for the thermal conductivity calculation is compiled based on literature [28][29][30][41]. In this literature there are procedures how to calculate the thermal conductivity of contacts and at the same time perform the calculation of thermal resistance. It is the calculation of thermal resistances  $R$  [ $\text{K} \cdot \text{W}^{-1}$ ] of individual parts of the construction and then the thermal conductivity is calculated as an inverted value of this thermal resistance, equation 5.2. For clarity and simplicity of the computation, thermal-conductive paths were created for each individual concept based on resistance as representatives of individual parts. Each part is marked with the letter  $R$  and a number. Connections (transitions between individual parts) are additionally marked with the small letter  $c$ . These maps are shown in annex A. On the basis of these maps, the total thermal resistances calculated by using the theory of addition of resistances in an electrical circuit.

$$C = \frac{1}{R} \quad (5.2)$$

In the calculation, the ideal - uniform and smooth - heat transfer through the material is considered. Heat propagation throughout the assembly is like an electric current propagation through an electrical circuit.

Due to the difficulty of the procedure, used equations of the whole calculation are not listed here. Procedure of the calculation is drafted in the before mentioned literature [28][29][30][41]. Only input parameters are listed here.

These parameters enter into the calculation of thermal conductivity of individual parts:

- Dimensions of individual parts
- Density and thermal conductivity of the materials, from which the parts are made
- Microhardness of individual parts
- Contact pressure between individual parts abutting each other
- In the case of threads, all thread dimensions

Such created model is applied on all concepts similarly, so that it is possible to evaluate and compare resulting parameters. Used materials for the concepts are listed in table 4.2. Both materials for constructions (Aluminium and Titanium alloy) are used in the calculation due to the possible comparison of the resulting parameters.

All calculations of thermal conductivities are done in *Microsoft Excel* due to their large number. The calculation of the total thermal resistance according to the compiled thermal ways, which are in individual concepts in annex A, is done by using *Java applet* by Paul Falstad. It is a simple simulator of electrical circuits [20].

In order for these calculations to be possible, the individual concepts are first modelled in *Catia V5 R21* and then schematically rendered in *AutoCAD Mechanical 2018*.

## 5.2. Outputs

The most important output parameters, as it was mentioned in previous chapter are thermal conductivity, weight and the specific parameter. For each concept, these parameters are listed in tables for every material used. Weights, from which the specific parameter is calculated and are listed in resulting tables, are weights of the whole set – flexible conductive component, the structure, MHS and the radiation plate. Weights of the constructions itself are listed separately.

The MHS weight is

$$m_0 = 0,173 \text{ kg [4]}$$

After that, for the possibility of comparison, are the resulting parameters of concepts with an added thin layer of PTFE (2 mm) to limit as much as possible the heat transfer to the construction of the concepts structure. This thin layer of PTFE is placed between all contacts of the structure with the MHS. The addition of PTFE is only possible in concepts of the first platform.

Annex B presents partial results for individual parts of the concepts, according to the conductivity maps, as they enter the calculation of the total thermal conductivity.

### **Output parameters for Concept A:**

The resulting values of thermal conductivity, weight and specific parameter for the concept A are listed in table 5.1 and the table 5.2 contains the resulting values of the construction itself. Tables 5.3 and 5.4 contain resulting values with added PTFE as insulator. The resulting thermal conductivity and calculated weight, based on the calculated volumes of the individual components and the materials density from table 4.2, include the radiation plate according to the calculation diagram in annex A2. The same is true for all concepts.



*Table 5.1: The resulting parameters of the concept A*

	Thermal conductivity	Weight	Specific parameter
	$W \cdot K^{-1}$	kg	-
<b>Aluminium alloy</b>	0,845	0,431	1,96
<b>Titanium alloy</b>	0,829	0,4742	1,748

*Table 5.2: The resulting parameters of the separate structure of concept A*

	Thermal conductivity	Weight	Specific parameter
	$W \cdot K^{-1}$	kg	-
<b>Aluminium alloy</b>	0,0097	0,0823	0,12
<b>Titanium alloy</b>	0,000544	0,1254	0,0043

*Table 5.3: The resulting parameters of the concept A with PTFE*

	Thermal conductivity	Weight	Specific parameter
	$W \cdot K^{-1}$	kg	-
<b>Aluminium alloy</b>	0,831	0,4496	1,85
<b>Titanium alloy</b>	0,7215	0,4927	1,46

*Table 5.4: The resulting parameters of the separate structure of concept A with PTFE*

	Thermal conductivity	Weight	Specific parameter
	$W \cdot K^{-1}$	kg	-
<b>Aluminium alloy</b>	0,0037	0,11545	0,032
<b>Titanium alloy</b>	0,00049	0,15994	0,00412

Two graphs are available for a clearer comparison. The first graph, figure 5.1, shows the values of entire assemblies and the second graph, figure 5.2, shows the values for individual structures.

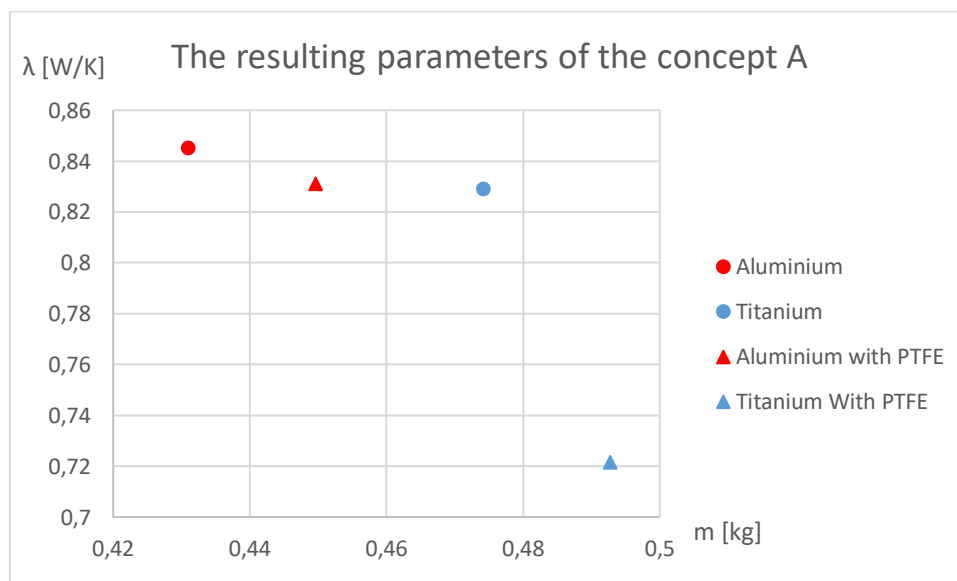


*Figure 5.1: The resulting parameters of the concept A*

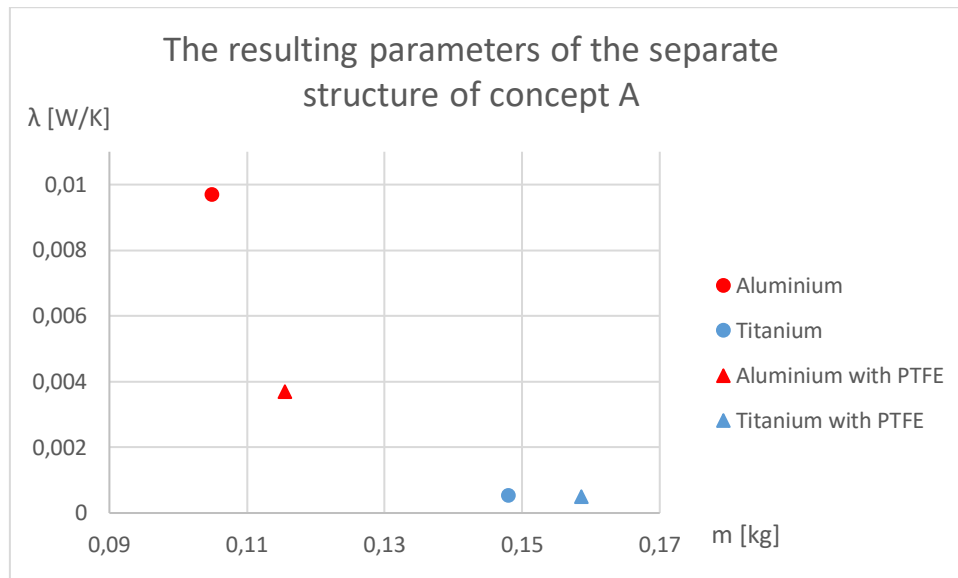


Figure 5.2: The resulting parameters of the separate structure of concept A

### Output parameters for Concept B:

The resulting values of thermal conductivity, weight and specific parameter for the concept B are listed in table 5.5 and table 5.6 contains resulting values of the construction itself. Table 5.7 and 5.8 contain resulting values with added PTFE as insulator.

Table 5.5: The resulting parameters of the concept B

	Thermal conductivity	Weight	Specific parameter
	$W \cdot K^{-1}$	kg	-
<b>Aluminium alloy</b>	0,985	0,4408	2,23
<b>Titanium alloy</b>	0,839	0,4893	1,715

Table 5.6: The resulting parameters of the separate structure of concept B

	Thermal conductivity	Weight	Specific parameter
	$W \cdot K^{-1}$	kg	-
<b>Aluminium alloy</b>	0,146	0,1146	1,724
<b>Titanium alloy</b>	0,0118	0,1631	0,088

Table 5.7: The resulting parameters of the concept B with PTFE

	Thermal conductivity	Weight	Specific parameter
	$W \cdot K^{-1}$	kg	-
<b>Aluminium alloy</b>	0,8467	0,4593	1,88
<b>Titanium alloy</b>	0,8137	0,5078	1,656

Table 5.8: The resulting parameters of the separate structure of concept B with PTFE

	Thermal conductivity	Weight	Specific parameter
	$W \cdot K^{-1}$	kg	-
<b>Aluminium alloy</b>	0,0059	0,125	0,0472
<b>Titanium alloy</b>	0,0034	0,1737	0,0196

Two graphs are available for a clearer comparison. The first graph, figure 5.3, shows the values of entire assemblies and the second graph, figure 5.4, shows the values for individual structures.

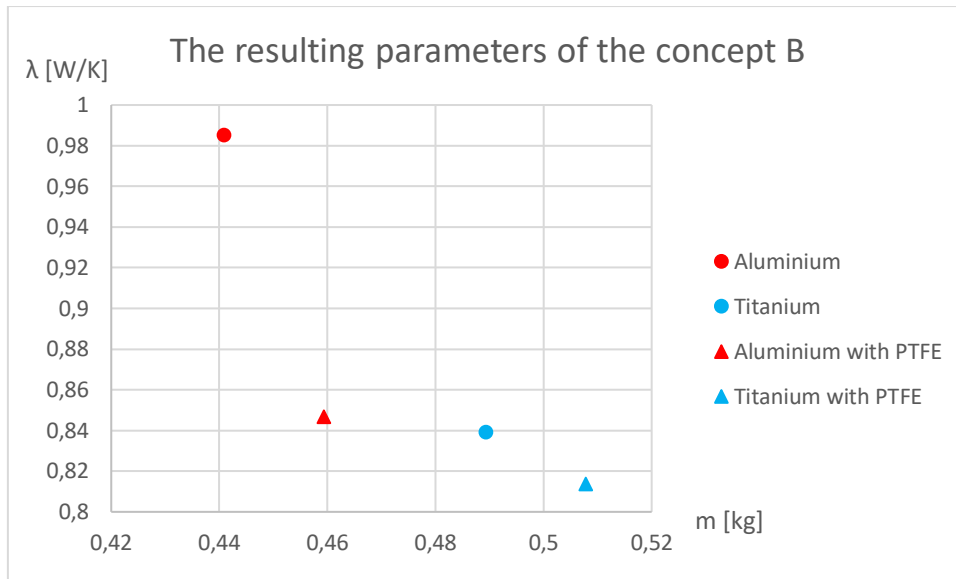


**Figure 5.3:** The resulting parameters of the concept B

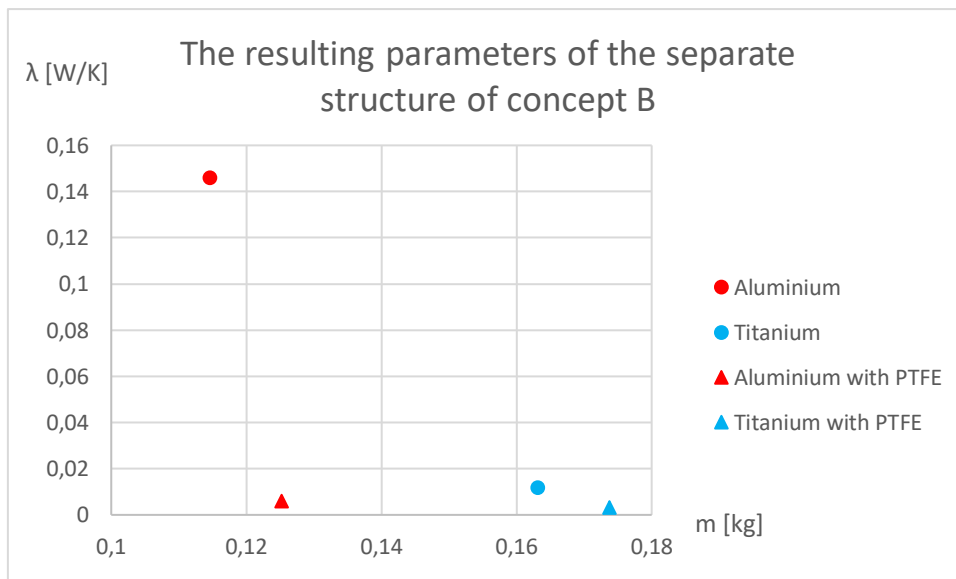


**Figure 5.4:** The resulting parameters of the separate structure of concept B

## Output parameters for Concept C:

The resulting values of thermal conductivity, weight and specific parameter for the concept C are listed in table 5.9 and table 5.10 contain resulting values of the construction itself. Table 5.11 and 5.12 contain resulting values with added PTFE as insulator.

*Table 5.9: The resulting parameters of the concept C*

	Thermal conductivity	Weight	Specific parameter
	$W \cdot K^{-1}$	kg	-
<b>Aluminium alloy</b>	1,748	0,6061	2,88
<b>Titanium alloy</b>	0,932	0,6583	1,416

*Table 5.10: The resulting parameters of the separate structure of concept C*

	Thermal conductivity	Weight	Specific parameter
	$W \cdot K^{-1}$	kg	-
<b>Aluminium alloy</b>	0,258	0,1629	2,93
<b>Titanium alloy</b>	0,0156	0,215	0,111

*Table 5.11: The resulting parameters of the concept C with PTFE*

	Thermal conductivity	Weight	Specific parameter
	$W \cdot K^{-1}$	kg	-
<b>Aluminium alloy</b>	0,8811	0,6183	1,31
<b>Titanium alloy</b>	0,869	0,6705	1,296

*Table 5.12: The resulting parameters of the separate structure of concept C with PTFE*

	Thermal conductivity	Weight	Specific parameter
	$W \cdot K^{-1}$	kg	-
<b>Aluminium alloy</b>	0,0204	0,17	0,12
<b>Titanium alloy</b>	0,0094	0,222	0,0423

Two graphs are available for a clearer comparison. The first graph, figure 5.5, shows the values of entire assemblies and the second graph, figure 5.6, shows the values for individual structures.

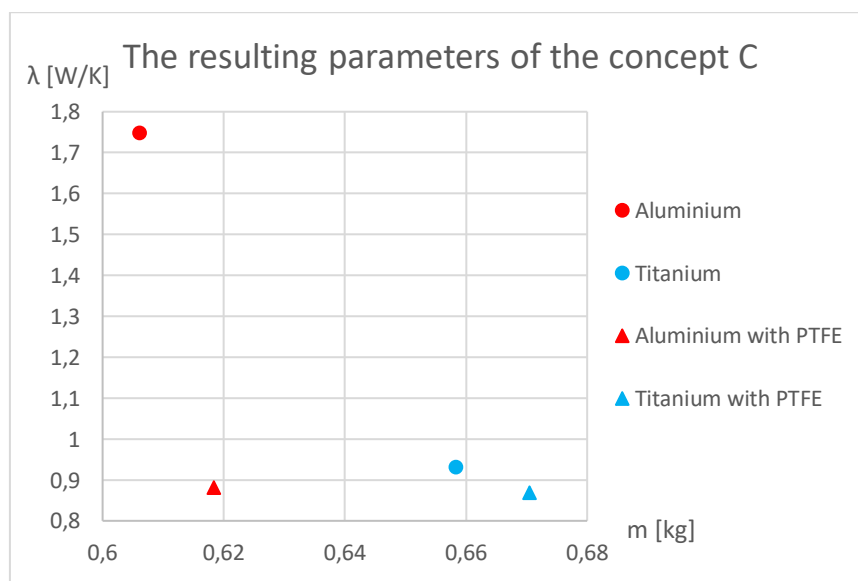


*Figure 5.5: The resulting parameters of the concept C*

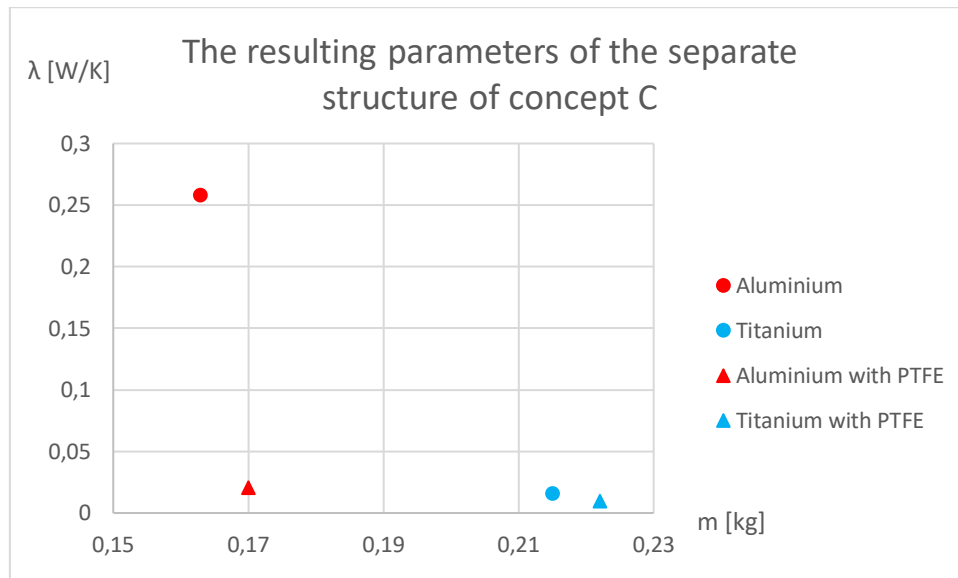


Figure 5.6: The resulting parameters of the separate structure of concept C

### Output parameters for Concept D:

The resulting values of thermal conductivity, weight and specific parameter for the concept D are listed in table 5.13. Since there is no connection between the heat source and the radiation plate outside the MHS in this configuration, there is no need to add PTFE. All heat flows through the MHS. The materials used for components baseplate and coldplate stay the same in this case and consist of the original MHS.

Table 5.13: The resulting parameters of the concept D

	<b>Thermal conductivity</b>	<b>Weight</b>	<b>Specific parameter</b>
	W · K <sup>-1</sup>	kg	-
<b>Current MHS</b>	1,2	0,173	6,9
<b>Concept D</b>	1,026	0,3357	3,056

The value of the total weight of only the new MHS modifications compared to the original variant is calculated as

$$m_{\text{MHS}} = 0,3047 \text{ kg}$$

## 6. Force analysis of concepts

This chapter deals with the analysis of load distribution from gravitational force to bolts, which connect the structures of the conceptual designs with the radiation plate. In chapter 6.1 the general procedure for the calculation of individual forces acting on bolts. In the following chapters, specific assignments and cases for individual concepts are given. For all concepts, the position values of center of gravity are deducted from Catia V5.

In calculations, two different values of gravitational force are used for each concept. The first value  $F_{g1}$  [N] is the force calculated based on the weight of each assembly  $m$  [kg] and the gravitational acceleration of Earth  $g_1 = 9,80665 \text{ m}\cdot\text{s}^{-2}$ , equation 6.1

$$F_g = m \cdot g \quad (6.1)$$

The second value  $F_{g2}$  [N] is calculated similarly, but with a different gravitational acceleration value. From the requirements of ESA [18], the MHS must be able, and thus the MHS attachment as well, to endure up to 20 times the gravitational acceleration of Earth. The substituted value of the gravitational acceleration is therefore  $g_2 = 196,133 \text{ m}\cdot\text{s}^{-2}$ .

### 6.1. Calculation procedure of magnitude of forces

It is necessary to introduce the coordinate system with axes  $x$ ,  $y$  and  $z$  for the calculations. The beginning of the coordinate system is located at the center of gravity for each concept. In this point gravitational force also acts, where its direction can be in all three axes. The whole calculation procedure is performed according to the literature [38].

As all concepts and their attachment points are symmetrical, it is possible to consider the arrangement of screws as groups of screws in two vertical rows. Another important consideration is that when forces act on the bolts perpendicular to their axis, all bolts participate equally in the load transfer. In the case of the resulting moment from the applied gravitational force, it is assumed that the load acting in the axis of the bolts from this moment is directly proportional to their distance from the center of rotation. This center of rotation for all concepts, due to their symmetry, is the point C shown on the screw layout diagrams for each concept.

The force acting on the bolt in the direction of its axis is calculated as

$$\bar{F} = \frac{F_g}{i} \text{ [N]} \quad (6.1)$$

where  $i$  is the number of screws. Similarly, based on consideration, the force acting perpendicular to the axis of the screw is distributed. In accordance with the consideration of the force in the axis of the screw from the resulting moment, it applies to forces at a non-zero distance from the axis of rotation

$$\frac{F_1}{l_1} = \frac{F_2}{l_2} = \dots = \frac{F_i}{l_i} \quad (6.2)$$

where  $l$  [m] is the distance of the screw from the axis of rotation. The maximum axial force  $F_1$  always acts on the furthest screw from the axis of rotation. All other forces can be expressed based on this maximum force as

$$F_i = \frac{F_1 \cdot l_i}{l_1} \text{ [N]} \quad (6.3)$$

For the moment then applies

$$M = F_g \cdot d \text{ [N}\cdot\text{m]} \quad (6.4)$$

$$M = F_1 \cdot l_1 + F_2 \cdot l_2 + \dots + F_i \cdot l_i \quad (6.5)$$

After substituting equation 6.3 into equation 6.5 and after adjustment, it is possible to get

$$M \cdot l_1 = F_1 \cdot l_1^2 + F_2 \cdot l_2^2 + \dots + F_i \cdot l_i^2 \quad (6.6)$$

From here it is possible to express the maximum force

$$F_1 = \frac{M \cdot l_1}{l_1^2 + l_2^2 + \dots + l_i^2} \text{ [N]} \quad (6.7)$$

In the case when there are several vertical rows in the joint, it is possible to modify equation 6.7 into

$$F_1 = \frac{M \cdot l_1}{i_s \cdot \sum_{j=1}^i l_j^2} \text{ [N]} \quad (6.8)$$

where  $i_s$  is the number of vertical rows of screws that is, the number of screws into which the maximum force  $F_1$  is distributed.

## 6.2. Magnitude of forces of concept A

In figure 6.1 the established coordinate system and the forces, which may affect the system are shown. Due to symmetry, the force acting in axis  $x$  is similar as the one acting in axis  $y$ , which is why it is not mentioned here. The position of the center of gravity of concept A is, due to symmetry, on the axis  $z$  and the distance from the bottom surface of the assembly, in the case of using aluminum alloy, is  $d_1 = 27,95$  mm and in the case of using titanium alloy the distance is  $d_2 = 28,12$  mm.

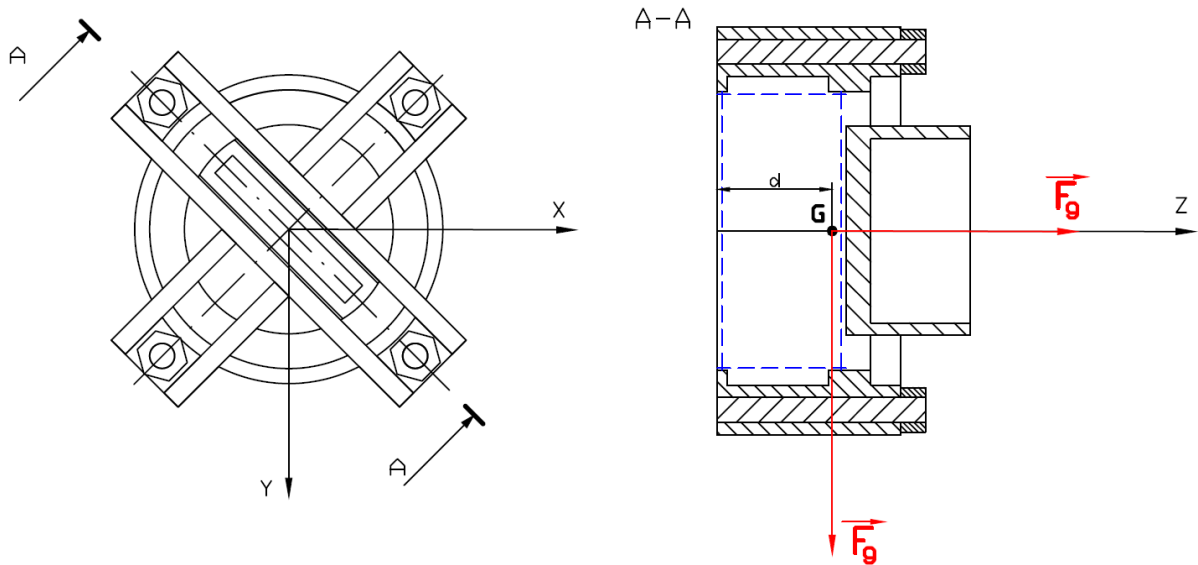


**Figure 6.1:** Forces and coordinate system of concept A

**Table 6.1:** Input values into the calculation of concept A

Mass of concept A with aluminium alloy	$m_{A1}$	0,431	kg
Mass of concept A with titanium alloy	$m_{A2}$	0,4742	kg
The first gravitational acceleration	$g_1$	9,80665	$m \cdot s^{-2}$
The second gravitational acceleration	$g_2$	196,133	$m \cdot s^{-2}$
Distance of the screw from the axis of rotation	$l_1$	0,0255	m
Distance of the center of gravity from the axis of rotation for aluminium alloy	$d_1$	0,02795	m
Distance of the center of gravity from the axis of rotation for titanium alloy	$d_2$	0,02812	m
Vertical rows of screws	$i_s$	2	-



For the situation when the gravitational force acts in the z-axis, therefore in the axis of the screws, equation 6.1 is used to calculate the forces in the screws. Similarly, forces distributed to the screws when loaded perpendicular to the screw axis are calculated and achieve similar values.

**Table 6.2:** Results of the force acting on the screw axis of concept A

Force	Formula	Result	Unit
$\overline{F}_{1,1}$	$\frac{m_{A1} \cdot g_1}{4}$	1,056	N
$\overline{F}_{1,2}$	$\frac{m_{A2} \cdot g_1}{4}$	1,16	N
$\overline{F}_{1,3}$	$\frac{m_{A1} \cdot g_2}{4}$	21,13	N
$\overline{F}_{1,4}$	$\frac{m_{A2} \cdot g_2}{4}$	23,25	N

For the calculation in a situation when the gravitational force acts perpendicular to the axes of the screws at a distance of  $d$  from the plane of screw placement, according to the diagram in the figure 6.2, the equation 6.8 is used. The diagram shows a simplified placement of screws in groups A and B and the center of rotation of the system C. This is also the case with other concepts.

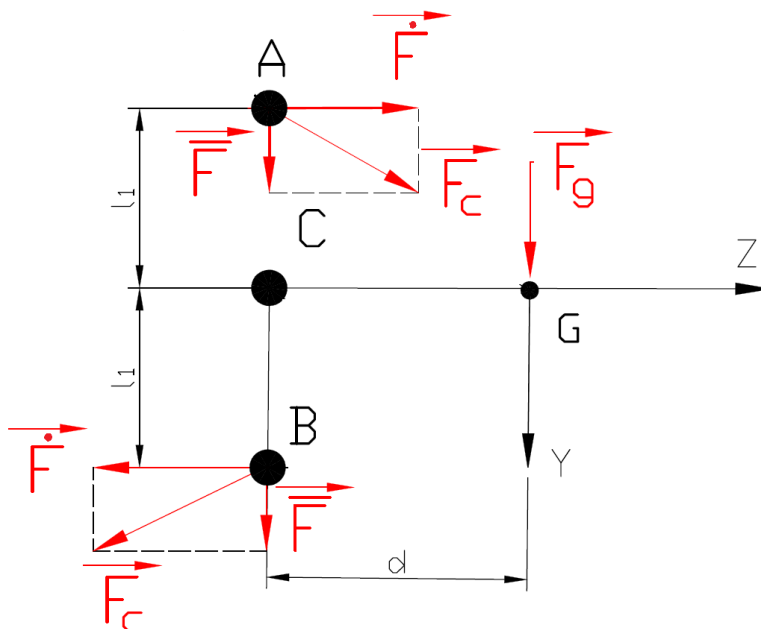


**Figure 6.2:** Diagram for the force acting in the y-axis of concept A

The load of each bolt from the transverse force acting perpendicular to its axis is calculated according to the equation 6.1. In this case,  $i = 4$  screws contribute to the force distribution.

**Table 6.3:** Results of the force acting perpendicular to the axis of the screw of concept A

Force	Formula	Result	Unit
$\dot{F}_{1,1}$	$\frac{m_{A1} \cdot g_1 \cdot d_1 \cdot l_1}{i_s \cdot l_1^2}$	2,32	N
$\dot{F}_{1,2}$	$\frac{m_{A2} \cdot g_1 \cdot d_2 \cdot l_1}{i_s \cdot l_1^2}$	2,564	N
$\dot{F}_{1,3}$	$\frac{m_{A1} \cdot g_2 \cdot d_1 \cdot l_1}{i_s \cdot l_1^2}$	46,33	N
$\dot{F}_{1,4}$	$\frac{m_{A2} \cdot g_2 \cdot d_2 \cdot l_1}{i_s \cdot l_1^2}$	51,3	N

**Table 6.4:** Results of the total force on one screw of concept A

Force	Formula	Result	Unit
$F_{c1,1}$	$\sqrt{\dot{F}_{1,1}^2 + \bar{F}_{1,1}^2}$	2,55	N
$F_{c1,2}$	$\sqrt{\dot{F}_{1,2}^2 + \bar{F}_{1,2}^2}$	2,81	N
$F_{c1,3}$	$\sqrt{\dot{F}_{1,3}^2 + \bar{F}_{1,3}^2}$	51	N
$F_{c1,4}$	$\sqrt{\dot{F}_{1,4}^2 + \bar{F}_{1,4}^2}$	56,3	N

### 6.3. Magnitude of forces of concept B

In figure 6.1 the established coordinate system and the forces, which may affect the system are shown. In this concept symmetry also applies, but the symmetry for the axis  $x$  and  $y$  is different. Therefore, it is necessary to calculate the action of forces in all three axes. The position of the center of gravity of concept B lies due to symmetry on the axis  $z$  and the distance from the bottom surface of assembly, in case of using aluminum alloy, is  $d_1 = 27,65$  mm and in the case of using titanium alloy the distance is  $d_2 = 27,62$  mm. Since the position of the center of gravity differs by only one hundredth of a millimeter, only one position of the center of gravity is considered.

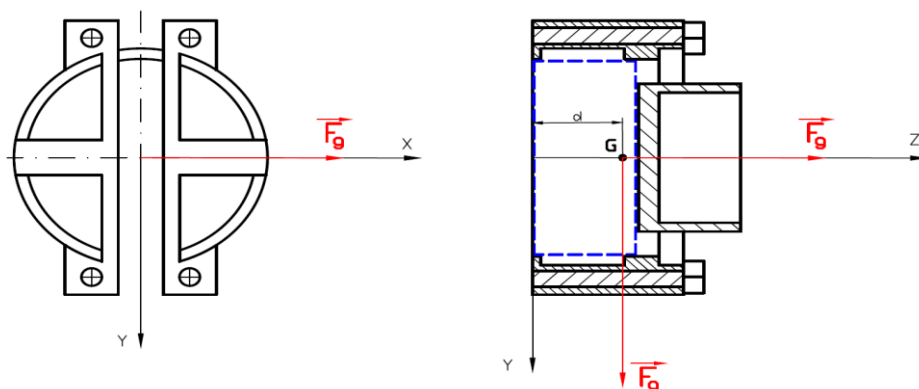


**Figure 6.3:** Forces and coordinate system of concept B

**Table 6.5:** Input values into the calculation of concept B

Mass of concept A with aluminium alloy	$m_{B1}$	0,4408	kg
Mass of concept A with titanium alloy	$m_{B2}$	0,4893	kg
The first gravitational acceleration	$g_1$	9,80665	$m \cdot s^{-2}$
The second gravitational acceleration	$g_2$	196,133	$m \cdot s^{-2}$
The first distance of the screw from the axis of rotation	$l_1$	0,012	m
The second distance of the screw from the axis of rotation	$l_2$	0,06882	m
Distance of the center of gravity from the axis of rotation for aluminium alloy	$d$	0,02765	m
Vertical rows of screws	$i_s$	2	-

For the situation when the gravitational force acts in the z-axis, therefore in the axis of the screws, equation 6.1 is used to calculate the forces in the screws. Similarly, forces distributed to the screws when loaded perpendicular to the screw axis are calculated and achieve similar values.

**Table 6.6:** Results of the force acting on the screw axis of concept B

Force	Formula	Result	Unit
$\overline{F_{2,1}}$	$\frac{m_{B1} \cdot g_1}{4}$	1,08	N
$\overline{F_{2,2}}$	$\frac{m_{B2} \cdot g_1}{4}$	1,2	N
$\overline{F_{2,3}}$	$\frac{m_{B1} \cdot g_2}{4}$	21,61	N
$\overline{F_{2,4}}$	$\frac{m_{B2} \cdot g_2}{4}$	24	N

For the calculation in a situation when the gravitational force acts perpendicular to the axes of the screws at a distance of  $d$  from the plane of screw placement, according to the diagrams in figure 6.4 and 6.5, the equation 6.8 is used. Since the symmetry along the axes  $x$  and  $y$  is not similar, it is necessary to calculate the forces acting perpendicular to the screws for two different distances of screws from the axis of rotation.

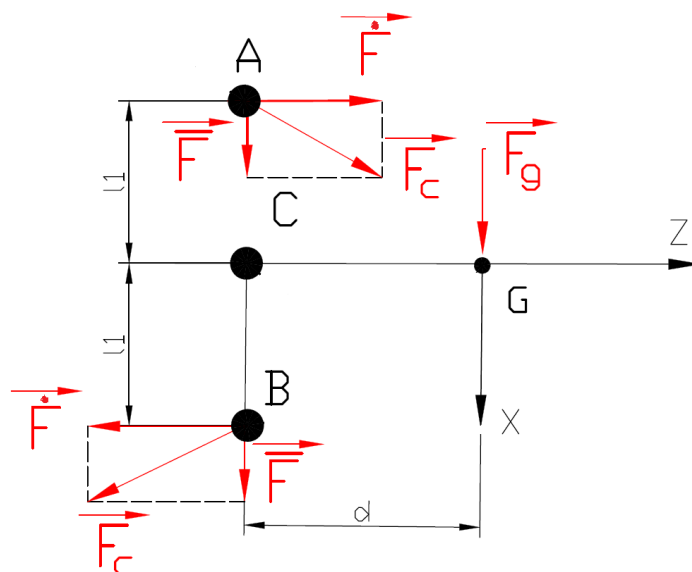


Figure 6.4: The first diagram for the force acting in the x-axis of concept B

Table 6.7: Results of the force in x-axis acting perpendicular to the axis of the screw of concept B

Force	Formula	Result	Unit
$\dot{F}_{2,1}$	$\frac{m_{B1} \cdot g_1 \cdot d \cdot l_1}{i_s \cdot l_1^2}$	5	N
$\dot{F}_{2,2}$	$\frac{m_{B2} \cdot g_1 \cdot d \cdot l_1}{i_s \cdot l_1^2}$	5,53	N
$\dot{F}_{2,3}$	$\frac{m_{B1} \cdot g_2 \cdot d \cdot l_1}{i_s \cdot l_1^2}$	99,6	N
$\dot{F}_{2,4}$	$\frac{m_{B2} \cdot g_2 \cdot d \cdot l_1}{i_s \cdot l_1^2}$	110,56	N

Table 6.8: Results of the total force in x-axis on one bolt of concept B

Force	Formula	Result	Unit
$F_{c2,1}$	$\sqrt{\dot{F}_{2,1}^2 + \bar{F}_{2,1}^2}$	5,12	N
$F_{c2,2}$	$\sqrt{\dot{F}_{2,2}^2 + \bar{F}_{2,2}^2}$	5,66	N
$F_{c2,3}$	$\sqrt{\dot{F}_{2,3}^2 + \bar{F}_{2,3}^2}$	102	N
$F_{c2,4}$	$\sqrt{\dot{F}_{2,4}^2 + \bar{F}_{2,4}^2}$	113,1	N

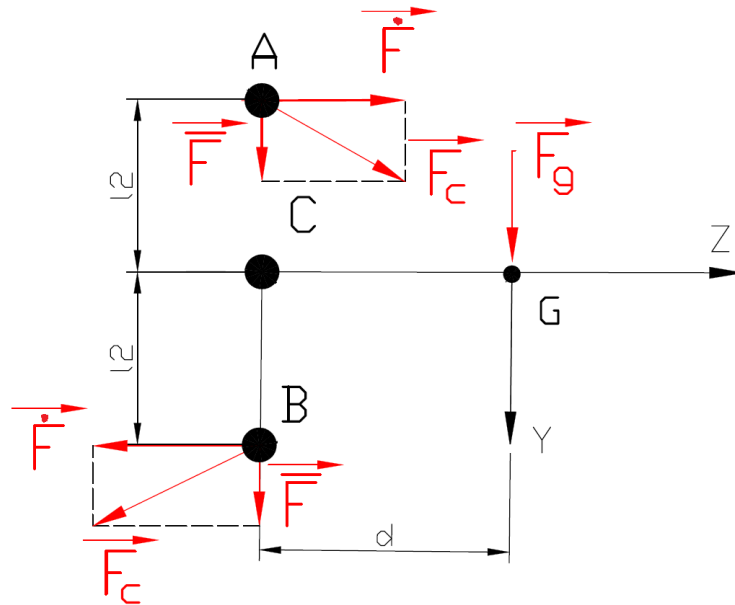


Figure 6.5: The second diagram for the force acting in the y-axis of concept B

Table 6.9: Results of the force in y-axis acting perpendicular to the axis of the bolt of concept B

Force	Formula	Result	Unit
$\dot{F}_{2,1}$	$\frac{m_{B1} \cdot g_1 \cdot d \cdot l_2}{i_s \cdot l_2^2}$	0,87	N
$\dot{F}_{2,2}$	$\frac{m_{B2} \cdot g_1 \cdot d \cdot l_2}{i_s \cdot l_2^2}$	0,96	N
$\dot{F}_{2,3}$	$\frac{m_{B1} \cdot g_2 \cdot d \cdot l_2}{i_s \cdot l_2^2}$	17,37	N
$\dot{F}_{2,4}$	$\frac{m_{B2} \cdot g_2 \cdot d \cdot l_2}{i_s \cdot l_2^2}$	19,28	N

Table 6.10: Results of the total force in y-axis on one bolt of concept B

Force	Formula	Result	Unit
$F_{c2,1}$	$\sqrt{\dot{F}_{2,1}^2 + \bar{F}_{2,1}^2}$	1,4	N
$F_{c2,2}$	$\sqrt{\dot{F}_{2,2}^2 + \bar{F}_{2,2}^2}$	1,54	N
$F_{c2,3}$	$\sqrt{\dot{F}_{2,3}^2 + \bar{F}_{2,3}^2}$	27,7	N
$F_{c2,4}$	$\sqrt{\dot{F}_{2,4}^2 + \bar{F}_{2,4}^2}$	30,8	N

## 6.4. Magnitude of forces of concept C

In figure 6.6 the established coordinate system and the forces, which may affect the system are shown. Due to symmetry, the force acting in axis  $x$  is similar as the one acting in axis  $y$ , which is why it is not mentioned here. The position of the centre of gravity of concept C is, due to symmetry, on the axis  $z$  and the distance from the bottom surface of the assembly, in the case of using aluminium alloy, is  $d_1 = 26,124$  mm and in the case of using titanium alloy the distance is  $d_2 = 24,98$  mm.

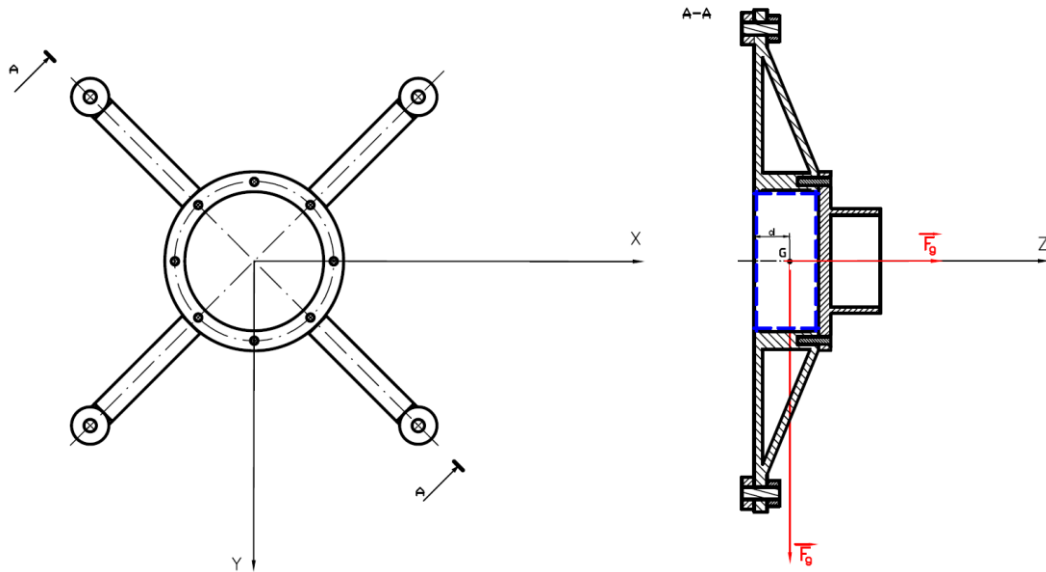


Figure 6.6: Forces and coordinate system of concept C

Table 6.11: Input values into the calculation of concept C

Mass of concept A with aluminium alloy	$m_{C1}$	0,6061	kg
Mass of concept A with titanium alloy	$m_{C2}$	0,6583	kg
The first gravitational acceleration	$g_1$	9,80665	$m \cdot s^{-2}$
The second gravitational acceleration	$g_2$	196,133	$m \cdot s^{-2}$
Distance of the screw from the axis of rotation	$l_1$	0,0661	m
Distance of the center of gravity from the axis of rotation for aluminium alloy	$d_1$	0,026124	m
Distance of the centre of gravity from the axis of rotation for titanium alloy	$d_2$	0,02498	m
Vertical rows of screws	$i_s$	2	-

For the situation when the gravitational force acts in the z-axis, therefore in the axis of the screws, equation 6.1 is used to calculate the forces in the screws. Similarly, forces distributed to the screws when loaded perpendicular to the screw axis are calculated and achieve similar values.

**Table 6.12:** Results of the force acting on the screw axis of concept C

Force	Formula	Result	Unit
$\overline{F_{3,1}}$	$\frac{m_{C1} \cdot g_1}{4}$	1,5	N
$\overline{F_{3,2}}$	$\frac{m_{C2} \cdot g_1}{4}$	1,614	N
$\overline{F_{3,3}}$	$\frac{m_{C1} \cdot g_2}{4}$	29,72	N
$\overline{F_{3,4}}$	$\frac{m_{C2} \cdot g_2}{4}$	32,3	N

For the calculation in a situation when the gravitational force acts perpendicular to the axes of the screws at a distance of  $d$  from the plane of screw placement, according to the diagram in the figure 6.7, the equation 6.8 is used.

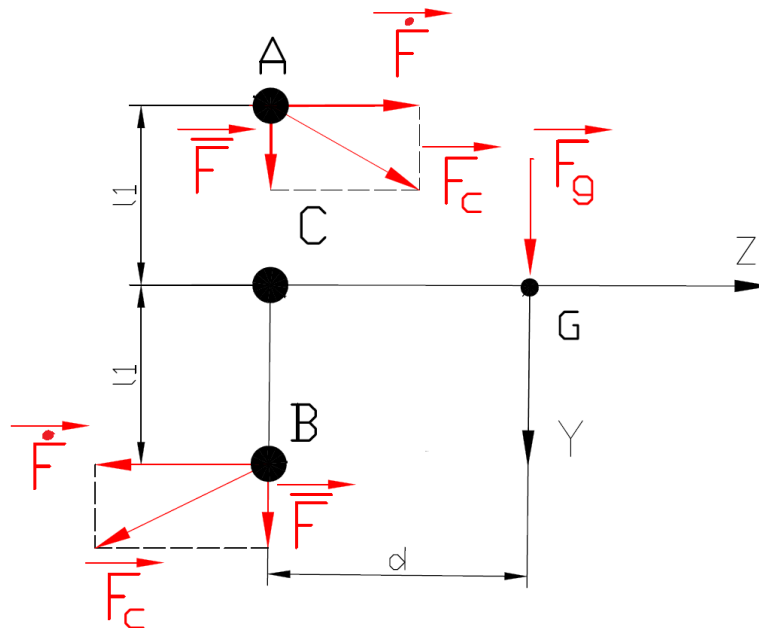


**Figure 6.7:** Diagram for the force acting in the y-axis of concept C

**Table 6.13:** Results of the force acting perpendicular to the axis of the screw of concept C

Force	Formula	Result	Unit
$\dot{F}_{3,1}$	$\frac{m_{C1} \cdot g_1 \cdot d_1 \cdot l_1}{i_s \cdot l_1^2}$	1,17	N
$\dot{F}_{3,2}$	$\frac{m_{C2} \cdot g_1 \cdot d_2 \cdot l_1}{i_s \cdot l_1^2}$	1,22	N
$\dot{F}_{3,3}$	$\frac{m_{C1} \cdot g_2 \cdot d_1 \cdot l_1}{i_s \cdot l_1^2}$	23,5	N
$\dot{F}_{3,4}$	$\frac{m_{C2} \cdot g_2 \cdot d_2 \cdot l_1}{i_s \cdot l_1^2}$	24,4	N

**Table 6.14:** Results of the total force on one screw of concept C

Force	Formula	Result	Unit
$F_{c3.1}$	$\sqrt{\dot{F}_{3.1}^2 + \bar{F}_{3.1}^2}$	1,9	N
$F_{c3.2}$	$\sqrt{\dot{F}_{3.2}^2 + \bar{F}_{3.2}^2}$	2	N
$F_{c3.3}$	$\sqrt{\dot{F}_{3.3}^2 + \bar{F}_{3.3}^2}$	37,9	N
$F_{c3.4}$	$\sqrt{\dot{F}_{3.4}^2 + \bar{F}_{3.4}^2}$	40,5	N

## 6.5. Magnitude of forces of concept D

In figure 6.6 the established coordinate system and the forces, which may affect the system are shown. Due to symmetry, the force acting in axis  $x$  is similar as the one acting in axis  $y$ , which is why it is not mentioned here. In this construction however, there is a certain change. Unlike previous concepts, this one is rigidly attached on both sides and not just one. This means that when force is applied in both the positive and negative directions of the  $z$ -axis, this force will not only distribute between the screws, but also on the surfaces that the MHS touches on both sides. It is thus possible to express, according to the equation 6.9, only the pressure exerted by the gravitational force MHS on the surface of the radiation plate, in the case of a force in the positive  $z$ -axis direction or on the surface of the box wall, in the case of a force in the negative  $z$ -axis direction.



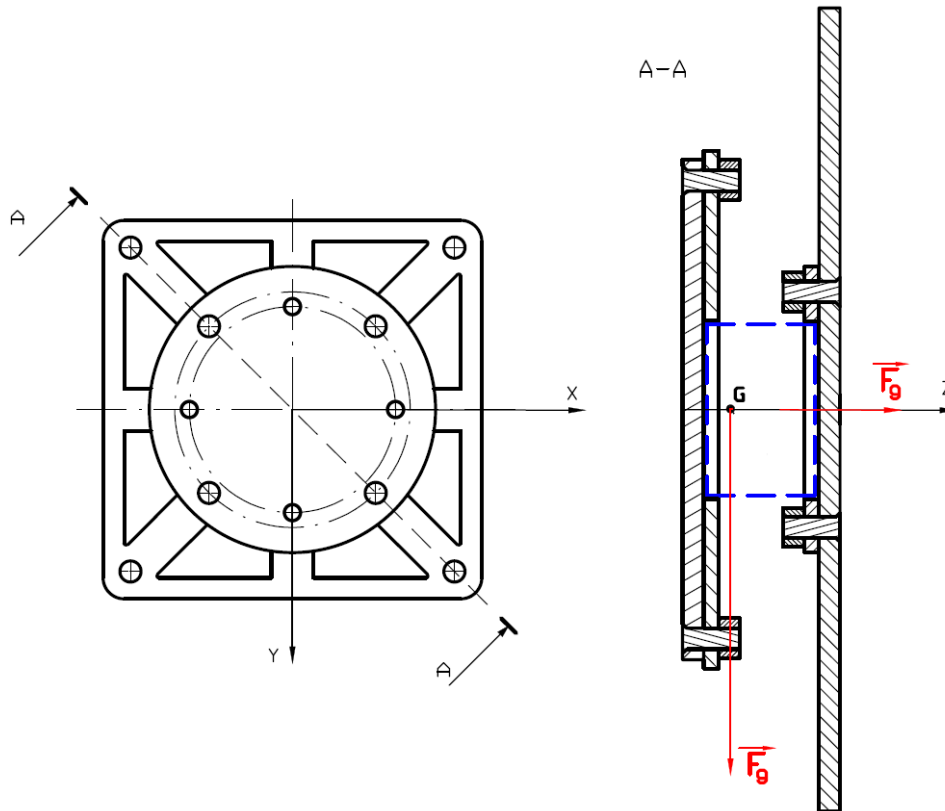


**Figure 6.8:** Forces and coordinate system of concept D

**Table 6.15:** Input values into the calculation of concept D

Mass of concept A with aluminium alloy	$m_D$	0,3357	kg
The first gravitational acceleration	$g_1$	9,80665	$m \cdot s^{-2}$
The second gravitational acceleration	$g_2$	196,133	$m \cdot s^{-2}$
Distance of the center of gravity from the axis of rotation	$d$	0,0066	m
Distance of the center of the group of screw from each of them	$r_1$	0,04087	m
Distance of the center of the group of screw from each of them	$r_2$	0,03117	m
Vertical rows of screws	$i_s$	2	-
Touch area of MHS and radiation plate	$S_1$	0,00351	$m^2$
Touch area of MHS and box	$S_2$	0,004255	$m^2$

Calculation of pressure from acting force

$$p = \frac{F}{S} \text{ [Pa]} \quad (6.9)$$

**Table 6.16:** Results of pressure induced by gravity of concept D

Force	Formula	Result	Unit
$p_{D4.1}$	$\frac{m_D \cdot g_1}{S_1}$	938	Pa
$p_{D4.2}$	$\frac{m_D \cdot g_1}{S_2}$	773,7	Pa
$p_{D4.3}$	$\frac{m_D \cdot g_2}{S_1}$	18 758	Pa
$p_{D4.4}$	$\frac{m_D \cdot g_2}{S_2}$	15 474	Pa

In the case of force acting perpendicular on the screw axis, the equation 6.8 is used. In this case, the center of the screw group is at another location. The distance  $d$  is in this case the distance of the center of gravity from the axis of rotation – point C. The diagram of the distribution of forces on the screws is shown in the figure 6.9.

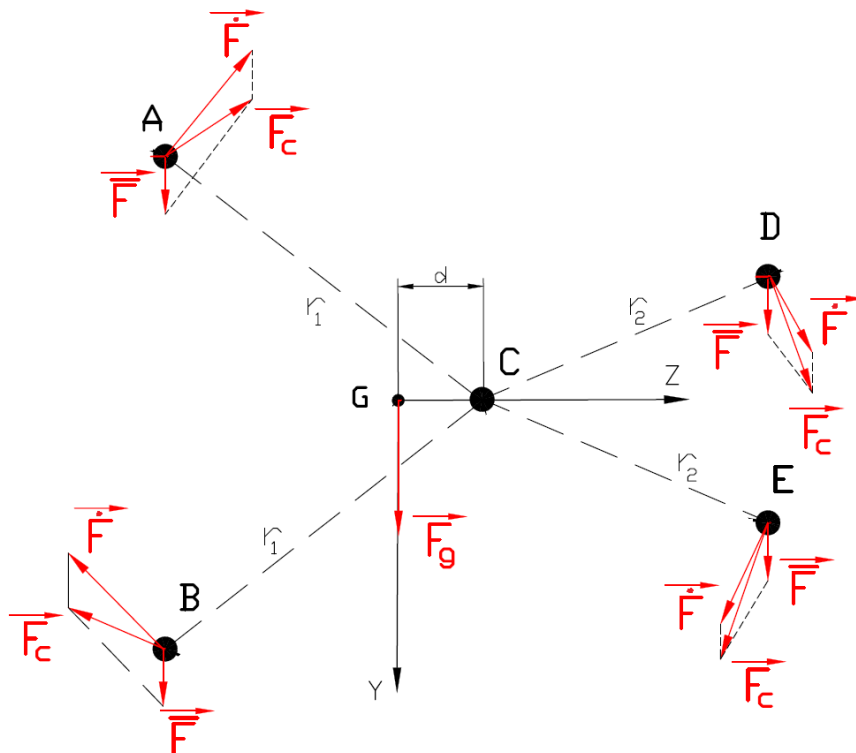


**Figure 6.9:** Diagram for the force acting in the y-axis of concept D

The load of each screw from the transverse force acting perpendicular to its axis is calculated according to the equation 6.1. In this case,  $i = 8$  screws contribute to the force distribution.

$$\overline{F}_{4,1} = \frac{m_D \cdot g_1}{i} = \frac{0,3357 \cdot 9,80665}{8} = 0,41 \text{ [N]}$$

$$\overline{F}_{4,2} = \frac{m_D \cdot g_2}{i} = \frac{0,3357 \cdot 196,133}{8} = 8,23 \text{ [N]}$$

**Table 6.17:** Results of the force acting perpendicular to the y-axis of the screw of concept D

Force	Formula	Result	Unit
$\dot{F}_{4,1}$	$\frac{m_D \cdot g_1 \cdot d \cdot r_1}{i_s \cdot r_1^2}$	0,27	N
$\dot{F}_{4,2}$	$\frac{m_D \cdot g_1 \cdot d \cdot r_2}{i_s \cdot r_2^2}$	0,35	N
$\dot{F}_{4,3}$	$\frac{m_D \cdot g_2 \cdot d \cdot r_1}{i_s \cdot r_1^2}$	5,32	N
$\dot{F}_{4,4}$	$\frac{m_D \cdot g_2 \cdot d \cdot r_2}{i_s \cdot r_2^2}$	7	N

**Table 6.18:** Results of the total force on one screw of concept D

Force	Formula	Result	Unit
$F_{c4,1}$	$\sqrt{\dot{F}_{4,1}^2 + \overline{F}_{4,1}^2}$	0,5	N
$F_{c4,2}$	$\sqrt{\dot{F}_{4,1}^2 + \overline{F}_{4,2}^2}$	0,54	N
$F_{c4,3}$	$\sqrt{\dot{F}_{4,2}^2 + \overline{F}_{4,3}^2}$	9,8	N
$F_{c4,4}$	$\sqrt{\dot{F}_{4,2}^2 + \overline{F}_{4,4}^2}$	10,87	N

## 7. Discussion

The aim for calculating the thermal conductivity of each concept is to find out to what extent they are conductive, possibly insulating. This is because through the construction of the concepts only in the first platform a stable thermal way around the MHS is created. However, if these concepts were not sufficiently insulating, the heat flow regulation function, which is provided by the MHS, would be lost.

According to the input parameters required for the thermal conductivity calculation, the material characteristics in tables 4.2 and 4.3, and the chosen construction dimensions based on the models, are by the procedure described in chapter 5.1 calculated thermal conductivities of all four concepts. Based on resistance theory, since the individual components of these concepts form resistances in the heat flow similarly as in an electrical circuit resistors resist the electrical current, the total thermal conductivity values of each concept are calculated, as well as the constructions. This is achieved by removing the MHS and its contacts with the construction from the thermal way. Thus, all the heat is going through the construction only. Then this calculation is done similarly for the case, where a 2 mm layer of Teflon (PTFE) is inserted into the MHS junctions with the construction. From the knowledge of density of the used material and the dimensions of the construction, the total weight of the assemblies and the constructions itself is also calculated. From the values of thermal conductivity and weight the specific parameter is gained as a means for comparison and evaluation, since the main goal of the concepts is to achieve the lowest total weight while also achieving the lowest thermal conductivity of the constructions itself.

From the resulting parameters listed in individual tables in chapter 5.2 the constructions can be judged between each other, or assess the change of thermal conductivity and weight within one construction when changing the material used.

Within the individual constructions, in all three cases a significant decrease of thermal conductivity of the construction can be seen, as well as an increase in weight due to the use of titanium alloy instead of an aluminium alloy. This is because the titanium alloy has a significantly lower thermal conductivity and greater density than the aluminium alloy. As can be seen from the comparison of the specific parameter, the increase in weight is relatively lower than the decrease in conductivity, which is the main goal.

*Table 7.1: Comparison of specific parameter of separate structures*

	Material	Specific parameter
		[-]
<b>Separate structure of concept A</b>	Aluminium alloy	0,12
	Titanium alloy	0,0043
<b>Separate structure of concept B</b>	Aluminium alloy	1,724
	Titanium alloy	0,088
<b>Separate structure of concept C</b>	Aluminium alloy	2,93
	Titanium alloy	0,111

From the point of view of the use of the material, the titanium alloy works better despite its weight increase due to its exceptionally low thermal conductivity. The final decision for the material will depend on the specific requirements, what maximum weight value of the whole assembly must be adhered to. Also, the options of technologies for the construction production

from both materials must be taken account into this decision. In this respect, aluminium alloy offers a greater degree of variability and production possibilities.

During the comparison of the resulting values between the individual concepts, a significant increase in thermal conductivity and the specific parameter can be noticed for the third concept C. It is a demonstration of the importance of the construction as well, outside of the use of material. In the first two concepts, A and B when not considering the MHS, the heat is always transferred from the terminal of the flexible conductive component to the rest of the structure through several beams, which have a small area but longer length in the direction of the heat flow. Whereas in concept C there are no beams. Numerically, this can be seen in the values of resistance to heat flow in individual structures (annex B). The same trend is also observable when adding a thin PTFE tape.

In the case of adding this thin PTFE tape, a wanted and aimed reduction in thermal conductivity can be seen. This reduction is not in all concepts though, and especially for material change it is proportionally similar. From the resulting values follows, that by adding PTFE tape into a titanium alloy construction the thermal conductivity is reduced much less than by having an aluminium alloy construction. It follows that for alloys with generally low conductivity, the shape and dimensions of the components are more important. Whereas for alloys with higher thermal conductivity, the addition of additional insulator is more important.

*Table 7.2: Comparison of specific parameter of separate structures with PTFE*

	Material	Specific parameter
		[-]
<b>Separate structure of concept A</b>	Aluminium alloy	0,032
	Titanium alloy	0,00412
<b>Separate structure of concept B</b>	Aluminium alloy	0,0472
	Titanium alloy	0,0196
<b>Separate structure of concept C</b>	Aluminium alloy	0,12
	Titanium alloy	0,0423

The concept D cannot be compared with these methods. It does not contain any additional external structure outside the MHS, which would ensure the connection of the flexible conductive component and the radiation plate. Therefore, there is no danger of losing the heat regulation function as in the previous concepts because the changes are limited to the MHS. In the previous concepts from the whole first platform, the aim was to limit their heat conductivity. But in this case, the opposite is true. Here the aim is to achieve the highest thermal conductivity or at least achieve the smallest total reduction. By comparing the values between the original un-modified MHS and the new modified MHS, the total conductivity was reduced and there was an increase in weight. This was also reflected in the specific parameter, which was reduced by about half compared to the original MHS. However, the value of the total conductivity stayed above  $1 \text{ W} \cdot \text{K}^{-1}$ , which is a requirement for this project given by ESA.

In the force analysis of concepts, the aim is to determine the distribution and magnitude of forces acting on individual screws, with which the constructions are attached to the radiation plate and in the case of concept D also to the box wall. These forces arise from the loading force, which is the gravitational force of individual concepts. Based on the ESA requirements, where it is necessary that the MHS, and the construction as well, will endure 20 times the normal gravitational acceleration of Earth, the forces in the screws are calculated for two values of gravitational. At the same time, the resulting forces are calculated for two different weights given by two different materials of the concepts, except concept D.

After the introduction of the coordinate system into the centre of gravity of the concepts, it is obvious that two different cases of gravitational force can occur in space. Due to the multiple symmetry of concepts and the rotational symmetry of the MHS and its attachment in concepts, the gravitational force can act on one hand in the z axis passing through the axis of this rotational symmetry of concepts as well as in one of the axes x or y, as for the second axis of x or y the same case occurs. The concept B, however, does not offer the same symmetry along the axes x and y. It is therefore necessary to perform calculation along all three axes in concept B.

From the resulting values of the total forces acting on screws, summarized in table 7.3, it is evident, that the greatest forces acting on individual screws will show in concept B. The greatest magnitude of force is in concept B achieved under the action of gravitational force on the x-axis of the concept. At the same time, it is a case where the gravitational force is magnified to 20 times the gravitational acceleration of Earth. On the other hand, the smallest forces acting on the screws are in concept D. From this point of view, this concept would seem to be the most appropriate choice.

*Table 7.3: Comparison of total forces*

	Force	Value		Force	Value
		[N]			[N]
<b>Total forces of concept A</b>	$F_{c1.1}$	2,55	<b>Total forces of concept B</b>	$F_{c2.1}$	5,12
	$F_{c1.2}$	2,81		$F_{c2.2}$	5,66
	$F_{c1.3}$	51		$F_{c2.3}$	102
	$F_{c1.4}$	56,3		$F_{c2.4}$	113,1
<b>Total forces of concept C</b>	$F_{c3.1}$	1,9	<b>Total forces of concept D</b>	$F_{c4.1}$	0,5
	$F_{c3.2}$	2		$F_{c4.2}$	0,54
	$F_{c3.3}$	37,9		$F_{c4.3}$	9,8
	$F_{c3.4}$	40,5		$F_{c4.4}$	10,87

The next step leading to the final selection of a suitable construction is the strength or FEA analysis. This analysis should showcase, if the concepts and their individual parts are able to endure all loads, from gravitational force based on the chosen level of safety that will be required. If the concepts will also satisfy this analysis, even with greater safety than required, the purposeful phase of optimization may occur so that the lower possible weight of the concepts will be achieved. In case the concepts or any of the concepts would not be suitable, another iteration with modified dimensions would happen. In both cases another total thermal control, determination of the distribution of forces into the screws, according to the procedure given in this thesis, and subsequently again FEA analysis would occur.

From the resulting values, comparison of individual concepts and derived final considerations, it is possible to select the most suitable concept and material. The most suitable material appears to be titanium alloy due to its exceptionally low thermal conductivity and small weight gain compared to aluminium alloy. Of the concepts based on the analysis of thermal conductivity and the distribution of forces on the screws, concept A with titanium alloy is the most suitable.

## 8. Conclusion

Based on the project given by ESA, dealing with the issue of MHS as a heat dissipation regulator from devices inside the spacecrafts, there was a demand for the creation of conceptual designs of MHS constructions integrated into the satellite. This Master thesis deals with this topic. The goal is, based on the suitable literature perform a search of components used in present time for the MHS construction and securing the thermal way for the heat dissipation. The next part contains the aim to design, based on given requirements, concepts for the MHS construction and then perform thermal control and determine the force distribution into attachment points of the construction.

First part of the Master thesis deal with the description and analysis of individual and important part for heat dissipation and within the heat path. MHS is a part of the passive thermal control. This is due to the fact, that it does not need any external energy source for its function. MHS is capable of dissipating and regulating heat based on PCM material that it contains. For this reason, the search is focused primarily on the parts from the passive thermal control, as they are a part of a suitable thermal way for the heat dissipation through MHS. Because there is vacuum in the open space, and during the mission fulfilment there are no other bodies located in the immediate location of the satellite – it must get rid of the redundant heat generated from electrical devices through radiation. The so-called radiation plate exists for this reason. The plate is constructed and contains required surface modifications so that it can emit to the greatest extent – radiate heat to the surrounding space. For this reason, it is situated and mounted on the exterior of the satellite or may also be part of the satellite wall itself. For cases where the satellite is moving close to the planets or the satellite's radiators are facing the sun, Louvers are usually placed in front of the radiators. These serve to ensure that the radiators do not receive a large amount of radiation from the space. Radiators have such a form that they are able, in addition to very effective emission of radiation into space, also easily receive this radiation, both by radiation and conduction. Thanks to this attribute of radiators, the most suitable placement of MHS is a place, where direct contact between MHS and the radiator occurs. Based on this knowledge, form of the concepts unfolds for the MHS structure. Since the devices inside the satellite, as heat sources, are not always located directly at the satellite walls, it is necessary to include in the heat path a component that will be able to transmit to a certain distance up to the MHS. This member can be, for example, a flexible conductive component mentioned in chapter 3.5.

The created concepts of the MHS structure integrated into the satellite structure, which are part of the second part of this thesis, must ensure fixed and constant connections of this flexible conductive component with the MHS. Based on more specific requirements, that are mentioned in the conclusion of chapter 3 and in the first subchapters of the chapter 4, which include, for example:

- Fixation of the flexible conductive component to the MHS and the MHS to the radiation plate
- Reinsurance of the lowest thermal conductivity, so that the MHS functions is not disturbed
- Construction ergonomics, so that is does not influence the satellite interior

four concepts of the MHS structure are designed into the satellite construction. Each of these concepts is designed for a different mounting method.

- Concept A – designed as an external construction, where the flexible conductive component needs to be integrated. MHS is then inserted into the assembly. The whole assembly is screwed to the radiation plate with four screws.
- Concept B – designed as an external construction for the case, where the flexible conductive component cannot be integrated through the concept. It is therefore possible to add it to the concept from the side. MHS it is then inserted into the concept structure and it is again screwed to the radiation plate with four screws.
- Concept C – designed as an external construction, where the flexible conductive component is not inserted, but it is screwed from one side. The MHS is then inserted into this structure. At the same time, it is designed in such a way that it is screwed to the frame around the radiation plate.
- Concept D – this is not an external structure, but only a modification of the external parts of the MHS. The concept is also designed to be screwed to the radiation plate and at the same time screwed to the box with electronics as a heat source.

In the next part of this work, the calculation of thermal conductivity of these concepts is done for two different types of materials – aluminium a titanium alloy. From the resulting values of the calculation it follows, that the titanium alloys are more effective for the concepts even at the cost of a slight increase of weight. At the same time, the results showed that by adding a thin PTFE tape into the contact points of the MHS with the concept construction the heat transfer through the structure is significantly reduced. The lowest values of the specific parameter, which gives the ratio of thermal conductivity and weight of the structure, is achieved by concept A. From the point of thermal conductivity, this concept is most suitable. The concept D is also very suitable, which on the contrary achieves a large specific parameter, which is desirable in this case, mainly due to its low weight, but the total thermal conductivity after the modification of parts of MHS decreased significantly.

From other calculations, that deal with the force distribution on individual screws in contact places of the construction and also is another part of this work, the most suitable concept is D. This is mainly because it is fastened with more screws on both sides compared to other concepts. When considering and comparing all the resulting values, concept A generally appears to be the most advantageous when using a titanium alloy with a thin PTFE strip at the points of contact of the MHS with the structure.

For the next part of the development of the MHS structure installed into the satellite construction, a concept should be selected, where the properties are universally the most advantageous.



## 9. Bibliography

- [1] 2019 CuTS® Catalog: TAI's Copper Thermal Strap Standard Product Line [online]. In: 2019 [cit. 2020-05-18]. Dostupné z: <https://www.techapps.com/cuts-catalog>
- [2] ČERNOCH, Jakub. Vývoj struktury pro efektivní přenos tepla. Brno, 2020. Dostupné také z: <https://www.vutbr.cz/studenti/zav-prace/detail/125297>. Diplomová práce. Vysoké učení technické v Brně, Fakulta strojního inženýrství, Letecký ústav. Vedoucí práce Jakub Mašek.
- [3] BANDEEN, William R. a Tomas H. VONDER HAAR. *EARTH ALBEDO AND EMITTED RADIATION*. Washington D.C.: NASA, 1971.
- [4] BONTANO, Giuseppe, MASSIMO, Conte, ADAMI, Marco. *Miniaturized Thermal Switch, Breadboard Tests and Design Selection Report*. Aero Sekur, August 2017, 52 pages. TN05 301609 A, Rev. A.
- [5] BONTANO, Giuseppe, MASSIMO, Conte, ADAMI, Marco. *Miniaturized Thermal Switch, Detailed Design Report*. Aero Sekur, August 2017, 29 pages. TN06 301609 A, Rev. A.
- [6] BOUSHON, Katelyn E. *Thermal analysis and control of small satellites in low Earth orbit*. Missouri, 2018. Master's Thesis. Missouri University of Science and Technology. Vedoucí práce Henry Pernicka.
- [7] DORNIER SYSTEM, "Phase Change Materials", Internal Report, Dornier System GmbH, Friedrichshafen, Germany, 1971.
- [8] ECSS-E-HB-31-01 PART 5A. *Space engineering: Thermal design hand book – Part 5: Structural Materials: Metallic and Composite*. 5 December 2011. Noordwijk, The Netherlands: ECSS Secretariat, 2011.
- [9] ECSS-E-HB-31-01 PART 6A. *Space engineering: Thermal design hand book – Part 6: Thermal Control Surfaces*. 5 December 2011. Noordwijk, The Netherlands: ECSS Secretariat, 2011.
- [10] ECSS-E-HB-31-01 PART 7A. *Space engineering: Thermal design hand book – Part 7: Insulations*. 5 December 2011. Noordwijk, The Netherlands: ECSS Secretariat, 2011.
- [11] ECSS-E-HB-31-01 PART 8A. *Space engineering: Thermal design hand book – Part 8: Heat pipes*. 5 December 2011. Noordwijk, The Netherlands: ECSS Secretariat, 2011.
- [12] ECSS-E-HB-31-01 PART 9A. *Space engineering: Thermal design hand book – Part 9: Radiators*. 5 December 2011. Noordwijk, The Netherlands: ECSS Secretariat, 2011.
- [13] ECSS-E-HB-31-01 PART 10A. *Space engineering: Thermal design hand book – Part 10: Phase-Change Capacitors*. 5 December 2011. Noordwijk, The Netherlands: ECSS Secretariat, 2011.

- 
- [14] ECSS-E-HB-31-01 PART 11A. *Space engineering: Thermal design hand book – Part 11: Electrical Heating*. 5 December 2011. Noordwijk, The Netherlands: ECSS Secretariat, 2011.
- [15] ECSS-E-HB-31-01 PART 12A. *Space engineering: Thermal design hand book – Part 12: Louvers*. 5 December 2011. Noordwijk, The Netherlands: ECSS Secretariat, 2011.
- [16] ECSS-E-HB-31-01 PART 15A. *Space engineering: Thermal design hand book – Part 15: Existing satellites*. 5 December 2011. Noordwijk, The Netherlands: ECSS Secretariat, 2011.
- [17] ECSS-E-HB-32-22A. *Space engineering: Insert design handbook*. 20 March 2011. Noordwijk, The Netherlands: ECSS Secretariat, 2011.
- [18] ESA SOW HEAT SWITCH. *Statement of Work, Miniaturised Heat Switch, Annex 1: Preliminary Functional Specification*. European Space Agency: AG Noordwijk zh, The Netherlands, published: 11. 05. 2011, 24 pages. TEC-MTT/2011/3756/In/SL. Appendix 1 to ITT 1-6801/11/NL/NA
- [19] *ESA Structures: Composite Joints and Inserts* [online]. European Space Agency, 2007 [cit. 2020-06-08]. Dostupné z: [http://www.esa.int/TEC/Structures/SEM95EWUP4F\\_0.html](http://www.esa.int/TEC/Structures/SEM95EWUP4F_0.html)
- [20] FALSTAD, Paul. Online simulátor elektronických obvodů. OLMR, Vít. *Vyvoj.hw.cz: profesionální elektronika* [online]. 2014, 2005 [cit. 2020-06-22]. Dostupné z: <http://www.falstad.com/circuit/index.html>
- [21] G. GILMORE, David. *Spacecraft Thermal Control Handbook: Volume I: Fundamental Technologies*. 2nd ed. El Segundo, California: The Aerospace Press, VA: American Institute of Aeronautics and Astronautics, 2002. ISBN 1-884989-11-X.
- [22] *IDA Science and Technology Policy Institute: Global Trends in Small Satellites* [online]. Institute for Defense Analyses, 2017 [cit. 2020-05-12]. Dostupné z: <https://www.ida.org/>
- [23] *Jet Propulsion Laboratory: Spacecraft* [online]. California: California Institute of Technology [cit. 2020-05-15]. Dostupné z: [https://www.jpl.nasa.gov/news/press\\_kits/insight/launch/mission/spacecraft/](https://www.jpl.nasa.gov/news/press_kits/insight/launch/mission/spacecraft/)
- [24] KARAM, Robert D., ZARCHAN, Paul, ed. *Satellite Thermal Control for Systems Engineers*. Volume 181. Virginia 20191-4344: American institute of Aeronautics and Astronautics, 1998. ISBN 1-56347-276-7.
- [25] KUPLÍK, V. *Stavební konstrukce z požárního hlediska*. Praha: Grada Publishing, 2006. ISBN 80-247-1329-2.
- [26] MAŠEK, J. *Funkční zkouška tepelného spínače pro prostředí planety Mars*. Brno: Vysoké učení technické v Brně, Fakulta strojního inženýrství, 2016. 129 s. Vedoucí diplomové práce Ing. Robert Popela, Ph.D.

- [27] MAŠEK, J., HORÁK, M., ZIKMUND, P., *Miniaturized Thermal Switch Report on BB Testing* Brno: V technické v Brně, Fakulta strojního inženýrství, 2017
- [28] M.M Yovanovich, *New Contact and Gap Correlations for Conforming Rough Surface*, AIAA-81-1164, presented at AIAA 16th Thermophysics Conference, Palo Alto, CA., June 1981.
- [29] M.M Yovanovich, *Theory and Applications of Constriction and Spreading Resistance Concepts for Microelectronic Thermal Management*, Cooling Techniques for Computers, Editor Win Aung, Hemisphere Publishing Corporation, 1991, pp. 277- 332.
- [30] M.M Yovanovich and V.W. Antonetti, *Applications of Thermal Contact Resistance Theory to Electronic Packages*, Advances in Thermal Modeling of Electronic Components and Systems, Vol. 1, Editors A.Bar-Cohen and A.D. Kraus, Hemisphere Publishing Corporation, 1998, pp. 79-128.
- [31] Nature's Crusaders: *Decrease global warming by raising crops with a high albedo* [online]. WordPress.com, 2008 [cit. 2020-03-19]. Dostupné z: <https://naturescrusaders.wordpress.com/2009/02/20/decrease-global-warming-by-raising-crops-with-a-high-albedo/albedo-dartmouth/>
- [32] *New Horizons: NASA's Mission to Pluto and the Kuiper Belt* [online]. Baltimore (Maryland): The Johns Hopkins University Applied Physics Laboratory, 2020 [cit. 2020-05-15]. Dostupné z: <http://pluto.jhuapl.edu/>
- [33] POPELA, R., MAŠEK, J. *Heat Switch Design Overview & Advanced MHS definition*, Brno: Vysoké učení technické v Brně, Fakulta strojního inženýrství, 2017
- [34] RAVENETTI, Mario, MORGANTI, Francesco, BATTOCCHIO, Luciano. *Miniaturized Heat Switch, Requirement Document*. Aero Sekur, July 2012, 23 pages. TN02 310609 A, Rev. A.
- [35] RELEA, E, L WEISS, R KUSSMAUL, M ZOGG, G RAMSTEIN a K WEGENER. Precisely Adjustable Inserts for Stiffness-Driven CFRP Sandwich Structures. In: *Procedia CIRP* [online]. Elsevier B.V, 2017, 66, s. 294-299 [cit. 2020-06-08]. DOI: 10.1016/j.procir.2017.03.175. ISSN 2212-8271. Dostupné z: <https://www-sciencedirect-com.ezproxy.lib.vutbr.cz/science/article/pii/S2212827117303578>
- [36] RICHMOND, J. A. *Adaptive Thermal Modeling Architecture for Small Satellite Applications*. Cambridge, 2010. Master thesis. Massachusetts Institute of Technology.
- [37] R.D. Karam, *Satellite Thermal Control for Systems Engineers*. Reston, VA: American Institute of Aeronautics and Astronautics, Inc., 1998.
- [38] SHIGLEY, Joseph E., Charles R. MISCHKE a Richard G. BUDYANS. *Konstruování strojních součástí*. Brno: Vutium, 2010. ISBN 978-80-214-2629-0.
- [39] *Shutterstock* [online]. Shutterstock, 2020 [cit. 2020-04-12]. Dostupné z: <https://www.shutterstock.com/cs/search/heat+transfer+radiation>

- [40] *United Launch Alliance* [online]. 2019 [cit. 2020-06-14]. Dostupné z: <https://www.ulalaunch.com/>
- [41] V.W. Antonetti and M.M Yovanovich, *Thermal Contact Resistance in Microelectronic Equipment*, Thermal Management Concepts in Microelectronic Packaging From Component to Systems, ISHM Technical Monograph Series 6984-003, 1984, pp. 135-151.
- [42] *Wilhelm Böllhoff GmbH & Co. KG: A strong joint* [online]. Germany, 2020 [cit. 2020-06-08]. Dostupné z: <https://www.boellhoff.com/de-en/index.php>
- [43] Y. A. Cengel, *Heat Transfer A Practical Approach*. Boston, MA: McGraw-Hill, Inc., 1998.
- [44] ZAPATA, Edgar. *The State of PlayUS Space Systems Competitiveness: Prices, Productivity, and Other Measures of Launchers & Spacecraft* [online]. October 11, 2017, , 25 [cit. 2020-06-14]. Dostupné z: <https://ntrs.nasa.gov/archive/nasa/casi.ntrs.nasa.gov/20170009967.pdf>
- [45] ECSS-Q-ST-70-36C. *Space product assurance: Material selection for controlling stress-corrosion cracking*. 6 March 2009. Noordwijk, The Netherlands: ECSS Secretariat, 2009.

## List of figures

*Figure 1.1: First type of location of heat switch*

*Figure 1.2: Second type of location of heat switch*

*Figure 1.3: Original concept MHS*

*Figure 1.4: Original conductive structure*

*Figure 1.5: Deployment of individual members*

*Figure 2.1: Modes of heat transfer*

*Figure 2.2: Modes of radiation*

*Figure 2.3: The range of thermal conductivity of various materials at room temperature*

*Figure 3.1: Heater*

*Figure 3.2: Heat-pipe schematic*

*Figure 3.3: Structure of IUE*

*Figure 3.4: Structure of InSight*

*Figure 3.5: Radiator*

*Figure 3.6: Louvers*

*Figure 3.7: Detail of control element*

*Figure 3.8: Effective thermal conductivity of MLI as compared with other insulation materials*

*Figure 3.9: Surface properties by type of finish*

*Figure 3.10: Thermal conductivity vs. mean temperature for several fibrous insulations*

*Figure 3.11: Composition of a typical MLI blanket*

*Figure 3.12: Effect of gas pressure on thermal conductivity*

*Figure 3.13: Electronic box*

*Figure 3.14: Electronic box built up from modules*

*Figure 3.15: Thermally conductive component from the company TAI*

*Figure 3.16: Typical Insert*

*Figure 3.17: Typical basic Insert*

*Figure 3.18: Three types of insert assembly*

*Figure 3.19: Partially potted insert*

*Figure 3.20: Cut of insert*

*Figure 4.1: The first system diagram*

*Figure 4.2: The second system diagram*

*Figure 4.3: The third system diagram*

*Figure 4.4: The fourth system diagram*

*Figure 4.5: Basic dimensions of first type termination*

*Figure 4.6: Basic dimensions of second type termination*

*Figure 4.7: Composition of concept A*

*Figure 4.8: Basic dimensions of concept A*

*Figure 4.9: Disassembled assembly of concept A*

*Figure 4.10: Composition of concept B*

*Figure 4.11: Basic dimensions of concept B*

*Figure 4.12: Disassembled assembly of concept B*

*Figure 4.13: Composition of concept C*

*Figure 4.14: Basic dimensions of concept C*

*Figure 4.15: Disassembled assembly of concept C*

*Figure 4.16: Concept D*

**Figure 4.17:** Basic dimensions of concept D

**Figure 4.18:** Composition of concept D

**Figure 4.19:** Disassembled assembly of concept D

**Figure 5.1:** The resulting parameters of the concept A

**Figure 5.2:** The resulting parameters of the separate structure of concept A

**Figure 5.3:** The resulting parameters of the concept B

**Figure 5.4:** The resulting parameters of the separate structure of concept B

**Figure 5.5:** The resulting parameters of the concept C

**Figure 5.6:** The resulting parameters of the separate structure of concept C

**Figure 6.1:** Forces and coordinate system of concept A

**Figure 6.2:** Diagram for the force acting in the y-axis of concept A

**Figure 6.3:** Forces and coordinate system of concept B

**Figure 6.4:** The first diagram for the force acting in the x-axis of concept B

**Figure 6.5:** The second diagram for the force acting in the y-axis of concept B

**Figure 6.6:** Forces and coordinate system of concept C

**Figure 6.7:** Diagram for the force acting in the y-axis of concept C

**Figure 6.8:** Forces and coordinate system of concept D

**Figure 6.9:** Diagram for the force acting in the y-axis of concept D

## List of tables

*Table 2.1: Albedo of planets*

*Table 2.2: Examples of heat transfer coefficient*

*Table 2.3: The thermal conductivities of some materials in 25 °C*

*Table 3.1: Examples of temperature ranges*

*Table 3.2: Types of radiators*

*Table 3.3: Explanations for the graph*

*Table 3.4: Price for 1 kg launched into LEO*

*Table 4.1: List of concepts*

*Table 4.2: List of materials for concepts*

*Table 4.3: Thermal Interface/contact Conductivity*

*Table 5.1: The resulting parameters of the concept A*

*Table 5.2: The resulting parameters of the separate structure of concept A*

*Table 5.3: The resulting parameters of the concept A with PTFE*

*Table 5.4: The resulting parameters of the separate structure of concept A with PTFE*

*Table 5.5: The resulting parameters of the concept B*

*Table 5.6: The resulting parameters of the separate structure of concept B*

*Table 5.7: The resulting parameters of the concept B with PTFE*

*Table 5.8: The resulting parameters of the separate structure of concept B with PTFE*

*Table 5.9: The resulting parameters of the concept C*

*Table 5.10: The resulting parameters of the separate structure of concept C*

*Table 5.11: The resulting parameters of the concept C with PTFE*

*Table 5.12: The resulting parameters of the separate structure of concept C with PTFE*

*Table 5.13: The resulting parameters of the concept D*

*Table 6.1: Input values into the calculation of concept A*

*Table 6.2: Results of the force acting on the screw axis of concept A*

*Table 6.3: Results of the force acting perpendicular to the axis of the bolt of concept A*

*Table 6.4: Results of the total force on one screw of concept A*

*Table 6.5: Input values into the calculation of concept B*

*Table 6.6: Results of the force acting on the screw axis of concept B*

*Table 6.7: Results of the force in x-axis acting perpendicular to the axis of the screw of concept B*

*Table 6.8: Results of the total force in x-axis on one bolt of concept B*

*Table 6.9: Results of the force in y-axis acting perpendicular to the axis of the bolt of concept B*

*Table 6.10: Results of the total force in y-axis on one bolt of concept B*

*Table 6.11: Input values into the calculation of concept C*

*Table 6.12: Results of the force acting on the screw axis of concept C*

*Table 6.13: Results of the force acting perpendicular to the axis of the screw of concept C*

*Table 6.14: Results of the total force on one screw of concept C*

*Table 6.15: Input values into the calculation of concept D*

*Table 6.16: Results of pressure induced by gravity*

*Table 6.17: Results of the force acting perpendicular to the y-axis of the screw of concept D*

*Table 6.18: Results of the total force on one screw of concept C*

*Table 7.1: Comparison of specific parameter of separate structures*

*Table 7.2: Comparison of specific parameter of separate structures with PTFE*

*Table 7.3: Comparison of total forces*

## List of short cuts and symbols

Symbol	Unit	Description
$\alpha$	-	Absorptivity
$\varepsilon$	-	Emissivity
$\theta$	°	Incident angle
$\lambda$	$\text{W}\cdot\text{m}^{-1}\cdot\text{K}^{-1}$	Coefficient of thermal conductivity
$\rho$	$\text{kg}\cdot\text{m}^{-3}$	Mass density
$\sigma$	$\text{W}\cdot\text{m}^{-2}\cdot\text{K}^{-4}$	Stefan-Boltzmann constant
A	$\text{m}^2$	Area
$A_f$	$\text{m}^2$	Area of radiation plate
$A_j$	$\text{m}^2$	Area of honeycomb structure
ATCS	-	Active thermal control system
BUT	-	Brno University of Technology
C	$\text{W}\cdot\text{K}^{-1}$	Thermal conductivity
d	m	Distance of the center of gravity from the axis of rotation
$d_e$	m	Depth
$\frac{dT}{dX}$	$\text{K}\cdot\text{m}^{-1}$	Temperature gradient
E	Pa	Young's Modulus
$E_0$	$\text{W}\cdot\text{m}^{-2}$	Radiation intensity (black body)
$E_g$	$\text{W}\cdot\text{m}^{-2}$	Radiation intensity (grey body)
$E_\alpha$	$\text{W}\cdot\text{m}^{-2}$	Heat flux by Albedo radiation
$E_p$	$\text{W}\cdot\text{m}^{-2}$	Heat flux by Planetary radiation
$E_s$	W	Radiant performance
ESA	-	European Space Agency
F	N	Force
$\bar{F}$	N	The force acting on the bolt in the direction of its axis
$\dot{F}$	N	Force acting perpendicular to the axis of the screw
$F_c$	N	Total force
$F_g$	N	Gravity



---

g	$\text{m}\cdot\text{s}^{-2}$	Gravitational acceleration
$G_s$	$\text{W}\cdot\text{m}^{-2}$	Solar constant
h	$\text{W}\cdot\text{m}^{-2}$	Heat transfer coefficient of convection
IR	-	Infra-red
i	-	Number of screws
$i_s$	-	Nuber of vertical rows of screws
$k_{\text{eff}}$	-	Effective thermal conductivity
L	m	Distance of the Earth from the Sun
l	-	Distance of the screw from the axis of rotation
LEO	-	Low Earth Orbit
m	kg	Weight
$m_0$	kg	Weight of current MHS design
$m_{\text{MHS}}$	kg	Weight of new MHS modification
MHS	-	Miniaturized Heat Switch
MLI	-	Multilayer Insulation
NASA	-	National Aeronautics and Space Administration
PCM	-	Phase-Change Materials
PTCS	-	Passive thermal control system
$Q_c$	J	Heat flux of conduction
$Q_v$	W	Heat of convection
r	m	Radius of the Sun
R	$\text{K}\cdot\text{W}^{-1}$	Thermal resistance
Re	Pa	Yield Strength
S	$\text{m}^2$	Touch area of MHS
s	$\text{W}\cdot\text{m}^{-2}$	Solar constant
$S_p$	-	Specific parameter
T	K	Temperature
TCS	-	Thermal control system
t	s	Time
ULA	-	United Launch Alliance

# Appendix

- A1 List of used parts in original concept of MHS
- A2 List of used parts in concept A
- A3 List of used parts in concept B
- A4 List of used parts in concept C
- A5 List of used parts in concept D
- B1 Intermediate calculation values for concept A
- B2 Intermediate calculation values for concept B
- B3 Intermediate calculation values for concept C
- B4 Intermediate calculation values for concept D

## A1 List of used parts in original concept of MHS

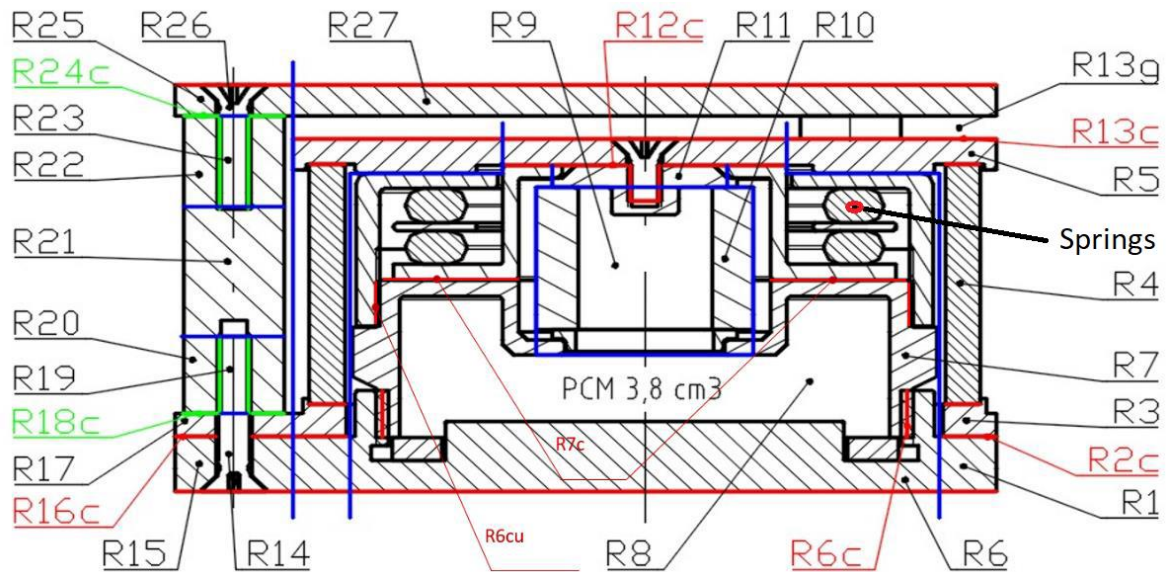


*Figure A1.1: Deployment of individual members of MHS [n]*

- R1 – Base plate (part 1)
- R3 – Base braid textile (part 1)
- R4 – Braid textile
- R5 – Cold plate
- R6 – Base plate (part 2)
- R7 – Container wax
- R8 – Paraffin (part 1)
- R9 – Paraffin (part 2)
- R10 – Bellow assy
- R11 – Upper flange
- R14 – Bolt for Elastomer insulator (bottom – part 1)
- R15 – Base plate (part 3)
- R17 – Base braid textile (part 2)
- R19 – Bolt for Elastomer insulator (bottom – part 2)
- R20 – Elastomer insulator (part 1)
- R21 – Elastomer insulator (part 2)
- R22 – Elastomer insulator (part 3)
- R23 – Bolt for Elastomer insulator (upper – part 1)
- R25 – Contact plate (part 1)
- R26 – Bolt for Elastomer insulator (upper – part 2)
- R27 – Contact plate (part 2)

## A2 List of used parts in concept A

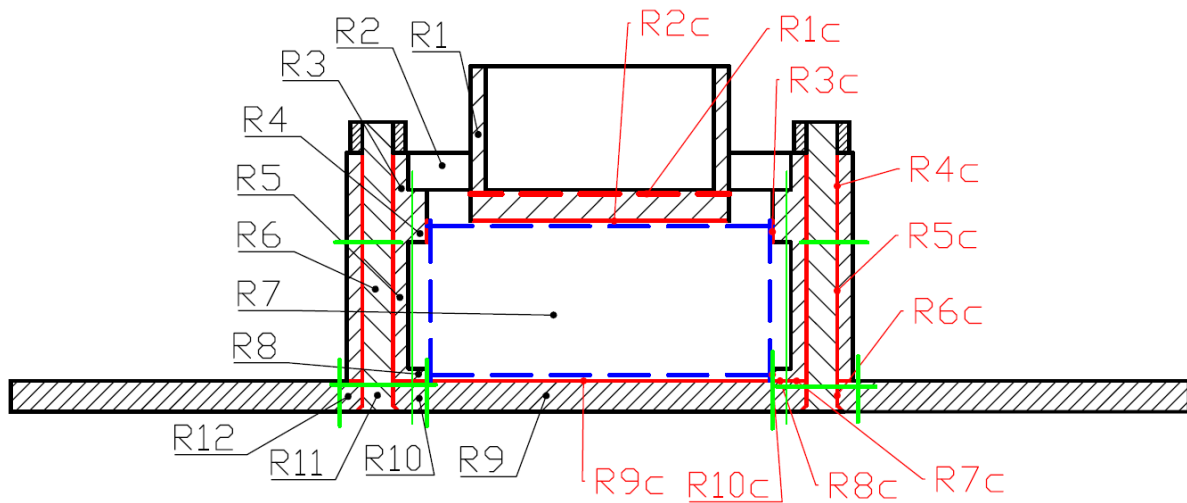


**Figure A2.1:** Deployment of individual members of Concept A

- R1 – Termination of the first flexible conductive component
- R2 – Beam
- R3 – Column (part 1)
- R4 – Upper belt
- R5 – Column (part 2)
- R6 – Bolt (part 1)
- R7 – MHS
- R8 – Lower belt
- R9 – Radiation plate (part 1)
- R10 – Radiation plate (part 2)
- R11 – Bolt (part 2)
- R12 – Radiation plate (part 3)

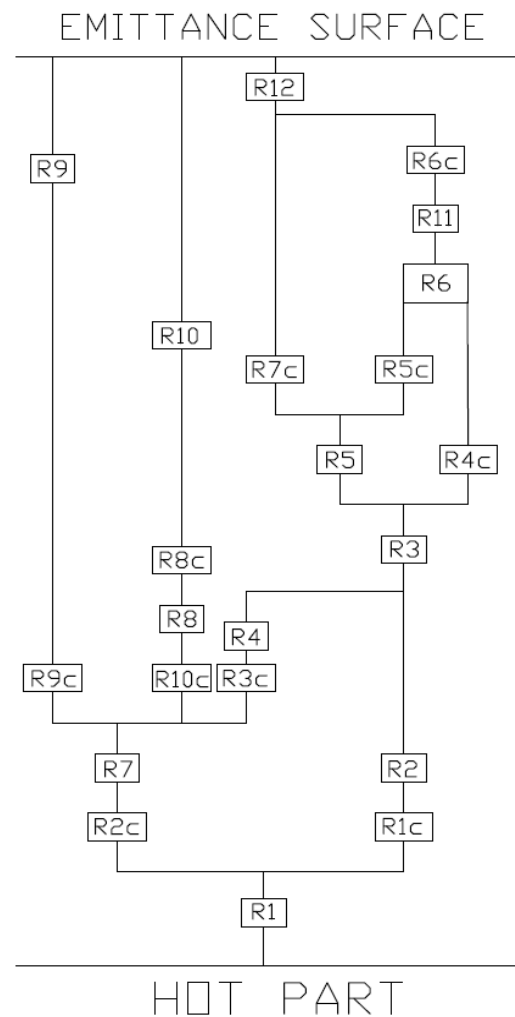


**Figure A2.2:** Heat path of the concept A

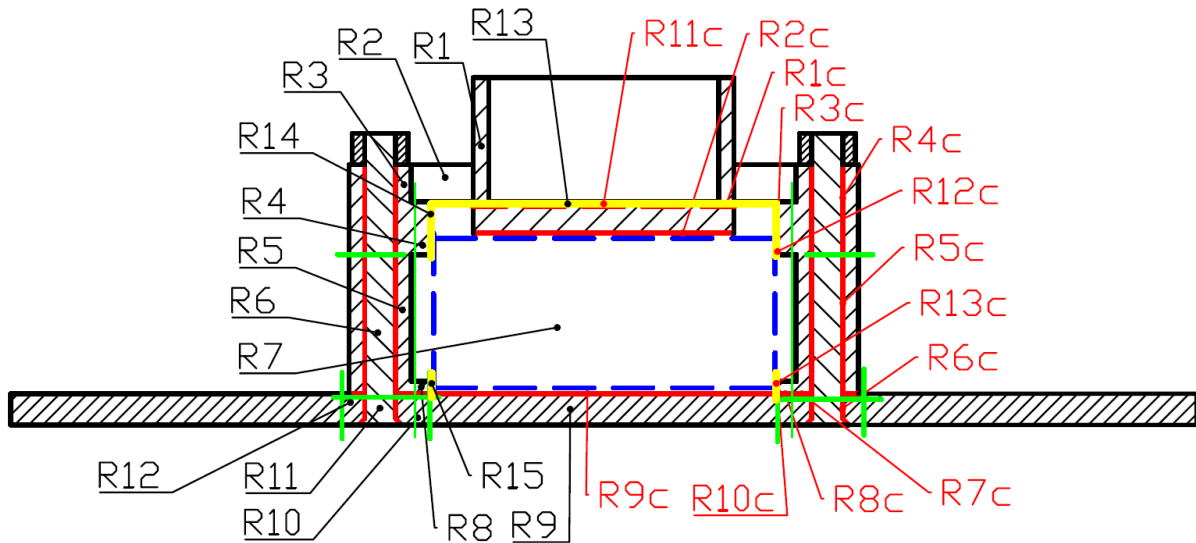


**Figure A2.3:** Deployment of individual members of Concept A with PTFE

- R13 – Upper PTFE (part 1)
- R14 – Upper PTFE (part 2)
- R15 – Lower PTFE

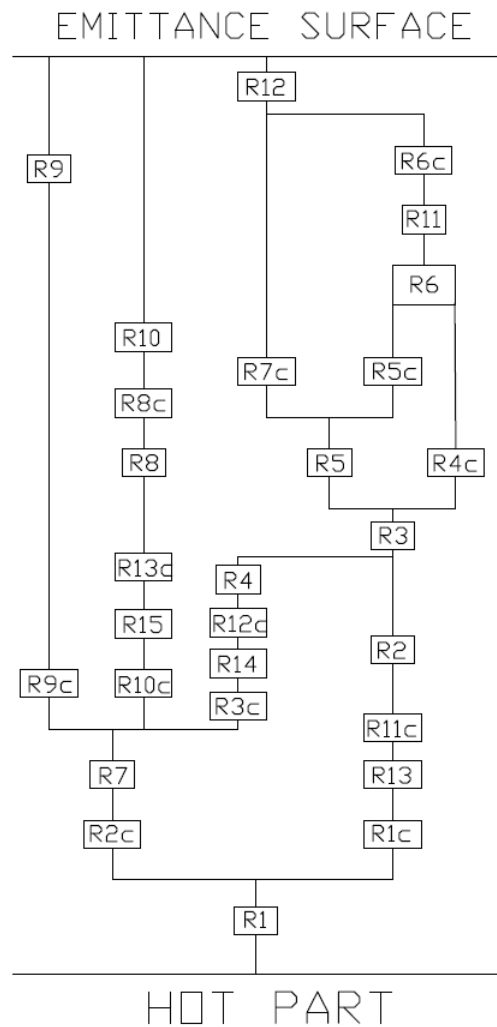


**Figure A2.4:** Heat path of the concept A with PTFE

### **A3 List of used parts in concept B**

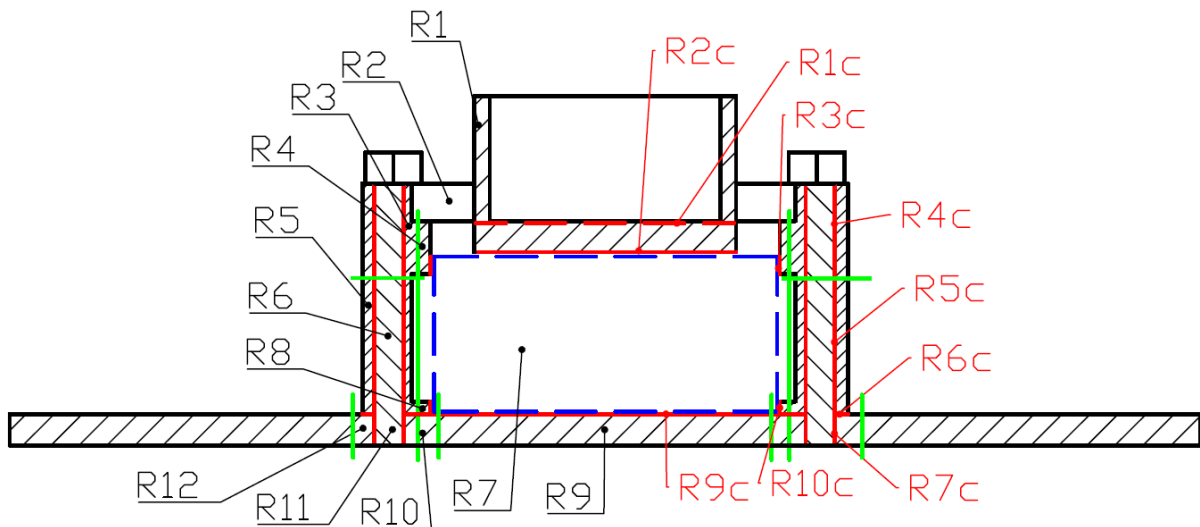


**Figure A3.1:** Deployment of individual members of Concept **B** (part 1)

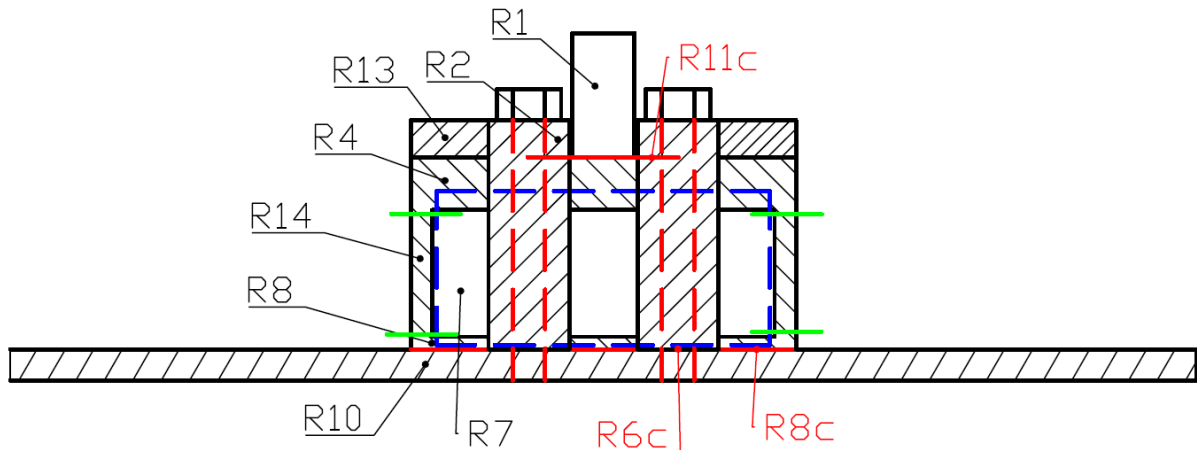


**Figure A3.2:** Deployment of individual members of Concept **B** (part 2)

- R1 – Termination of the first flexible conductive component
- R2 – First beam
- R3 – Column (part 1)
- R4 – Upper belt
- R5 – Column (part 2)
- R6 – Bolt (part 1)
- R7 – MHS
- R8 – Lower belt
- R9 – Radiation plate (part 1)
- R10 – Radiation plate (part 2)
- R11 – Bolt (part 2)
- R12 – Radiation plate (part 3)
- R13 – Second beam
- R14 – Rib

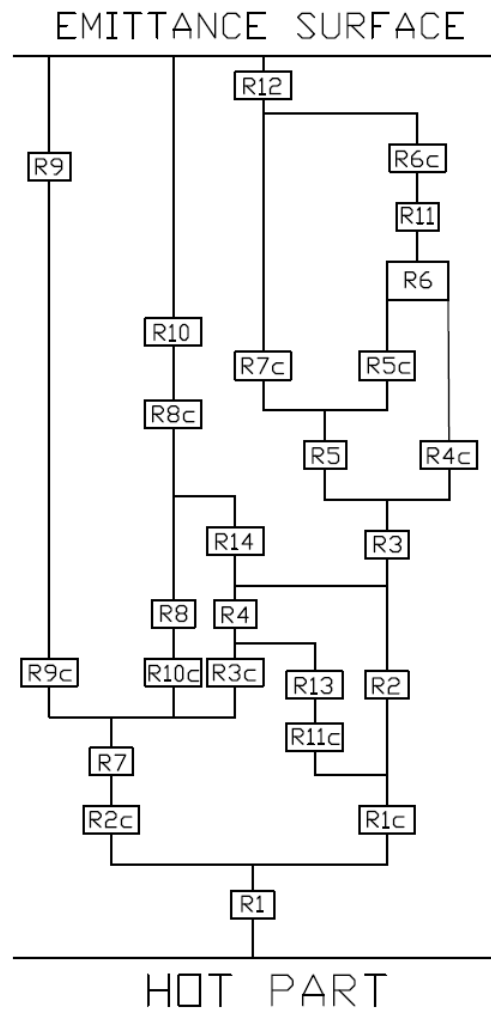


**Figure A3.3:** Heat path of the concept **B**

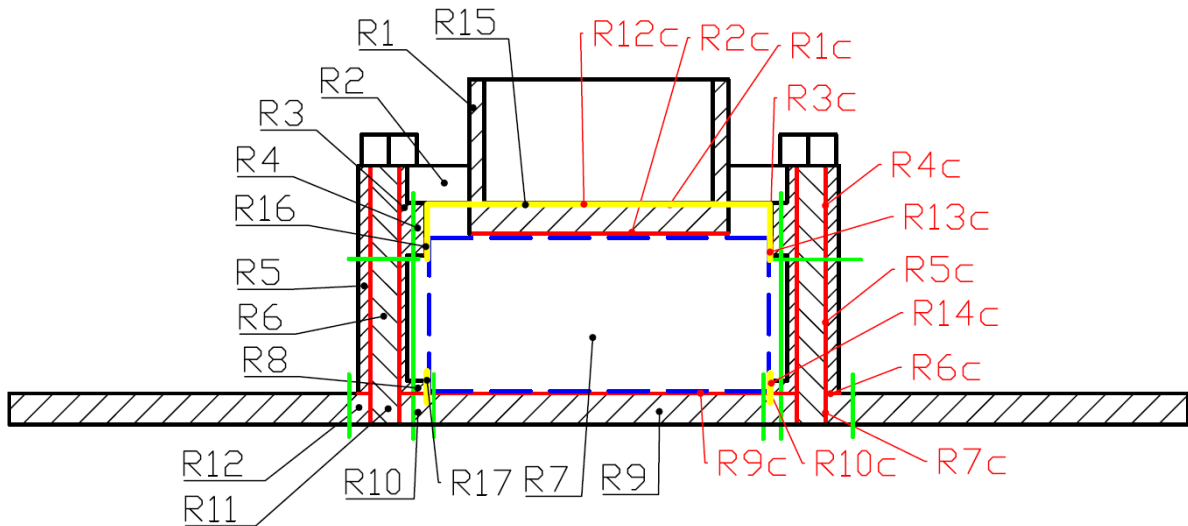


**Figure A3.4:** Deployment of individual members of Concept **B** with PTFE

- R15 – Upper PTFE (part 1)
- R16 – Upper PTFE (part 2)
- R17 – Lower PTFE

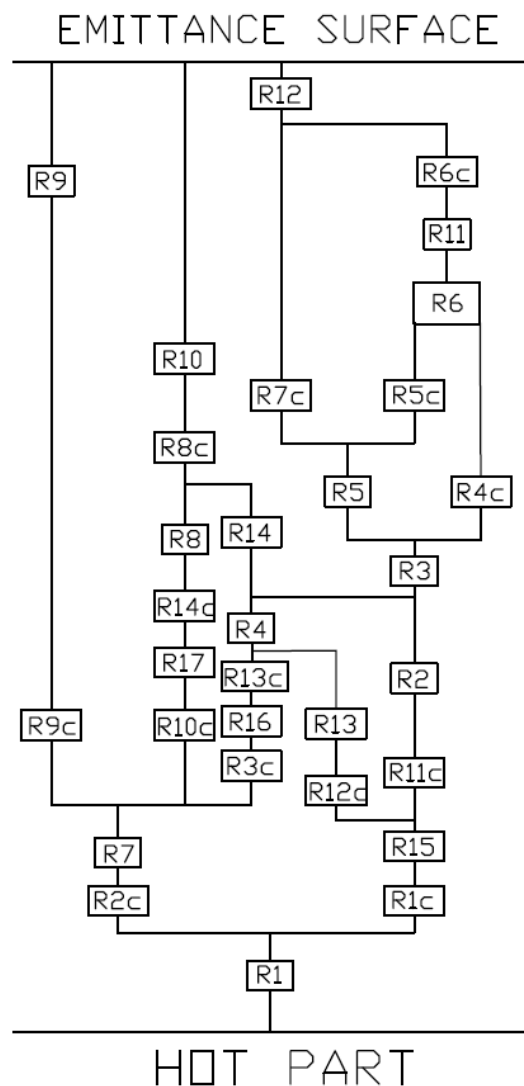


**Figure A3.5:** Heat path of the concept **B** with PTFE



## A4 List of used parts in concept C

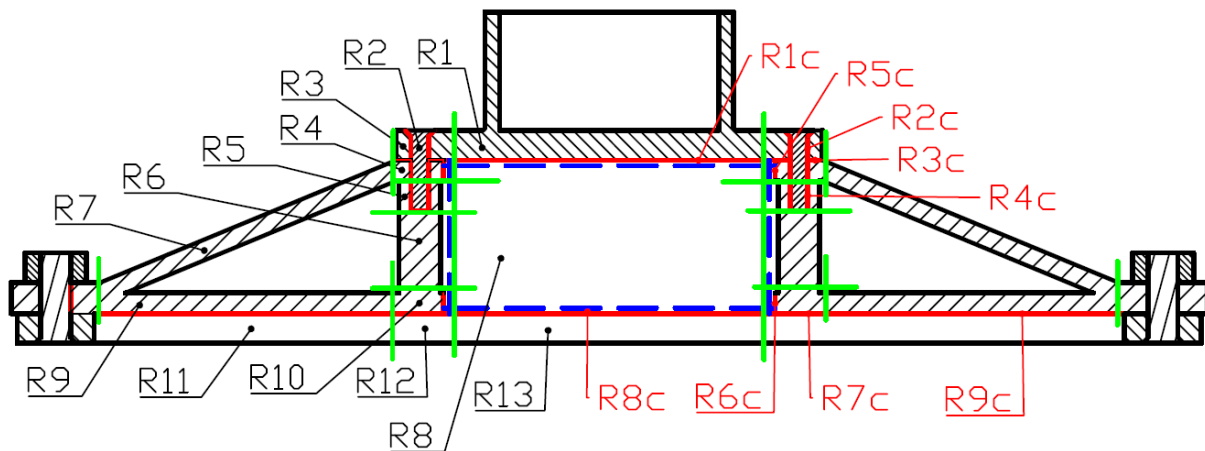


**Figure A4.1:** Deployment of individual members of Concept C

- R1 – Termination of the second flexible conductive component (part 1)
- R2 – Bolt
- R3 – Termination of the second flexible conductive component (part 2)
- R4 – Column (part 1)
- R5 – Column (part 2)
- R6 – Column (part 3)
- R7 – Upper rib
- R8 – MHS
- R9 – Lower rib
- R10 – Column (part 4)
- R11 – Radiation plate (part 1)
- R12 – Radiation plate (part 2)
- R13 – Radiation plate (part 3)

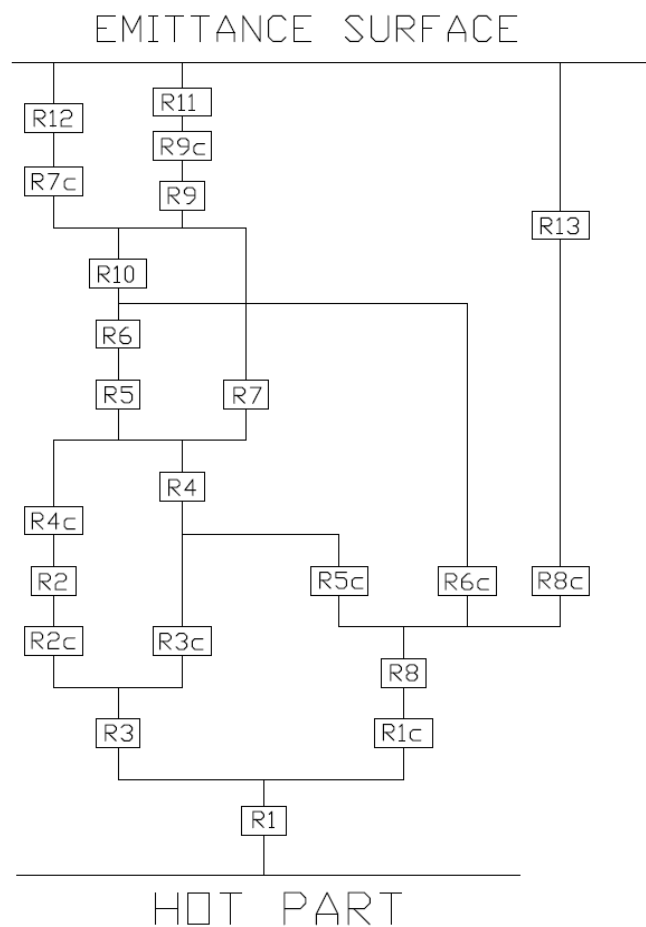


**Figure A4.2:** Heat path of the concept C

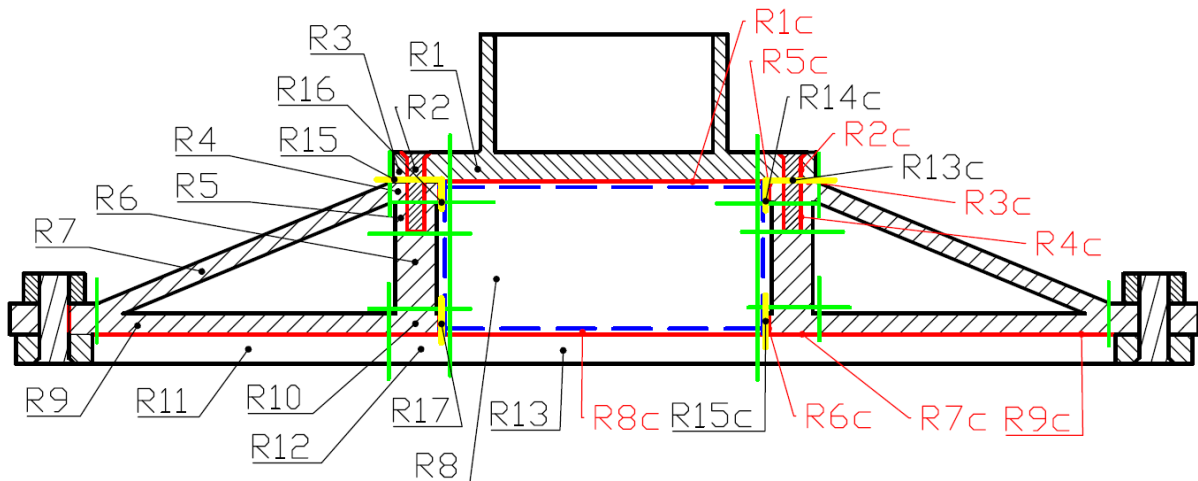


**Figure A4.3:** Deployment of individual members of Concept C with PTFE

- R15 – Upper PTFE (part 1)
- R16 – Upper PTFE (part 2)
- R17 – Lower PTFE

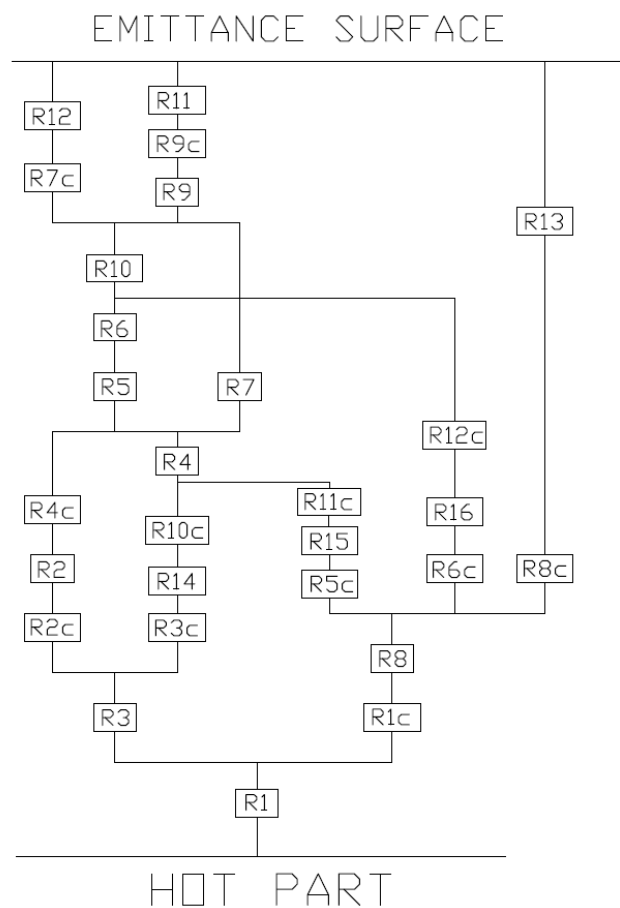


**Figure A4.4:** Heat path of the concept C with PTFE

## **A5 List of used parts in concept D**

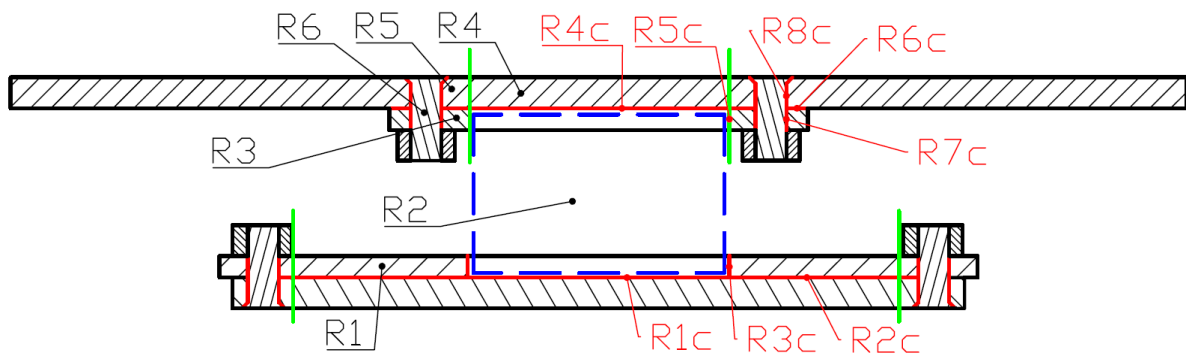


**Figure A4.1:** Deployment of individual members of Concept D

- R1 – Outside part of baseplate of MHS
- R2 – MHS
- R3 – Outside part of coldplate of MHS
- R4 – Radiation plate (part 1)
- R5 – Radiation plate (part 1)
- R6 – Bolt

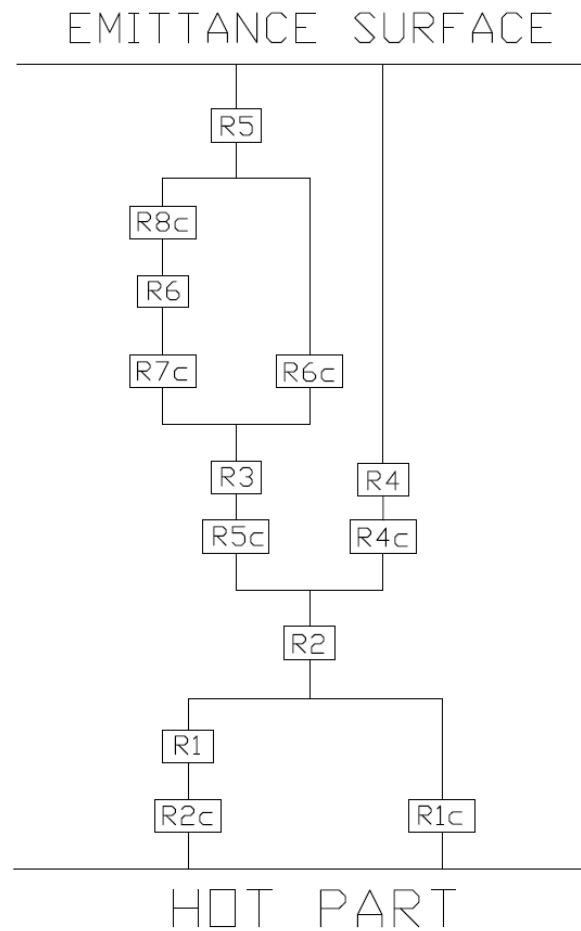


**Figure A4.2:** Heat path of the concept D

## **B1 Intermediate calculation values for concept A**

For used material Aluminium 2024:

<b>R</b>	<b>Volume</b>	<b>Thermal Conductivity</b>	<b>Thermal contact Conductivity</b>	<b>Thermal Resistance</b>
	[m3]	[W/mK]	[W/m2K]	[K / W]
R1	8,32E-06	391		0,1229589
R1_01	6,93E-06	391		0,009229
<b>R1c</b>			3864,79985	0,5454166
R2	6,96E-06	120		100,69444
<b>R2c</b>			6785,898763	0,1063542
R3	5,35E-06	120		1,3091369
<b>R3c</b>			3864,79985	0,4202106
R4	4,49E-06	120		0,016718
<b>R4c</b>			5693077,9	0,0001928
R5	8,27E-06	120		2,0223908
<b>R5c</b>			5693077,9	0,0001248
R6	2,9E-06	16		117,45635
<b>R6c</b>			5966595,373	0,0005335
R7				0,833
<b>R7c</b>			2904,399608	0,9325711
R8	1,06E-06	120		0,0710513
<b>R8c</b>			2904,399608	0,6191851
R9	4,93E-06	155		0,0052388
R9_01	1,29E-06	155		0,0449041
<b>R9c</b>			4766,415797	0,0851809
R10	1,11E-06	155		0,0232047
R10_01	2,92E-07	155		0,1988971
<b>R10c</b>			3864,79985	0,7353686
R11	3,93E-07	16		15,915494
R12	7,38E-07	155		0,1397966
R12_01	1,94E-07	155		1,1982565

For used material Titanium Grade 5:

<b>R</b>	<b>Volume</b>	<b>Thermal Conductivity</b>	<b>Thermal contact Conductivity</b>	<b>Thermal Resistance</b>
	[m <sup>3</sup> ]	[W/mK]	[W/m <sup>2</sup> K]	[K / W]
R1	8,32E-06	391		0,1229589
R1_01	6,93E-06	391		0,009229
<b>R1c</b>			228,6424122	9,2193123
R2	6,96E-06	6,7		1803,4826
<b>R2c</b>			6785,898763	0,1063542
R3	5,35E-06	6,7		23,447228
<b>R3c</b>			228,6424122	7,1029255
R4	4,49E-06	6,7		0,2994261
<b>R4c</b>			1330729,461	0,0008248
R5	8,27E-06	6,7		36,221924
<b>R5c</b>			1330729,461	0,0005339
R6	2,9E-06	16		117,45635
<b>R6c</b>			5966595,373	0,0005335
R7				0,833
<b>R7c</b>			275,7863474	9,8212224
R8	1,06E-06	6,7		1,2725608
<b>R8c</b>			622,7758341	2,8876537
R9	4,93E-06	155		0,0052388
R9_01	1,29E-06	155		0,0449041
<b>R9c</b>			4766,415797	0,0851809
R10	1,11E-06	155		0,0232047
R10_01	2,92E-07	155		0,1988971
<b>R10c</b>			228,6424122	12,43012
R11	3,93E-07	16		15,915494
R12	7,38E-07	155		0,1397966
R12_01	1,94E-07	155		1,1982565

For used material Aluminium 2024 + PTFE:

<b>R</b>	<b>Volume</b>	<b>Thermal Conductivity</b>	<b>Thermal contact Conductivity</b>	<b>Thermal Resistance</b>
	[m3]	[W/mK]	[W/m2K]	[K / W]
R1	8,32E-06	391		0,1229589
R1_01	6,93E-06	391		0,009229
<b>R1c</b>			19,19844926	53,731731
R2	6,96E-06	120		100,69444
<b>R2c</b>			6785,898763	0,1063542
R3	5,35E-06	120		1,3091369
<b>R3c</b>			19,19844926	84,59173
R4	4,49E-06	120		0,016718
<b>R4c</b>			5693077,9	0,0001928
R5	8,27E-06	120		2,0223908
<b>R5c</b>			5693077,9	0,0001248
R6	2,9E-06	16		117,45635
<b>R6c</b>			5966595,373	0,0005335
R7				0,833
<b>R7c</b>			2904,399608	0,9325711
R8	1,06E-06	120		0,0710513
<b>R8c</b>			2904,399608	0,6191851
R9	4,93E-06	155		0,0052388
R9_01	1,29E-06	155		0,0449041
<b>R9c</b>			4766,415797	0,0851809
R10	1,11E-06	155		0,0232047
R10_01	2,92E-07	155		0,1988971
<b>R10c</b>			19,19844926	148,03553
R11	3,93E-07	16		15,915494
R12	7,38E-07	155		0,1397966
R12_01	1,94E-07	155		1,1982565
R13	4,93E-06	0,23		3,5305001
R14	2,99E-06	0,23		5,8149413
R15	7,04E-07	0,23		24,7135
<b>R11c</b>			19,17299438	109,94244
<b>R12c</b>			19,17299438	34,878133
<b>R14c</b>			19,17299438	98,821377

For used material Titanium Grade 5 + PTFE:

<b>R</b>	<b>Volume</b>	<b>Thermal Conductivity</b>	<b>Thermal contact Conductivity</b>	<b>Thermal Resistance</b>
	[m3]	[W/mK]	[W/m2K]	[K / W]
R1	8,32E-06	391		0,1229589
R1_01	6,93E-06	391		0,009229
<b>R1c</b>			19,1984493	53,731731
R2	6,96E-06	6,7		1803,4826
<b>R2c</b>			6785,89876	0,1063542
R3	5,35E-06	6,7		23,447228
<b>R3c</b>			19,1984493	84,59173
R4	4,49E-06	6,7		0,2994261
<b>R4c</b>			1330729,46	0,0008248
R5	8,27E-06	6,7		36,221924
<b>R5c</b>			1330729,46	0,0005339
R6	2,9E-06	16		117,45635
<b>R6c</b>			5966595,37	0,0005335
R7				
<b>R7c</b>			275,786347	9,8212224
R8	1,06E-06	6,7		1,2725608
<b>R8c</b>			622,775834	2,8876537
R9	4,93E-06	155		0,0052388
R9_01	1,29E-06	155		0,0449041
<b>R9c</b>			4766,4158	0,0851809
R10	1,11E-06	155		0,0232047
R10_01	2,92E-07	155		0,1988971
<b>R10c</b>			19,1984493	148,03553
R11	3,93E-07	16		15,915494
R12	7,38E-07	155		0,1397966
R12_01	1,94E-07	155		1,1982565
R13	4,93E-06	0,23		3,5305001
R14	2,99E-06	0,23		5,8149413
R15	7,04E-07	0,23		24,7135
<b>R11c</b>			18,5721934	113,49902
<b>R12c</b>			18,5721934	36,006423
<b>R14c</b>			18,5721934	102,0182

## **B2 Intermediate calculation values for concept B**

For used material Aluminium 2024:

<b>R</b>	<b>Volume</b>	<b>Thermal Conductivity</b>	<b>Thermal contact Conductivity</b>	<b>Thermal Resistance</b>
	[m3]	[W/mK]	[W/m2K]	[K / W]
R1	8,32E-06	391		0,1229589
R1_01	6,93E-06	391		0,009229
R1c			3864,79985	0,8261354
R2	2,83E-06	120		40,972222
R2c			6785,898763	0,1063542
R3	6,89E-06	120		1,0171156
R3c			3864,79985	0,4455353
R4	4,23E-06	120		0,0177255
R4c			5693077,9	0,0001928
R5	1,06E-05	120		1,5712682
R5c			5693077,9	0,0001248
R6	2,9E-06	16		117,45635
R6c			27826031,15	0,0001144
R7				0,833
R7c			622,7758341	3,3790282
R8	9,96E-07	120		0,0753333
R8c			2904,399608	0,6191851
R9	4,93E-06	155		0,0052388
R9_1	1,29E-06	155		0,0449041
R9c			4766,415797	0,0851809
R10	1,11E-06	155		0,0232047
R10_1	2,92E-07	155		0,1988971
R10c			3864,79985	0,7796868
R11	3,93E-07	16		15,915494
R11c			3864,79985	1,1448921
R12	9,5E-07	155		0,108613
R12_01	2,49E-07	155		0,9309687
R13	2,54E-06	120		2,9444444
R14	1,23E-06	120		5,6478405



For used material Titanium Grade 5:

<b>R</b>	<b>Volume</b>	<b>Thermal Conductivity</b>	<b>Thermal contact Conductivity</b>	<b>Thermal Resistance</b>
	[m3]	[W/mK]	[W/m2K]	[K / W]
R1	8,32E-06	391		0,1229589
R1_01	6,93E-06	391		0,009229
<b>R1c</b>			228,6424122	13,964373
R2	2,83E-06	6,7		733,83085
<b>R2c</b>			6785,898763	0,1063542
R3	6,89E-06	6,7		18,216996
<b>R3c</b>			228,6424122	7,5309952
R4	4,23E-06	6,7		0,3174715
<b>R4c</b>			1330729,461	0,0008248
R5	1,06E-05	6,7		28,142118
<b>R5c</b>			1330729,461	0,0005339
R6	2,9E-06	16		117,45635
<b>R6c</b>			2642211,008	0,0012047
R7				0,833
<b>R7c</b>			622,7758341	3,3790282
R8	9,96E-07	6,7		1,3492539
<b>R8c</b>			275,7863474	6,5208483
R9	4,93E-06	155		0,0052388
R9_1	1,29E-06	155		0,0449041
<b>R9c</b>			4766,415797	0,0851809
R10	1,11E-06	155		0,0232047
R10_1	2,92E-07	155		0,1988971
<b>R10c</b>			228,6424122	13,179242
R11	3,93E-07	16		15,915494
<b>R11c</b>			228,6424122	19,352397
R12	9,5E-07	155		0,108613
R12_01	2,49E-07	155		0,9309687
R13	2,54E-06	6,7		52,736318
R14	1,23E-06	6,7		101,15535

For used material Aluminium 2024 + PTFE:

<b>R</b>	<b>Volume</b>	<b>Thermal Conductivity</b>	<b>Thermal contact Conductivity</b>	<b>Thermal Resistance</b>
	[m3]	[W/mK]	[W/m2K]	[K / W]
R1	8,32E-06	391		0,1229589
R1_01	6,93E-06	391		0,009229
<b>R1c</b>			19,19844926	53,731731
R2	2,83E-06	120		40,972222
<b>R2c</b>			6785,898763	0,1063542
R3	6,89E-06	120		1,0171156
<b>R3c</b>			19,19844926	89,689792
R4	4,23E-06	120		0,0177255
<b>R4c</b>			5693077,9	0,0001928
R5	1,06E-05	120		1,5712682
<b>R5c</b>			5693077,9	0,0001248
R6	2,9E-06	16		117,45635
<b>R6c</b>			27826031,15	0,0001144
R7				0,833
<b>R7c</b>			622,7758341	3,3790282
R8	9,96E-07	120		0,0753333
<b>R8c</b>			2904,399608	0,6191851
R9	4,93E-06	155		0,0052388
R9_1	1,29E-06	155		0,0449041
<b>R9c</b>			4766,415797	0,0851809
R10	1,11E-06	155		0,0232047
R10_1	2,92E-07	155		0,1988971
<b>R10c</b>			19,19844926	156,95714
R11	3,93E-07	16		15,915494
<b>R11c</b>			19,17299438	166,5284
R12	9,5E-07	155		0,108613
R12_01	2,49E-07	155		0,9309687
R13	2,54E-06	120		2,9444444
R14	1,23E-06	120		5,6478405
R15	4,93E-06	0,23		3,5305001
R16	2,99E-06	0,23		5,8149413
R17	7,04E-07	0,23		24,7135
<b>R12c</b>			19,17299438	230,78183
<b>R13c</b>			19,17299438	34,878133
<b>R14c</b>			19,17299438	98,821377

For used material Titanium Grade 5 + PTFE:

<b>R</b>	<b>Volume</b>	<b>Thermal Conductivity</b>	<b>Thermal contact Conductivity</b>	<b>Thermal Resistance</b>
	[m3]	[W/mK]	[W/m2K]	[K / W]
R1	8,32E-06	391		0,1229589
R1_01	6,93E-06	391		0,009229
<b>R1c</b>			19,1984493	53,731731
R2	2,83E-06	6,7		733,83085
<b>R2c</b>			6785,89876	0,1063542
R3	6,89E-06	6,7		18,216996
<b>R3c</b>			19,1984493	89,689792
R4	4,23E-06	6,7		0,3174715
<b>R4c</b>			1330729,46	0,0008248
R5	1,06E-05	6,7		28,142118
<b>R5c</b>			1330729,46	0,0005339
R6	2,9E-06	16		117,45635
<b>R6c</b>			2642211,01	0,0012047
R7				0,833
<b>R7c</b>			622,775834	3,3790282
R8	9,96E-07	6,7		1,3492539
<b>R8c</b>			275,786347	6,5208483
R9	4,93E-06	155		0,0052388
R9_1	1,29E-06	155		0,0449041
<b>R9c</b>			4766,4158	0,0851809
R10	1,11E-06	155		0,0232047
R10_1	2,92E-07	155		0,1988971
<b>R10c</b>			19,1984493	156,95714
R11	3,93E-07	16		15,915494
<b>R11c</b>			18,5721934	171,91551
R12	9,5E-07	155		0,108613
R12_01	2,49E-07	155		0,9309687
R13	2,54E-06	6,7		52,736318
R14	1,23E-06	6,7		101,15535
R15	4,93E-06	0,23		3,5305001
R16	2,99E-06	0,23		5,8149413
R17	7,04E-07	0,23		24,7135
<b>R12c</b>		18,5721934 1	18,5721934	238,24751
<b>R13c</b>		18,5721934 1	18,5721934	36,006423
<b>R14c</b>		18,5721934 1	18,5721934	102,0182

## **B3 Intermediate calculation values for concept C**

For used material Aluminium 2024:

<b>R</b>	<b>Volume</b>	<b>Thermal Conductivity</b>	<b>Thermal contact Conductivity</b>	<b>Thermal Resistance</b>
	[m3]	[W/mK]	[W/m2K]	[K / W]
R1	8,32E-06	391		0,1229589
R1_01	1,23E-05	391		0,0051919
<b>R1c</b>			6785,898763	0,0598311
R2	7,63E-07	16		119,36621
<b>R2c</b>			8453506,547	0,0003138
R3	7,76E-06	391		0,0082398
<b>R3c</b>			3864,79985	0,1667233
R4	5,43E-06	120		0,0187936
<b>R4c</b>			9415126,665	0,0001657
R5	1,26E-06	120		1,3262912
<b>R5c</b>			3864,79985	0,4202106
R6	4,28E-06	120		3,009869
<b>R6c</b>			3864,79985	0,4202106
R7	7,7E-06	120		13,095238
<b>R7c</b>			2904,399608	0,2140542
R8				0,833
<b>R8c</b>			4766,415797	0,0851809
R9	7,34E-06	120		12,407407
<b>R9c</b>			2904,399608	0,1697088
R10	5,63E-06	120		0,0181329
R11	1,62E-05	155		0,0254401
R11_01	4,26E-06	155		0,2180581
R12	3,22E-06	155		0,0080219
R12_01	8,44E-07	155		0,0687593
R13	4,93E-06	155		0,0052388
R13_01	1,29E-06	155		0,0449041

For used material Titanium Grade 5:

<b>R</b>	<b>Volume</b>	<b>Thermal Conductivity</b>	<b>Thermal contact Conductivity</b>	<b>Thermal Resistance</b>
	[m3]	[W/mK]	[W/m2K]	[K / W]
R1	8,32E-06	391		0,1229589
R1_01	1,23E-05	391		0,0051919
<b>R1c</b>			6785,898763	0,0598311
R2	7,63E-07	16		119,36621
<b>R2c</b>			8453506,547	0,0003138
R3	7,76E-06	391		0,0082398
<b>R3c</b>			228,6424122	2,8181648
R4	5,43E-06	6,7		0,3366018
<b>R4c</b>			2200740,382	0,000709
R5	1,26E-06	6,7		23,754469
<b>R5c</b>			228,6424122	7,1029255
R6	4,28E-06	6,7		53,908101
<b>R6c</b>			228,6424122	7,1029255
R7	7,7E-06	6,7		234,54158
<b>R7c</b>			275,7863474	2,2542776
R8				0,833
<b>R8c</b>			4766,415797	0,0851809
R9	7,34E-06	6,7		222,22222
<b>R9c</b>			275,7863474	1,7872611
R10	5,63E-06	6,7		0,3247681
R11	1,62E-05	155		0,0254401
R11_01	4,26E-06	155		0,2180581
R12	3,22E-06	155		0,0080219
R12_01	8,44E-07	155		0,0687593
R13	4,93E-06	155		0,0052388
R13_01	1,29E-06	155		0,0449041

For used material Aluminium 2024 + PTFE:

<b>R</b>	<b>Volume</b>	<b>Thermal Conductivity</b>	<b>Thermal contact Conductivity</b>	<b>Thermal Resistance</b>
	[m3]	[W/mK]	[W/m2K]	[K / W]
R1	8,32E-06	391		0,1229589
R1_01	1,23E-05	391		0,0051919
<b>R1c</b>			6785,898763	0,0598311
R2	7,63E-07	16		119,36621
<b>R2c</b>			8453506,547	0,0003138
R3	7,76E-06	391		0,0082398
<b>R3c</b>			19,19844926	33,562711
R4	5,43E-06	120		0,0187936
<b>R4c</b>			9415126,665	0,0001657
R5	1,26E-06	120		1,3262912
<b>R5c</b>			19,19844926	84,59173
R6	4,28E-06	120		3,009869
<b>R6c</b>			19,19844926	84,59173
R7	7,7E-06	120		13,095238
<b>R7c</b>			2904,399608	0,2140542
R8				0,833
<b>R8c</b>			4766,415797	0,0851809
R9	7,34E-06	120		12,407407
<b>R9c</b>			2904,399608	0,1697088
R10	5,63E-06	120		0,0181329
R11	1,62E-05	155		0,0254401
R11_01	4,26E-06	155		0,2180581
R12	3,22E-06	155		0,0080219
R12_01	8,44E-07	155		0,0687593
R13	4,93E-06	155		0,0052388
R13_01	1,29E-06	155		0,0449041
R14	3,1E-06	0,23		5,6030608
R15	1,23E-06	0,23		14,122
R16	1,23E-06	0,23		14,122
<b>R10c</b>			19,17299438	33,60727
<b>R11c</b>			19,19844926	84,59173
<b>R12c</b>			19,19844926	84,59173

For used material Titanium Grade 5 + PTFE:

<b>R</b>	<b>Volume</b>	<b>Thermal Conductivity</b>	<b>Thermal contact Conductivity</b>	<b>Thermal Resistance</b>
	[m <sup>3</sup> ]	[W/mK]	[W/m <sup>2</sup> K]	[K / W]
R1	8,32E-06	391		0,1229589
R1_01	1,23E-05	391		0,0051919
<b>R1c</b>			6785,89876	0,0598311
R2	7,63E-07	16		119,36621
<b>R2c</b>			8453506,55	0,0003138
R3	7,76E-06	391		0,0082398
<b>R3c</b>			19,1984493	33,562711
R4	5,43E-06	6,7		0,3366018
<b>R4c</b>			2200740,38	0,000709
R5	1,26E-06	6,7		23,754469
<b>R5c</b>			19,1984493	84,59173
R6	4,28E-06	6,7		53,908101
<b>R6c</b>			19,1984493	84,59173
R7	7,7E-06	6,7		234,54158
<b>R7c</b>			275,786347	2,2542776
R8				0,833
<b>R8c</b>			4766,4158	0,0851809
R9	7,34E-06	6,7		222,22222
<b>R9c</b>			275,786347	1,7872611
R10	5,63E-06	6,7		0,3247681
R11	1,62E-05	155		0,0254401
R11_01	4,26E-06	155		0,2180581
R12	3,22E-06	155		0,0080219
R12_01	8,44E-07	155		0,0687593
R13	4,93E-06	155		0,0052388
R13_01	1,29E-06	155		0,0449041
R14	3,1E-06	0,23		5,6030608
R15	1,23E-06	0,23		14,122
R16	1,23E-06	0,23		24,7135
<b>R10c</b>			18,5721934	34,694448
<b>R11c</b>			18,5721934	87,44417
<b>R12c</b>			18,5721934	87,44417

## **B4 Intermediate calculation values for concept D**

<b>R</b>	<b>Volume</b>	<b>Thermal Conductivity</b>	<b>Thermal Interface/contact Conductivity</b>	<b>Thermal Resistance</b>
	[m3]	[W/mK]	[W/m2K]	[K / W]
R1	1,1E-05	391		0,0028533
<b>R1c</b>			4766,415797	0,0851809
R2				0,833
<b>R2c</b>			4766,415797	0,1160662
R3	3,82E-06	391		0,0076595
<b>R3c</b>			4766,415797	0,179521
R4	4,93E-06	155		0,0052388
R4_01	1,29E-06	155		0,0449041
<b>R4c</b>			4766,415797	0,0851809
R5	2,34E-06	155		0,0110409
R5_01	6,14E-07	155		0,0946365
<b>R5c</b>			5111611,666	0,0008896
R6	6,68E-07	16		27,05634
<b>R6c</b>			5966595,373	0,0005335